TANDEM MASS SPECTROMETRIC ANALYSES OF NOVEL SYNTHETIC NEOGLYCOLIPIDS AND AMPHIPHILIC CARBOHYDRATE MOLECULES

CÉLINE VAILLANT

Tandem mass spectrometric analyses of novel synthetic neoglycolipids and amphiphilic carbohydrate molecules

By Céline Vaillant

A thesis submitted to the School of Graduate Studies in partial fulfilment of the requirements for the degree of Master of Science

Department of Chemistry

Faculty of Science

Memorial University of Newfoundland

September 2008

St John's Newfoundland

Dedication

For the ones who were, are and will be...

ABSTRACT:

This thesis describes the mass spectrometric and low-energy induced collision analyses of the protonated molecules obtained from a series of novel synthetic amphiphilic neoglycolipid cholesteryl derivatives using electrospray ionization. It also confirms the *in situ* internal elimination of the polyethoxy-spacer linkers occurring with the simultaneous formation of a C-glycoside ion-species produced by an intramolecular complex ion-molecule reaction occurring in the ionization source interface and in the collision cell of the tandem mass spectrometer.

The novel series of synthetic neoglycolipids described in this thesis varied in size and composition. They were composed of a similar cholesterol (hydrophobic) head covalently attached to a variable length of different polyethoxy spacers, covalently linked to a polar carbohydrate (hydrophilic) head such as 2-acetamido-2-deoxy-β-D-glucopyranosyl or 2-azido-2-deoxy-β-D-glucopyranosyl units.

The novel formation of a different type of $[\text{C-glycoside+H-N}_2]^+$ ion-species formed during the ESI-MS and ESI-MS/MS analyses of the neoglycolipid series containing the 2-azido-2-deoxy-glucopyranosyl moiety is also described in this thesis.

The difference in the chemical structures of neoglycolipids affects the low-energy induced collision fragmentation and the abundance of the resulting product ions. Data on diastereisomers, anomers and constitutional isomers of the neoglycolipids fragmentation were compared to verify the presence of the C-glycoside ion species.

Finally, the analyses of a series of new synthetic simple glycolipids, *N*-acetyl-glycosides and *N*-glycoside derivatives, which do not contain the cholesteryl aglycon portion, were carried out to determine the fragmentation pathway and to observe the similarity with the fragmentation pathway of the carbohydrate portion of the studied neoglycolipids.

Acknowledgments

I would like to thank Dr Joseph H. Banoub, Adjunct Professor in the Biochemistry and Chemistry Departments at Memorial University of Newfoundland, and Senior Scientist in Special Projects at Department of Fisheries and Oceans (DFO), who was my supervisor during my Masters of Science thesis, for his help, kindness, advice and intellectual assistance; as well as Dr Travis Fridgen and Dr Christina Bottaro, Professors in the Chemistry Department at Memorial University of Newfoundland (MUN), who were members of my supervisory committee, for their helpful advice.

Thanks to the DFO for making me feel welcome in their laboratories. I met nice people during these two last years in the building. Thanks to George Sheppard, biological research technician at DFO, for his help in fixing the mass spectrometer; and Howard Hodder, biological research technician, for his help during chemistry experiments and also for his help regarding the writing of my thesis.

I would like to thank Viola Martin, secretary at MUN's Chemistry Department, who has been more than helpful during these two years to provide me with any kind of information I needed.

I would like to thank Professor Paul Boullanger and his colleagues, who are working at the Laboratoire de Chimie Organique II, Glycochimie, Université Claude Bernard at Lyon, for their help in chemistry and for the creation of the series of neoglycolipids; Professor Jon Amster, Liz Hoffman and their colleagues for the acquisition of the FT-ICR MS data in their laboratories at the Department of Chemistry,

University of Georgia in United States; Professor Giorgi Gianluca and his colleagues, for the realization of ESI-Ion trap-MS analysis in their laboratories at Dipartimento di Chimica, University of Sienna in Italy; Dr Paris Georghiou and Dr Hassan Al-Saraierh who helped to synthesize, in the chemistry laboratories at Memorial University of Newfoundland, the cholesta,3-5,diene. Also,I would like to thank Dr.Paris Georghiou to help me naming some of the molecules.

I would like to thank Alexandra Belzeve and Kathy Northee who helped me with the analysis of the protected neoglycoconjugates and in a future project during their summer internship at DFO.

I would like to thank my parents for encouraging me during these two years and especially my mother. She told me recently: "It is a great Art to be a mother". I can say that her own Art was really useful and more than needed. Even though the Atlantic Ocean was separating us, she has that special power.

I would like to thank my friends Paula, Paul Hawkins and their daughter Matilda, whom I considered as my Newfie family, for their encouradgment. I also want to thank my friend Gillian Boone who took some of her time to read my thesis and correct some points. I would like to thank my friends from the Volley Ball Graduate Team: Kyla Brake and Jiyi Liu for their encouradgments. Thanks to my friend Octavia Dobre and her family for their support.

Thanks to my friends Anas El Aneed, Andry Ratsimandresy and Dounia Hamoutene, whom I met at DFO, for guiding and encouraging me.

I would like to thank Adam Choi, for being my closest supporter during the writing of the thesis.

Finally I would like to thank the NSERC, SGS, MUN, GSU and DFO for providing financial assistance to realize my research.

Thanks to the Writing Centre for their help in correcting the grammar part of the thesis.

Table of Contents

DEDICATION I

ABSTRACT: II

ACKNOWLEDGMENTS IV

TABLE OF CONTENTS VII

LIST OF TABLES XIII

LIST OF SCHEMES XXII

LIST OF ABBREVIATIONS XXV

LIST OF APPENDICES XXVI

CHAPTER 1: INTRODUCTION 1

1.1. Liposomes, neoglycoconjugates, C-glycosides *1*

1.1.1. History *1*

1.1.2. Liposomes *2*

1.1.3. Neoglycolipids *3*

1.1.4. Glycoside derivatives *4*

1.2. Formation of a C-glycoside ion-species formed by CID in the collision cell of the tandem MS/MS *5*

CHAPTER 2: EXPERIMENTAL 16

2.1. Synthesis 17

2.1.1. Synthesis of 2-acetamido-2-deoxy-glycosyl-containing glycolipids (1-4, 9-10) 17

2.1.2. Synthesis of per-O-acetylated-2-acetamido-2-deoxy-D-glycopyranosyl neoglycolipids (5-6) 20

2.1.3. Synthesis of 2-azido-2-deoxy-β-D-galactopyranosyl neoglycolipids (7-8, 11-12) 21

2.1.4. Synthesis of simple glycolipids (13-15) 23

2.2. Instrument Methods 25

2.2.1. ESI mass spectrometry 25

2.2.2. Low-energy CID-MS/MS 25

2.2.3. Product ion scanning experiments 27

2.2.4. CID-MS^n or quasi MS^n analysis 27

2.3. ESI-MS and ESI-MS/MS analyses of the different series of neoglycolipids 28

2.3.1. Analysis of a new series of 2-acetamido-2-deoxyglycosyl-containing neoglycolipids (1-4) 28

2.3.2. Analysis of a new series of 2-acetamido-2-deoxy-D-glycopyranosyl per-O-acetylated neoglycolipids (5-6) 29

2.3.3. Analysis of 2-azido-2-deoxy-β-D-galactopyranosyl neoglycolipids (7-8, 11-12) 29

2.3.4. Analysis of simple glycolipids (13-15) 30

CHAPTER 3: ANALYSIS OF A SERIES OF NEW 2-ACETAMIDO-2-DEOXY-GLYCOSYL-CONTAINING NEOGLYCOLIPIDS 31

3.1. Free neoglycolipids analysis results 31

3.2. 8-(Cholest-5-en-3-β-yloxy)-3,6-dioxaoctyl-2-acetamido-2-deoxy-β-D-glucopyranoside (1) 32

3.2.1. QqTOF-MS analysis 32

3.2.2. CID-MS/MS analysis of the protonated molecule 34

3.2.3. Formation of a C-glycoside ion-species 36

3.3. 8-(Cholest-5-en-3-β-yloxy)-3,6-dioxaoctyl-2-acetamido-2-deoxy-3-O-β-D-galactopyranosyl-α-D-galactopyranoside (3) 38

3.3.1. QqTOF-MS analysis 38

3.3.2. CID-MS/MS of the protonated molecule 38

3.3.3. Formation of the [C-glycoside]$^+$ and [C-glycoside + H-DGal]$^+$ ion-species 42

3.4. 11-(Cholest-5-en-3-β-yloxy)-3,6,9-trioxaundecyl-α-L-fucopyranoside (4) 46

3.5. Discussion 49

CHAPTER 4: 2-ACETAMIDO-2-DEOXY-D-GLYCOPYRANOSYL PER-O-ACETYLATED NEOGLYCOLIPIDS 54

4.1. Mass spectrometric analyses of the 2-acetamido-2-deoxy-D-glycopyranosyl per-O-acetylated neoglycolipids 54

4.2. 8-(Cholest-5-en-3-β-yloxy)-3,6-dioxaoctyl-2-acetamido-4,6-di-O-acetyl-3-O-(2,3,4,6-tetra-O-acetyl-β-D-galactopyranosyl)-2-deoxy-α-D-galactopyranose (5)... 54

4.2.1. Qq-TOF analysis 54

4.2.2. CID-MS/MS analysis of the protonated molecule 56

4.2.3. CID-MS/MS of the sugar-spacer and the sugar 58

4.3. Cholest-5-en-3-β-yl-2-acetamido-3,4,6-tri-O-acetyl-2-deoxy-β-L-glucopyranoside (6) 60

4.3.1. QqTOF-MS analysis 60

4.3.2. CID-MS/MS analysis of the protonated molecule 61

4.3.3. CID-MS/MS of the [SugarOH]⁺ 63

4.4. Discussion 66

CHAPTER 5: THE FORMATION OF A NEW C-GLYCOSIDE ION-SPECIES FROM A NEW NEOGLYCOLIPID SERIES CONTAINING THE 2-AZIDO-2-DEOXY-B-D-GALACTOPYRANOSYL RESIDUE MOIETY 68

5.1. Mass spectrometric analyses 70

5.2. Partially O-acetylated galacto azido neoglycolipid 70

5.2.1. 8-(Cholest-5-en-3-β-yloxy)-3,6-dioxaoctyl-3-O-(2,3,4,6-tetra-O-acetyl-β-D-galactopyranosyl)-2-azido-4,6-O-benzylidene-2-deoxy-β-D-galactopyranoside (7). 70

5.2.1.1. QqToF analysis 70

5.2.1.2. CID-MS/MS of the protonated molecule 73

5.2.2. 8-(Cholest-5-en-3-β-yloxy)-3,6-dioxaoctyl 3-O-(2,3,4,6-tetra-O-acetyl-β-D-galactopyranosyl)-2-azido-2-deoxy-α-D-galactopyranoside (8) 86

5.2.2.1. QqToF analysis 86

5.2.2.2. CID-MS/MS analyses of the protonated molecule 87

5.2.2.3. CID-MS/MS of the $[M+H-N_2]^+$ ion 90

5.2.2.4. CID-MS/MS of the [SugarSpacer]$^+$ ion 91

5.2.2.5. CID-MS/MS of the $[C\text{-glycoside}+H-N_2]^+$ ion-species 94

5.3. Discussion 94

CHAPTER 6: DIFFERENTIATION OF ANOMERS AND CONSTITUTIONAL ISOMERS OF SOME NEOGLYCOLIPIDS 98

6.1. Differentiation of diastereoisomeric anomers 99

6.1.1. 8-(Cholest-5-en-3-β-yloxy)-3,6-dioxaoctyl-2-azido-4,6-O-benzylidene-2-deoxy-α-D-galactopyranoside (11) vs 8-(cholest-5-en-3-β-yloxy)-3,6-dioxaoctyl-2-azido-4,6-O-benzylidene-2-deoxy-β-D-galactopyranoside (12) 99

6.1.2. 8-(Cholest-5-en-3-β-yloxy)-3,6-dioxaoctyl-2-azido-4,6-O-benzylidene-2-deoxy-α-D-galactopyranoside (11) 100

6.1.3. 8-(Cholest-5-en-3-β-yloxy)-3,6-dioxaoctyl-2-azido-4,6-O-benzylidene-2-deoxy-β-D-galactopyranoside (12) 104

6.1.3.1. CID-MS/MS of the protonated molecule 105

6.1.3.2. CID-MS/MS of the $[M+H-N_2]^+$ 106

6.1.3.3. CID-MS/MS of the $[C\text{-glycoside}+H]^+$ ion-species 108

6.1.3.4. CID-MS/MS of the $[C\text{-glycoside}+H-N_2]^+$ ion-species 110

6.1.4. Discussion 111

6.1.5. Cholest-5-en-3-β-yl-2-acetamido-2-deoxy-β-L-glucopyranoside (2) vs cholest-5-en-3-β-yl-2-acetamido-2-deoxy-β-D-glucopyranoside (9) 117

6.2. Differentiation of constitutional isomers 121

6.2.1. 8-(Cholest-5-en-3-β-yloxy)-3,6-dioxaoctyl-2-acetamido-2-deoxy-3-O-β-D-galactopyranosyl-α-D-galactopyranoside (3) vs 8-(cholest-5-en-3-β-yloxy)-3,6-dioxaoctyl-2-acetamido-2-deoxy-4-O-β-D-galactopyranosyl-β-D-glucopyranoside (10) 121

CHAPTER 7: SIMPLE NEOGLYCOLIPID CONTAINING THE 2-DEOXY-2-N-ACETYL OR 2-DEOXY-2-AMINO-GLUCOSAMINYL RESIDUES 127

7.1. Ethoxy-[2-2-ethoxy]-dodecanoxyl-2-N-acetyl-2-deoxy-β-glucopyranoside (13) 128

7.2. Octanoxyl-2-N-acetyl-2-deoxy-β-D-glucopyranoside (14) 133

7.3. Undecyloxyl-2-amino-2-deoxy-β-D-glucopyranoside (15) 136

7.4. Discussion 141

CONCLUSION 143

FUTURE WORK 146

REFERENCES 148

APPENDICES 155

List of Tables

Table 3. 1: Relative intensity and *m/z* values obtained for each product ion from the product ion scan (CID-MS/MS) of the protonated molecule of $[M+H]^+$ "1".....35

Table 3. 2: Relative intensity and *m/z* values of the different product ions derived from the CID-MS/MS analysis of the 8-(cholest-5-en-3-β-yloxy)-3,6-dioxaoctyl-2-acetamido-2-deoxy-3-*O*-β-D-galactopyranosyl-α-D-galactopyranoside, molecule "3". 40

Table 6. 1: Comparison of the product ion relative intensities and *m/z* obtained during the acquisition of the CID-MS/MS of both molecules 11 and 12 112

Table 6. 2: Relative intensities and *m/z* obtained for each product ions, when acquiring the tandem mass spectrometry of the protonated molecule $[M+H]^+$ of the molecules 2 and 9.....119

Table 6. 3: Product ions *m/z* and relative intensities obtained from the scans of the protonated molecules 3 and 10 by low collision energy tandem mass spectrometric analyses.....125

Table 7. 1: Data obtained from the full conventional scan and the CID-MS/MS-QqToF analyses of the protonated molecule of 1-ethoxy-[2-2-ethoxy]-dodecanoxyl-2-*N*-acetyl-2-deoxy-β- glucopyranoside (13) 129

Table 7. 2: Data obtained from the full conventional scan and the CID-MS/MS-QqToF analyses of the protonated molecule octanoxyl-2-*N*-acetyl-2-deoxy-β-D-glucopyranoside (14). 136

Table 7. 3: Data from full scan and CID-MS/MS analysis of the undecyloxyl-2-amino-2-deoxy-β-D-glucopyranoside, molecule "15". 140

List of Figures

Figure 1.1: Liposome representation with encapsulation of drug (http://en.wikipedia.org/wiki/Liposome) 2

Figure 2.1: Structures of free-acetylated neoglycolipid cholesteryl derivatives 1-4 17

Figure 2.2: Structures of neoglycolypid cholesteryl derivatives 9-10 19

Figure 2.3: Structures of per-O-acetylated cholesteryl neoglycolipid derivatives 5 and 6 20

Figure 2.4: Structures of azido cholesteryl neoglycolipid derivatives 7, 8, 11 and 12 21

Figure 2.5: Structures of simple glycolipids 13-15 23

Figure 3.1: Full scan analysis of 8-(cholest-5-en-3-β-yloxy)-3,6-dioxaoctyl-2-acetamido-2-deoxy-β-D-glucopyranoside neoglycolipid-molecule " 1". 34

Figure 3.2: CID-MS/MS of the protonated molecule $[M+H]^+$ of (8-(cholest-5-en-3-β-yloxy)-3,6-dioxaoctyl 2-acetamido-2-deoxy-β-D-glucopyranoside), molecule "1", CE=15eV. 35

Figure 3.3: *Quasi*-MS^3 of the ion-species $[C\text{-glycoside}+H]^+$ arising from 8-(cholest-5-en-3-β-yloxy)-3,6-dioxaoctyl-2-acetamido-2-deoxy-β-D-glucopyranoside , molecule "1". 37

Figure 3.4: CID-MS/MS of the protonated molecule $[M+H]^+$ of the 8-(cholest-5-en-3-β-yloxy)-3,6-dioxaoctyl-2-acetamido-2-deoxy-3-*O*-β-D-galactopyranosyl-α-D-galactopyranoside, molecule"3". 39

Figure 3.5: Second-generation tandem mass spectrometry or *quasi*-MS^3 of *m/z* 734.37, of the 8-(cholest-5-en-3-β-yloxy)-3,6-dioxaoctyl-2-acetamido-2-deoxy-3-*O*-β-D-galactopyranosyl-α-D-galactopyranoside, molecule "3".....43

Figure 3.6: Second-generation mass spectrometry analysis or *quasi*-MS^3 of the *m/z* 572, product ion derived from the 8-(cholest-5-en-3-β-yloxy)-3,6-dioxaoctyl-2-acetamido-2-deoxy-3-*O*-β-D-galactopyranosyl-α-D-galactopyranoside, molecule "3".....44

Figure 3.7: Probable fragmentations occurring for disaccharides[61].....45

Figure 3.8: Tandem mass spectrum of the 11-(cholest-5-en-3-β-yloxy)-3,6,9-trioxaundecyl-α-L-fucopyranoside (molecule "4") protonated molecule $[M+H]^+$ at *m/z* 709.06 by ESI-QqTOF-MS/MS.....46

Figure 4.1: Full scan spectrum of 8-(cholest-5-en-3-β-yloxy)-3,6-dioxaoctyl 2-acetamido-4,6-di-*O*-acetyl-3-*O*-(2,3,4,6-tetra-*O*-acetyl-β-D-galactopyranosyl)-2-deoxy-α-D-galactopyranose, molecule "5".....55

Figure 4.2: CID-MS/MS of the protonated molecule 8-(cholest-5-en-3-β-yloxy)-3,6-dioxaoctyl 2-acetamido-4,6-di-*O*-acetyl-3-*O*-(2,3,4,6-tetra-*O*-acetyl-β-D-galactopyranosyl)-2-deoxy-α-D-galactopyranose $[M+H]^+$ at *m/z* 1136.27, molecule "5".....57

Figure 4.3: ESI-MS of the cholest-5-en-3-β-yl-2-acetamido-3,4,6-tri-*O*-acetyl-2-deoxy-β-L-glucopyranoside, molecule "6".....60

Figure 4.4: Tandem mass spectrometry analysis of the precursor ion $[M+H]^+$ at *m/z* 716.55, molecule "6".....62

Figure 4.5: Second-generation tandem mass spectrometry of the $[SugarOH]^+$ also called $[L\text{-}GlcNAcOH]^+$, molecule "6". 63

Figure 5.1: Full scan ESI-MS analysis of 8-(cholest-5-en-3-β-yloxy)-3,6-dioxaoctyl-3-*O*-(2,3,4,6-tetra-*O*-acetyl-β-D-galactopyranosyl)-2-azido-4,6-*O*-benzylidene-2-deoxy-β-D-galactopyranoside, molecule "7". DP 100V FP 150V DP2 5V 71

Figure 5.2: Full scan ESI-MS analysis of 8-(cholest-5-en-3-β-yloxy)-3,6-dioxaoctyl-3-*O*-(2,3,4,6-tetra-*O*-acetyl-β-D-galactopyranosyl)-2-azido-4,6-*O*-benzylidene-2-deoxy-β-D-galactopyranoside, molecule "7". DP 100V FP 150V DP2 10V 72

Figure 5.3: CID-MS/MS scan of the protonated molecule 8-(cholest-5-en-3-β-yloxy)-3,6-dioxaoctyl-3-*O*-(2,3,4,6-tetra-*O*-acetyl-β-D-galactopyranosyl)-2-azido-4,6-*O*-benzylidene-2-deoxy-β-D-galactopyranoside (molecule 7) at *m/z* 1124.32..... 74

Figure 5.4: CID-MS/MS spectrum region from *m/z* 990 to 1130 of the 8-(cholest-5-en-3-β-yloxy)-3,6-dioxaoctyl-3-*O*-(2,3,4,6-tetra-*O*-acetyl-β-D-galactopyranosyl)-2-azido-4,6-*O*-benzylidene-2-deoxy-β-D-galactopyranoside, molecule "7"..... 75

Figure 5.5: CID-MS/MS spectrum region from *m/z* 740 to 980 of the 8-(cholest-5-en-3-β-yloxy)-3,6-dioxaoctyl-3-*O*-(2,3,4,6-tetra-*O*-acetyl-β-D-galactopyranosyl)-2-azido-4,6-*O*-benzylidene-2-deoxy-β-D-galactopyranoside, molecule "7"..... 76

Figure 5.6: Possible structure of the *m/z* 780.02 ion..... 77

Figure 5.7: Possible ion for *m/z* 766.60 77

Figure 5.8: CID-MS/MS spectrum region from *m/z* 560 to 760 of the 8-(cholest-5-en-3-β-yloxy)-3,6-dioxaoctyl-3-*O*-(2,3,4,6-tetra-*O*-acetyl-β-D-galactopyranosyl)-2-azido-4,6-*O*-benzylidene-2-deoxy-β-D-galactopyranoside, molecule "7"..... 78

Figure 5.9: Possible ion structures from the section *m/z* 560-760 79

Figure 5.10: CID-MS/MS spectrum from *m/z* 410 to 570 of the 8-(cholest-5-en-3-β-yloxy)-3,6-dioxaoctyl-3-*O*-(2,3,4,6-tetra-*O*-acetyl-β-D-galactopyranosyl)-2-azido-4,6-*O*-benzylidene-2-deoxy-β-D-galactopyranoside, molecule "7"..... 80

Figure 5.11: Different possibilities for the *m/z* ions found from 300 to 570 81

Figure 5.12: CID-MS/MS spectrum region from *m/z* 240 to 400 of the 8-(cholest-5-en-3-β-yloxy)-3,6-dioxaoctyl-3-*O*-(2,3,4,6-tetra-*O*-acetyl-β-D-galactopyranosyl)-2-azido-4,6-*O*-benzylidene-2-deoxy-β-D-galactopyranoside, molecule "7"..... 82

Figure 5.13: Tentative structure of the product ions from *m/z* 240 to 400 83

Figure 5.14: CID-MS/MS spectrum region from *m/z* 100 to 240 of the 8-(cholest-5-en-3-β-yloxy)-3,6-dioxaoctyl-3-*O*-(2,3,4,6-tetra-*O*-acetyl-β-D-galactopyranosyl)-2-azido-4,6-*O*-benzylidene-2-deoxy-β-D-galactopyranoside, molecule "7"..... 84

Figure 5.15: Possible ions from $[DGal]^+$ 85

Figure 5.16: Possible ions from both oxonium and benzene ring..... 85

Figure 5.17: CID-MS/MS spectrum of the protonated molecule 8-(cholest-5-en-3-β-yloxy)-3,6-dioxaoctyl 3-*O*-(2,3,4,6-tetra-*O*-acetyl-β-D-galactopyranosyl)-2-azido-2-deoxy-α-D-galactopyranoside (molecule "8") $[M+H]^+$ at *m/z* 1036.36. 88

Figure 5.18: CID-MS/MS of the $[SugarSpacer+H]^+$ ion at *m/z* 668.57 issued from the molecule of 8-(cholest-5-en-3-β-yloxy)-3,6-dioxaoctyl 3-*O*-(2,3,4,6-tetra-*O*-acetyl-β-D-galactopyranosyl)-2-azido-2-deoxy-α-D-galactopyranoside (molecule "8")..... 93

Figure 6.1: Representation of the molecules 11 and 12..... 99

Figure 6.2: Tandem mass spectrum of the protonated molecule $[M+H]^+$ of the compound 8-(cholest-5-en-3-β-yloxy)-3,6-dioxaoctyl-2-azido-4,6-*O*-benzylidene-2-deoxy-α-D-galactopyranoside, molecule "11". 100

Figure 6.3: Possible structures for the product ion at *m/z* 616 obtained during the CID-MS/MS of the $[M+H]^+$ protonated molecule, molecule "11" 101

Figure 6.4: Possible fragmentation pathway of the protonated molecule 8-(cholest-5-en-3-β-yloxy)-3,6-dioxaoctyl-2-azido-4,6-*O*-benzylidene-2-deoxy-α-D-galactopyranoside (molecule "11", part 1) 102

Figure 6.5: Possible fragmentation pathway of the protonated molecule 8-(cholest-5-en-3-β-yloxy)-3,6-dioxaoctyl-2-azido-4,6-*O*-benzylidene-2-deoxy-α-D-galactopyranoside (molecule "11", part 2) 103

Figure 6.6: Tandem mass spectrum of the protonated molecule $[M+H]^+$ of the 8-(cholest-5-en-3-β-yloxy)-3,6-dioxaoctyl-2-azido-4,6-di-*O*-benzylidene-2-deoxy-β-D-galactopyranoside (molecule "12") 106

Figure 6.7: CID-MS/MS of the ion $[M+H-N_2]^+$ with different collision energies 107

Figure 6.8: Third-generation tandem mass spectrometry of the $[C\text{-glycoside}+H-N_2]^+$ product ion at *m/z* 616.57, derived from the 8-(cholest-5-en-3-β-yloxy)-3,6-dioxaoctyl-2-azido-4,6-*O*-benzylidene-2-deoxy-β-D-galactopyranoside (molecule "12") 110

Figure 6.9: Comparison of the relative intensities of the product ions obtained during tandem mass spectrometry of the molecules 8-(cholest-5-en-3-β-yloxy)-3,6-dioxaoctyl-2-azido-4,6-*O*-benzylidene-2-deoxy-α-D-galactopyranoside ("11") and 8-

(cholest-5-en-3-β-yloxy)-3,6-dioxaoctyl-2-azido-4,6-*O*-benzylidene-2-deoxy-β-D-galactopyranoside ("12") 113

Figure 6.10: Representation of molecules 2 and 9 117

Figure 6.11: Low energy collision tandem mass spectrum of the protonated molecule of cholest-5-en-3-β-yl-2-acetamido-2-deoxy-β-D-glucopyranoside $[M+H]^+$ (molecule "9") 118

Figure 6.12: Low energy collision tandem mass spectrum of the protonated molecule cholest-5-en-3-β-yl-2-acetamido-2-deoxy-β-L-glucopyranoside $[M+H]^+$ (molecule "2") 118

Figure 6.13: Comparison of the relative abundances of the product ions obtained for diastereoisomers 2 and 9 120

Figure 6.14: Representation of the molecules 3 and 10 121

Figure 6.15: CID-MS/MS of the protonated molecule 8-(cholest-5-en-3-β-yloxy)-3,6-dioxaoctyl-2-acetamido-2-deoxy-4-*O*-β-D-galactopyranosyl-β-D-glucopyranoside $[M+H]^+$ (molecule "10") 123

Figure 6.16: CID-MS/MS of the protonated molecule 8-(cholest-5-en-3-β-yloxy)-3,6-dioxaoctyl-2-acetamido-2-deoxy-3-*O*-β-D-galactopyranosyl-α-D-glucopyranoside $[M+H]^+$, molecule 3 123

Figure 6.17: Comparison of the relative abundances of the product ions obtained for anomeric constitutional isomers 3 and 10 126

Figure 7.1: Representation of the molecules 13, 14 and 15 127

Figure 7.2: Conventional scan of the ethoxy-[2-2-ethoxy]-dodecanoxyl-2-*N*-acetyl-2-deoxy-β-glucopyranoside, molecule "13". 128

Figure 7.3: Tandem mass spectrometry of the protonated molecule $[M+H]^+$ of ethoxy-[2-2-ethoxy]-dodecanoxyl-2-*N*-acetyl-2-deoxy-β-glucopyranoside at *m/z* 522.61, molecule "13". 130

Figure 7.4: *Quasi*-MS^3 of *m/z* 204.48. 131

Figure 7.5: ESI-MS of the octanoxyl-2-*N*-acetyl-2-deoxy-β-D-glucopyranoside, molecule "14". 133

Figure 7.6: Low collision energy tandem mass spectrum of the precursor ion $[M+H]^+$ at *m/z* 334.57, molecule "14". 134

Figure 7.7: Full ESI-MS scan of the undecyloxyl-2-amino-2-deoxy-β-D-glucopyranoside (molecule "15"). 137

Figure 7.8: Tandem mass spectrum of the dimer protonated molecule $[2M+H]^+$ at *m/z* 667.61 138

Figure 7.9: CID-MS/MS of the precursor ion $[M+H]^+$ at *m/z* 334.61 of the undecyloxyl-2-amino-2-deoxy-β-D-glucopyranoside (molecule "15"). 139

List of Schemes

Scheme 1. 1: First concerted cleavage mechanism. 7

Scheme 1.2: Second concerted cleavage mechanism 9

Scheme 1. 3: General scheme for ion-molecule reaction propose to produce the observed [C-glycoside+H]$^+$ ion-species 11

Scheme 2. 1: The synthesis of molecule 2 according to Lafont and Boullanger [47] 18

Scheme 2. 2: Scheme for the synthesis of molecules 13 to 15 24

Scheme 2. 3: Deacylation of molecule 12 24

Scheme 3. 1: Proposed fragmentation pathway of 8-(cholest-5-en-3-β-yloxy)-3,6-dioxaoctyl 2-acetamido-2-deoxy-β-D-glucopyranoside, molecule "1" 36

Scheme 3. 2: Proposed fragmentation pathway of the 8-(cholest-5-en-3-β-yloxy)-3,6-dioxaoctyl-2-acetamido-2-deoxy-3-*O*-β-D-galactopyranosyl-α-D-galactopyranoside, molecule "3". 41

Scheme 3. 3: Ions resulting from the tandem mass spectrometry of the protonated molecule 11-(cholest-5-en-3-β-yloxy)-3,6,9-trioxaundecyl-α-L-fucopyranoside (molecule "4") [M+H]$^+$ 48

Scheme 3. 4: Representation of the two different [C-glycoside]$^+$ ion-species issued from the protonated molecule 8-(cholest-5-en-3-β-yloxy)-3,6-dioxaoctyl-2-acetamido-2-deoxy-3-*O*-β-D-galactopyranosyl-α-D-galactopyranoside (molecule"3"). 52

Scheme 4. 1: Proposed fragmentation pathway of 8-(cholest-5-en-3-β-yloxy)-3,6-dioxaoctyl-2-acetamido-4,6-di-*O*-acetyl-3-*O*-(2,3,4,6-tetra-*O*-acetyl-β-D-galactopyranosyl)-2-deoxy-α-D-galactopyranose, molecule "5". 59

Scheme 4. 2: Proposed fragmentation pathway for the molecule cholest-5-en-3-β-yl-2-acetamido-3,4,6-tri-*O*-acetyl-2-deoxy-β-L-glucopyranoside, molecule "6". 65

Scheme 4. 3: Lack of $[C\text{-glycoside}+H]^+$ formation from *O*-acetylated neoglycolipid cholesteryl derivatives. 67

Scheme 5. 1: Consecutive reactions occurring in the collision cell. 69

Scheme 5. 2: A possible fragmentation scheme obtained from the isolation of 8-(cholest-5-en-3-β-yloxy)-3,6-dioxaoctyl 3-*O*-(2,3,4,6-tetra-*O*-acetyl-β-D-galactopyranosyl)-2-azido-2-deoxy-α-D-galactopyranoside, molecule "8", protonated molecule $[M+H]^+$ from CID-MS/MS of *m/z* 1036.36 89

Scheme 5. 3: Proposed fragmentation pathway derived from the second generation tandem mass spectrum of the $[M+H-N_2]^+$ ion, molecule "8". 90

Scheme 5. 4: Proposed fragmentation pathway derived from the tandem mass spectrum of the $[SugarSpacer]^+$ ion at *m/z* 668.57, molecule "8". 92

Scheme 6. 1: Presumed product ions formed in the acquisition of *quasi*-MS^3 of the ion $[M+H-N_2]^+$ 108

Scheme 6. 2: Possible $[C\text{-glycoside}+H]^+$ fragmentation pathway derived from the second generation tandem mass spectrum 109

Scheme 6. 3: Possible consecutive reactions occurring *in situ* in the cell collision. 115

Scheme 7. 1: Proposed fragmentation pathway of the ethoxy-[2-2-ethoxy]-dodecanoxyl-2-*N*-acetyl-2-deoxy-β-glucopyranoside, molecule "13"..... 132

Scheme 7. 2: Proposed fragmentation pathway for the octanoxyl-2-*N*-acetyl-2-deoxy-β-D-glucopyranoside (molecule "14")..... 135

Scheme 7. 3: Proposal fragmentation pathway of the undecyloxyl-2-amino-2-deoxy-β-D-glucopyranoside (molecule "15")..... 140

List of Abbreviations

CID-QqTOF-MS/MS: *Collision Induced Dissociation-Triple Quadrupole-Time of Flight-tandem mass spectrometry*
ESI-QqTOF: *Electrospray Ionization Triple Quadrupole-Time of Flight*
N_3: *Azido*
FT-ICR-MS: *Fourier-Transform- Ion Cyclotron Resonance-Mass Spectrometer*
AIDs: *Acquired immune deficiency syndrome*
HIV: *Human immunodeficiency virus*
GalNAc: *N-acetyl-galactosamine*
DNA: *Deoxyribonucleic acid*
ESI: *Electrospray Ionization*
CID: *Collision Induced Dissociation*
Glc: *glucosamine*
DGal: *Dextrorotary-galactosamine*
LGlcNAc: *Laevorotatory or Levorotatory N-Acetyl-glucose*
MeONa: *Sodium methoxide*
MeOH: *Methanol*
GS: *Gas*
DP: *Declustering Potential*
FP: *Focusing Potential*
CE: *Collision energy*
MS^3: *second generation tandem mass spectrometry*
MS^4: *third generation tandem mass spectrometry*
m/z: *mass/to charge ratio. z : number of charges*
AcOH: *Acetyl hydroxide*
CH_2CO: *ketene*
OAc: *Oacetyl*
Ac: *Acetyl*
APPI: *Atmospheric pressure photoionization*
NH_3: *Ammonia*
eV: *electron Volt*
Da: *Dalton*
MALDI: *Matrix-assisted laser desorption/ionization*
C_6H_5CH: *Benzylidene*
$DGalN_3$: *Azido-D-galactosamine*
$PhCH_3$: *toluene*
FAB: *Fast Atom Bombardment*
EI: *Electron Ionization*
CI: *Chemical Ionization*

List of Appendices

Appendix 1: Flow conversion table for QSTAR XL (QSTAR XL System, Hardware Guide, Applied Biosystems, July 2002) 155

Chapter 1: Introduction

1.1. Liposomes, neoglycoconjugates, C-glycosides

1.1.1. History

The main goal in medicinal therapy is to be able to target specific cell-functions within the body. In the 1970's, it was determined that liposomes could be used as drug carriers. It was believed that a liposome, which could interact with the surface of the desired target cell, could be used as a vehicle to carry cell recognition molecules. In 1982, most articles regarding liposomes hailed them as a revolution for use as "guided missiles" in drug therapy.[1] The interest in using liposomes grew into applications as vaccine and diagnostic tools. However, problems have been encountered with using liposomes as a drug delivery system. In fact, "targeting" of liposomes to specific cells *in vivo* requires: i) access to the appropriate target cell; and ii) recognition and selective interaction with the target cell with little or no uptake by non-target cells.[1] The combination of liposome-drug also has to be non-toxic, and stable enough so that the concentration of the drug would still be effective when delivered to the target.[1]

1.1.2. Liposomes

A liposome is composed of a hydrophilic cyclic bilayer of membrane-type lipids that form a sphere with an interior hydrophilic compartment. This interior compartment contains biological fluids that allow this compartment to be a drug carrier.[2,3] Liposomes are often used as drug delivery systems due to their encapsulating properties (**Figure 1.1**). The encapsulated molecules can be carbohydrates, proteins or even DNA.

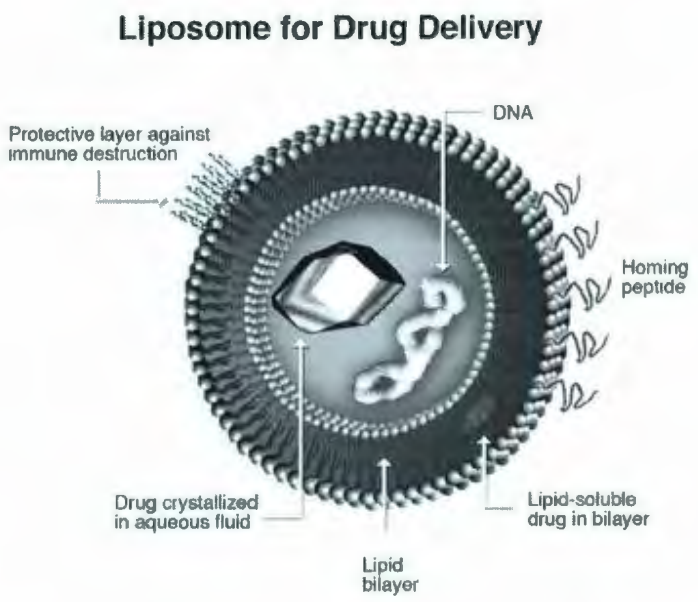

Figure 1.1: Liposome representation with encapsulation of drug (http://en.wikipedia.org/wiki/Liposome)

When injected into the body, membrane permeability will be affected, the liposome will change its structure, and lysis (drug delivery) will be induced.[4] Drug carriers can influence drug metabolism, toxicity or drug delivery to pharmacological receptors and can also prolong *in vivo* drug actions. Furthermore, when neoglycolipids are incorporated into a liposome, liposome life can be increased by half.[5,6] It should be noted,

however, that other kinds of drug carriers, such as antibodies, proteins, polysaccharides, synthetic polymers and other kinds of macromolecules are used for their therapeutic effects.[7]

1.1.3. Neoglycolipids

Glycoconjugates are composed of mono-, oligo- or polysaccharide carbohydrates, often called glycans,[4] connected by a covalent linkage to a protein (glycoprotein) or to a lipid (glycolipid).[2] These molecules are amphiphilic due to the difference in polarity between the polar head (glycan) and the non-polar lipid tail (lipid, protein).[8,9] A common methodology for using different specific glycoside antigens as medicinal vaccines is to encapsulate the carbohydrates inside a liposome.[10,11] There are various 2-amino-2-deoxy-β-glycopyranosides containing specific *O*-antigens that have been synthesized for their immunochemical and enzymological interests.[12] These can be found in human milk, blood, and virulent bacterial lipopolysaccharide antigens.[2] Consequently, the oligosaccharide moieties of the different glycoconjugates play an important role in the human body. They are involved in i) the blood group specificities, ii) extension of the life of liposomes by up to one-half in the blood stream, iii) creation of antibodies when a cell is invaded by a virus, and iv) enzyme action.[2]

Neoglycoconjugates are often found linked to the outer-cell membranes.[8] Their carbohydrate moiety, which is situated on the cell membrane, can have important functions such as cell-cell or cell-virus recognition.[2] It is important to note the utility of a spacer in neoglycolipids. According to several studies, the spacer connecting the

carbohydrate and lipid imparts stability to the molecule by acting as a balance between the hydrophilic and hydrophobic parts.[13,14] Moreover, this spacer facilitates embedding into the liposomes[14] and into the surface bilayer.[6] This oligoethyleneglycol allows easy recognition of the head group (key) by the target protein (lock or receptor).[10] These modifications of neoglycolipids may allow medicinal use as agents against AIDs, the HIV[6,15] and cancer.[6,14,15,16] In addition, they also can be used as vaccines,[6,16,17,18] and can play other roles such as raising antibodies,[17] being used as a bacterial antigen[19] or as an inhibitor.[3,18]

Some studies have shown that galactosamine can interact with T cells. For instance, if *N*-acetylgalactosamine is linked to a T cell, it will permit the creation of a non-hydrolysable vaccine.[16] Another experiment has shown that while a synthetic carbohydrate cannot function like a natural one (due to the chemical modifications), its effects resemble those of the natural one. John Schmieg *et al.*[20] have shown that synthetic carbohydrate can mimic T cell activity instead of stimulating it. However, this synthetic T cell was inhibiting Th_1, even though a natural T cell would produce Th and Th_2 cytokines. In the case of the neoglycolipids studied in this thesis, the cholesterol moiety acts as a membrane stabilizing agent.[21]

1.1.4. Glycoside derivatives

There are different types of glycoside derivatives which involve the presence of heteroatoms on the anomeric position *C*-1 such as *C*-1-*O*-, C-1-*N*-, and *C*-1-*C*-glycosides and they are all used in medicine.[5,7,15,16] However, in the treatment of HIV and HcV, it

recently appeared that *N*- and *C*-types of glycosides were preferable to an *O*-glycoside in some medical treatment.[22] While both are similar in their conformations, the *C*-glycosides are chemically more stable than *O*- and *N*-glycosides.[22] Finally, the various *C*-glycosidation reactions have been shown to be much more difficult to achieve than *O*- and/or *N*-glycosylations.[6]

The neoglycolipids studied in this thesis present in their structures two types of carbohydrate moieties: 2-deoxy-2-*N*-acetyl-β-glucosaminyl and 2-deoxy-2-*N*-acetyl-β-galactosaminyl. The hydrophobic part of these synthetic neoglycolipids is a building block for T and T_n antigens.[14]

1.2. Formation of a C-glycoside ion-species formed by CID in the collision cell of the tandem MS/MS

In previous publications,[5,23] it was tentatively proposed that a $[C\text{-glycoside}]^+$ ion-species was formed during electrospray ionization (ESI) by CID in the interface atmospheric region of the mass spectrometer and in the collision cell during acquisition of CID-MS/MS, from a series of 2-deoxy-2-amino-β-D-glucosamine- or a 2-deoxy-2-*N*-acetyl-β-D-glucosamine-containing neoglycolipid cholesteryl derivatives. The rational formation of this β-D-ion-species could not be explained from the model of the molecular structure of the neoglycolipid cholesteryl derivatives.

The chemical structure of this $[C\text{-glycoside}]^+$ ion-species was proposed by performing CID-MS/MS of this ions species which produced two major product ions, namely, the 2-deoxy-2-acetamido-glucosamine oxonium ion, and a protonated

cholestadiene. This CID-MS/MS analysis indicated that the precursor $[C\text{-glycoside}]^+$ derived from the 2-deoxy-2-*N*-acetyl-β-D-glucosamine neoglycolipid cholesteryl derivatives dissociates by two possible contiguous bond cleavages.

The first putative mechanism involves the elimination of the axial C-2 hydrogen of the sugar moiety, with consecutive cleavage of the anomeric C-1-steoridal C-3' bond. This forms the neutral 2-*N*-acetyl-2-deoxy-D-glucal fragment. The protonated cholestadiene observed at *m/z* 369.15 resulted, presumably, via the C-3'-C-4' double bond formation on the steroid nucleus, followed by protonation at the C-6' to produce the cholesta-3-ene tertiary carbocation (equivalent to a "protonated" cholestadiene) (**Scheme 1.1**).

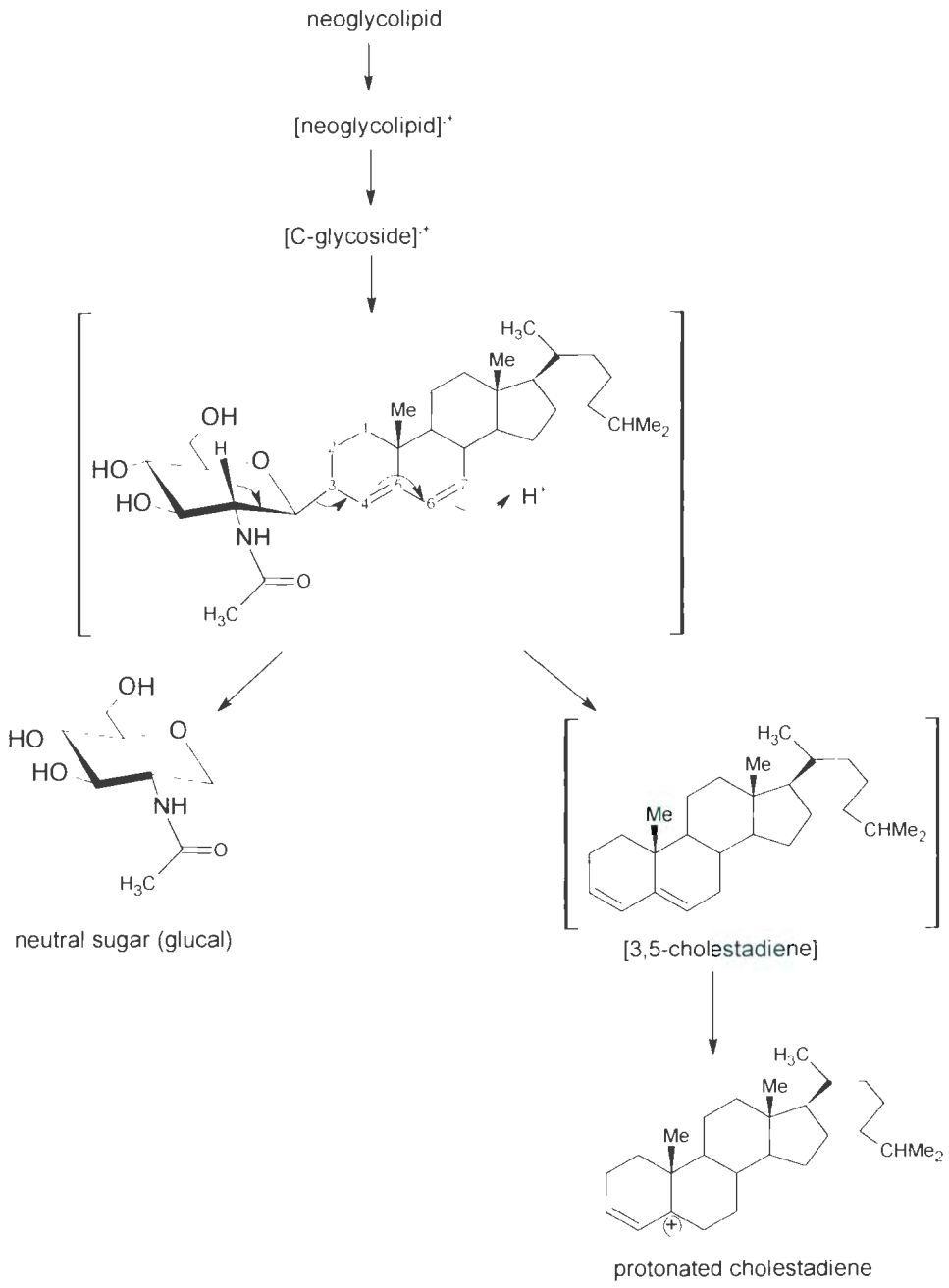

Scheme 1. 1: First concerted cleavage mechanism.

In the second putative mechanism, it was presumed that the precursor [C-glycoside] undergoes the C-1-steroidal C-3' bond cleavage as a result of anchimeric assistance from a lone pair of electrons from the ring oxygen. This forms the [Oxonium]$^{+}$ species which can be stabilized by the *N*-acetyl group which produces the corresponding 1,2-oxazolinium ion or [Oxazolinium]$^{+}$. The C-1-C-3' bond cleavage is facilitated by the protonation at C-7' of the cholesta-3,5-diene (**Scheme 1.2**).[23]

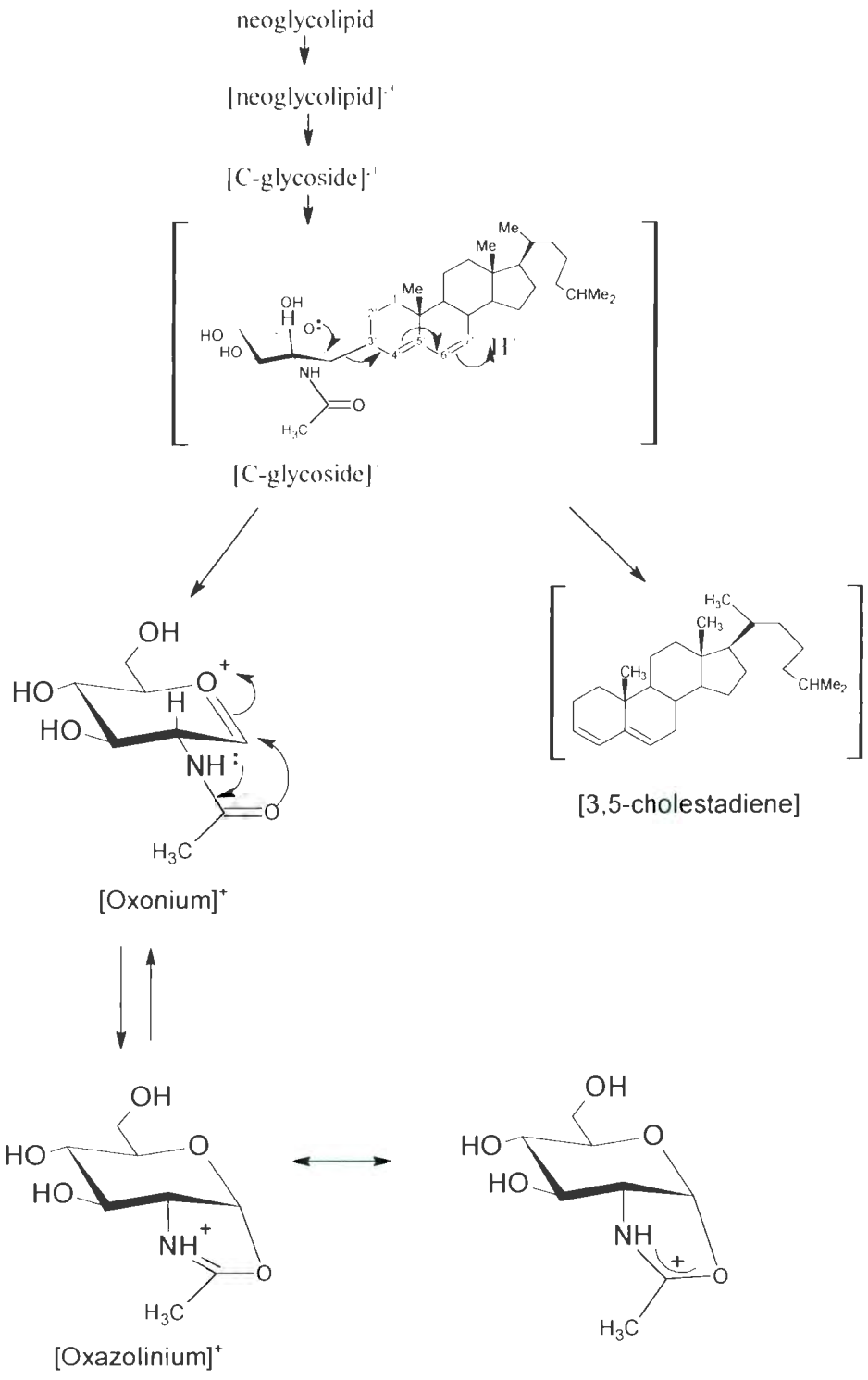

Scheme 2.2: Second concerted cleavage mechanism

The rationale proposed for the actual formation of the $[C\text{-glycoside}]^+$ ion-species, was that it resulted from an ion-molecule reaction which can occur in both the collision cell and within the ESI interface of the Turbo Ionspray source. The parent ion produced from the cholesteryl glycolipid ($[M+H]^+$ in **Scheme 1.3**) was postulated to undergo covalent bond cleavages analogous to that proposed for the CID-MS/MS analysis of the $[C\text{-glycoside}]^+$ above, in which an $[Oxonium]^+ \leftrightarrow [Oxazolinium]^+$ species and a neutral cholestadiene is formed, as well as the fragment(s) resulting from the "spacer" group. The $[Oxonium]^+ \leftrightarrow [Oxazolinium]^+$ ion then undergoes an electrophilic addition to the cholesta-3,5-diene at the C-3' position of the steroid, which concomitant loss of proton from the C-7' position and the formation of the C-3' C-glycosidic cholesta-4,6-diene observed at its corresponding protonated ion.

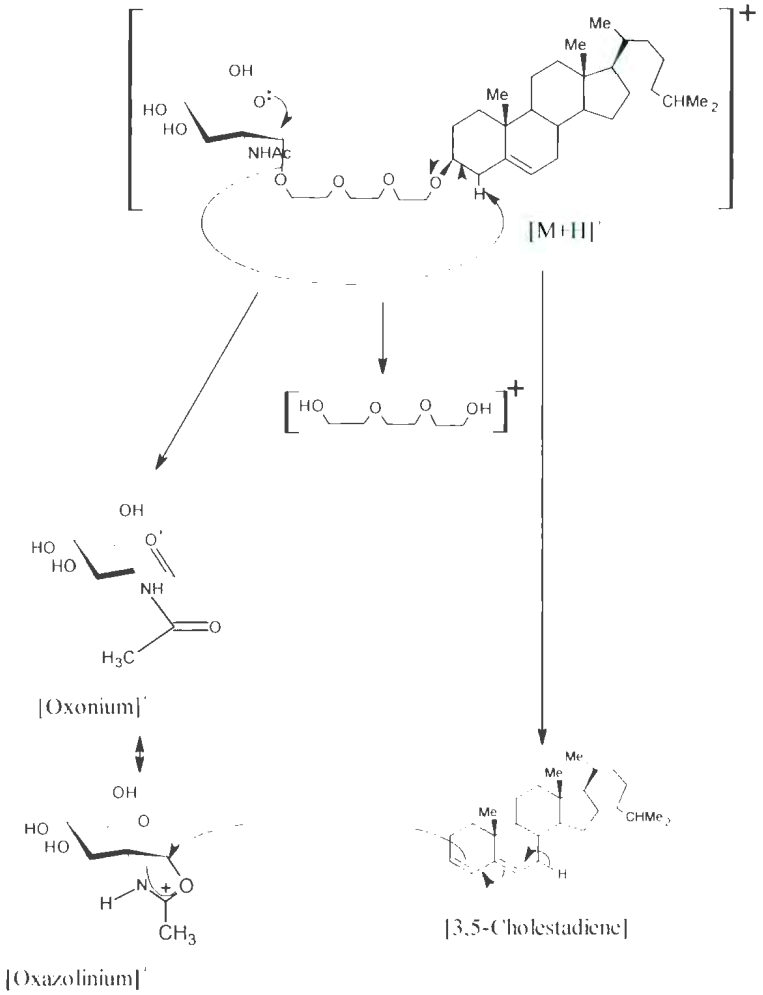

Scheme 1. 2: General scheme for ion-molecule reaction propose to produce the observed $[C\text{-glycoside+H}]^+$ ion-species.

In the case of the free 2-amino group on the sugar moiety (*i.e.* glucosamine), the electrophile is a 1,2-cyclic-aziridinium ion. The presence of the $[C\text{-glycoside}]^+$ ion-species was not observed; however, when the sugar moiety did not carry the *N*-acetyl derived participating group on the *C*-2.[23]

The C-glycoside ion-species was believed to be obtained in the gas-phase by an ion-molecule reaction, aided by intermolecular forces such as, for example, ion-dipole. Campbell *et al.*[24] demonstrated that an ion-molecule reaction occurred when screening the amido functionality with Fourier transform cyclotron resonance (FT-ICR). These rapid and spontaneous reactions are the most common ones for protonated molecules. They suggest that a proton transfer and a nucleophilic substitution occurred at the same time due to the endothermicity of the proton transfer step. It was also observed that the aromatic ring is essential for this reaction to occur. Finally, they obtained the same results using a triple quadrupole mass spectrometer as the ion source.

A literature survey revealed that gas phase CID-MS/MS fragmentations, under any different type of ionization is a unimolecular process. In addition, it has also been revealed that many ion-molecule reactions occur via mechanisms mediated by intermediate complexes, ranging from simple electrostatically or hydrogen-bonded species to covalently bonded complexes.[25]

As Liu and Anderson[25] stated: "Evidence for the role of complexes includes isotopic scrambling, forward–backward symmetric product angular distributions, and product branching and recoil energies consistent with statistical unimolecular decay of a

long-lived intermediate. In such reactions, it is safe to say that the breakup of the complex is a statistical process, signifying that it depends only on the total energy and angular momentum of the complex."

Furthermore, it has been reported that even for reactions mediated by a statistical complex, the reaction may be controlled by dynamics, *i.e.*, the rate-limiting step is sensitive to the details of reactant preparation, not simply on energy and angular momentum.[25]

Liu and Anderson[25] also cited that: "The fundamental assumption, in statistical reaction models, is that energy is randomized, *i.e.*, distributed statistically among all the energetically accessible states of the system. For statistical factors to control reaction, this randomization must occur prior to the rate-limiting step in the mechanism.[26,27,28] Inherent in this assumption is the requirement that energy exchange between different degrees of freedom be facile, so that energy randomization can be rapid compared to the reaction time. In addition, the rate of a particular process (*e.g.*, breakup of a complex, or interconversion between different complex isomers) is proportional to the total number of energetically accessible states (subject to angular momentum conservation) at the transition state (TS)."

Fukui stated that "statistical reactions tend to occur by paths close to the minimum energy path, as the density of states is highest for such paths."[25,29] To predict the behaviour of statistical mechanism, the energies, moments of inertia and vibrational frequencies for the complexes and transitions states that connect the reactants to various

product channels have to be calculated.[25] "For many ion-molecule reactions, there are no energy barriers to the approach of reactants, thus it is assumed that the initial ion-molecule complex forms efficiently".[25] The unimolecular rates for crossing the various transition states leading from the initial complex to other complexes as well as various product channels, are calculated using the transition-state-theory-based model such as the Rice-Ramsperger-Kassel-Marcus (RRKM) theory[30,31] or phase space theory.[26] Baer and Hase[26] realized that "the product branching is given by the ratio of the rates, and recoil energy distributions can also be calculated based on the assumption of statistical energy partitioning in the products. This basic approach has been successful in accounting for [their] many experimental observations, and these successes support the assumptions made in the statistical models."

Schranz and Sewell[32] demonstrated that detailed investigations of dynamic effects on chemical reactions, leads to reconsideration of the validity of the fast-energy exchange assumption inherent in the statistical approach. Reacting molecules might not necessarily follow the minimum energy pathway when kinetic energy is accounted for.[33,34] These phenomena would be due to the relationship between intra-molecular vibrational redistribution (IVR) and molecular structure.[33,34] Finally, Liu and Anderson[25] reported that in previous experiments "non-statistical effects have been seen in the variation of unimolecular lifetime with energy,[35,36] in product energy distributions,[37,38] product branching ratios,[39] and in the effects of electronic[40] and vibrational excitation."[41]

Therefore, after careful consideration, it was deemed probable that the CID-MS/MS C-glycoside ion-species formed might be produced from an ion-molecule

reaction occurring through an electrostatically bound transition complex, controlled by intramolecular forces. This presumes that during the "internal elimination" of the spacer, the activated complex transition state contains the positive 1,2-ozazolinium ion and the neutral molecule which are held in very close proximity by an electrostatic force which, in turn, almost certainly produces a covalent bond.

During this M.Sc. work, it became possible to rationalize that this unique and novel C-glycoside ion-species was formed by an "intramolecular" mechanism.

Future explanations for this phenomenon may result when complex gas-phase reactions of this described type are further explored. For these reasons, it was difficult to correctly name this product ion as: i) a covalent C-glycoside product ion or ii) an ion-molecule complex held by strong electrostatic forces. For simplicity, it was decided to call it the "C-glycoside" ion-species, as its molecular mass corresponds to that of the C-glycoside ion.

Therefore for expediency purposes, throughout this M.Sc. thesis, any formation of novel ion-molecule reaction species formed in the vacuum interface or the collision cell during CID analyses will be referred to as the "C-glycoside" ion-species.

Chapter 2: Experimental

The thesis deals with the experiments conducted by conventional ESI-MS and low energy CID-MS/MS on a novel synthetic neoglycoconjugate series, namely, 2-acetamido-2-deoxy-β-D-glycosyl-containing neoglycolipids (**Chapter 3** and **Chapter 6**), per-*O*-acetylated 2-acetamido-2-deoxy-β-D-glycopyranosyl neoglycolipid derivatives (**Chapter 4**), 2-azido-2-deoxy-β-D-galactopyranosyl neoglycolipids and their partially acetylated derivatives (**Chapter 5** and **Chapter 6**), and a series of simple glycolipids containing 2-deoxy-2-*N*-acetyl or 2-deoxy-2-amino-glucosaminyl residues (**Chapter 7**).

These experiments were conducted to confirm the purity of the neoglycolipids and glycolipids using mass spectrometry techniques. It was reported earlier that the neoglycolipids can facilitate the stability and gene transfer ability of liposomes.[42,43] Structural studies of liposomal formulations and liposomal-gene carriers are necessities for the pharmaceutical and therapeutic fields.[23] These neoglycolipids were synthesized by another laboratory (Laboratoire de Chimie Organique II, Glycochimie, Université Claude Bernard, Lyon-France) and were characterized using the following techniques: column chromatography, polarimetry, thin layer chromatography and nuclear magnetic resonance spectroscopy.

2.1. Synthesis

2.1.1. Synthesis of 2-acetamido-2-deoxy-glycosyl-containing glycolipids (1-4, 9-10)

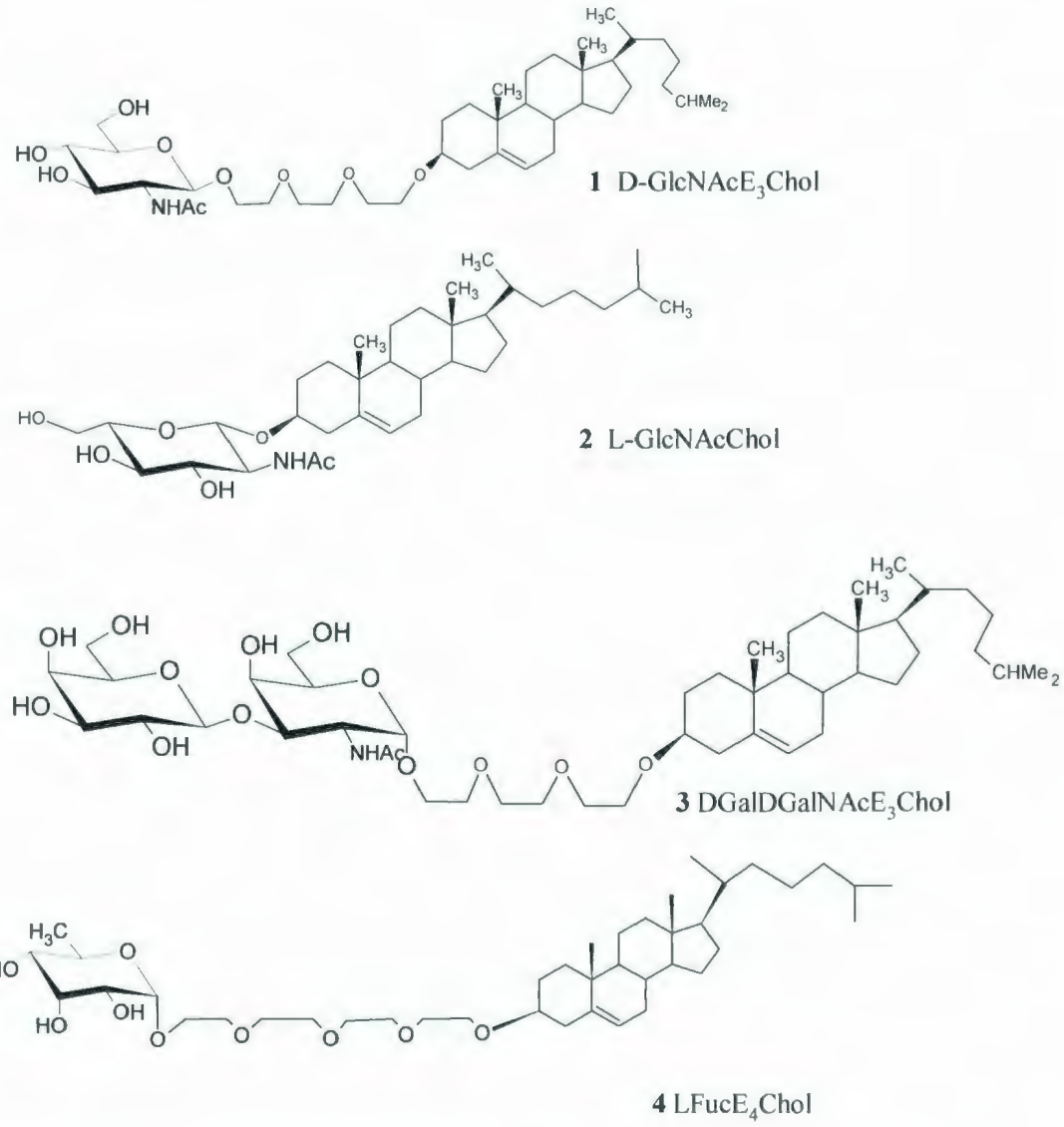

Figure 2.1: Structures of free-acetylated neoglycolipid cholesteryl derivatives 1-4

The synthesis of 8-(cholest-5-en-3-β-yloxy)-3,6-dioxaoctyl-2-acetamido-2-deoxy-β-D-glucopyranoside (D-GlcNAcE$_3$Chol) **1** (**Figure 2.1**) was previously reported and this molecule was synthesized for its efficacy against bacterial infections.[10,44] 8-(Cholest-5-en-3-β-yloxy)-3,6-dioxaoctyl-2-acetamido-2-deoxy-3-*O*-β-D-galactopyranosyl-α-D-galactopyranoside (D-Gal-D-GalNAcE$_3$Chol) **3** (**Figure 2.1**) was synthesized following the protocol of Boullanger *et al.*[45,46] Cholest-5-en-3-β-yl-2-acetamido-2-deoxy-β-L-glucopyranoside (L-GlcNAcChol, L-*N*-acetyl-glucosamine-cholesteryl) **2** **(Figure 2.1)** was synthesized according to the procedure of Lafont and Boullanger.[47] The deprotected 2-acetamido-2-deoxy-L-glucoside-*O*-acetylated-cholesteryl derivative was deacylated and deprotected using a catalytic amount of sodium methoxide (MeONa) in methanol (MeOH) (**Scheme 2.1**).

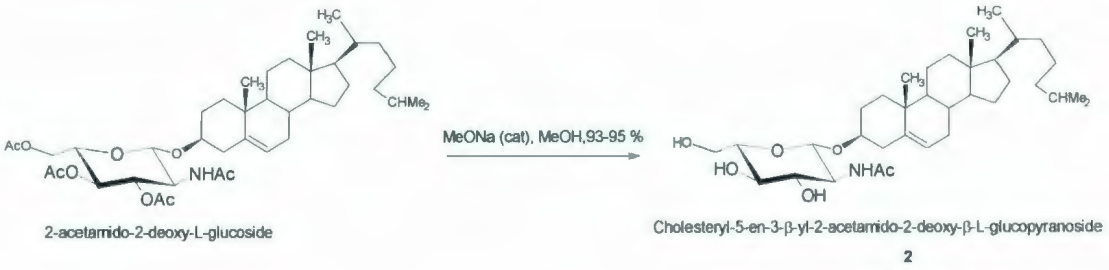

Scheme 2. 1: The synthesis of molecule 2 according to Lafont and Boullanger [47]

The use of the molecule 11-(cholest-5-en-3-β-yloxy)-3,6,9-trioxaundecyl-α-L-fucopyranoside (L-Fuc-E$_4$Chol) **4** **(Figure 2.1)** was reported by Bardonnet *et al;*[10] however, the synthesis of the compound was not described.

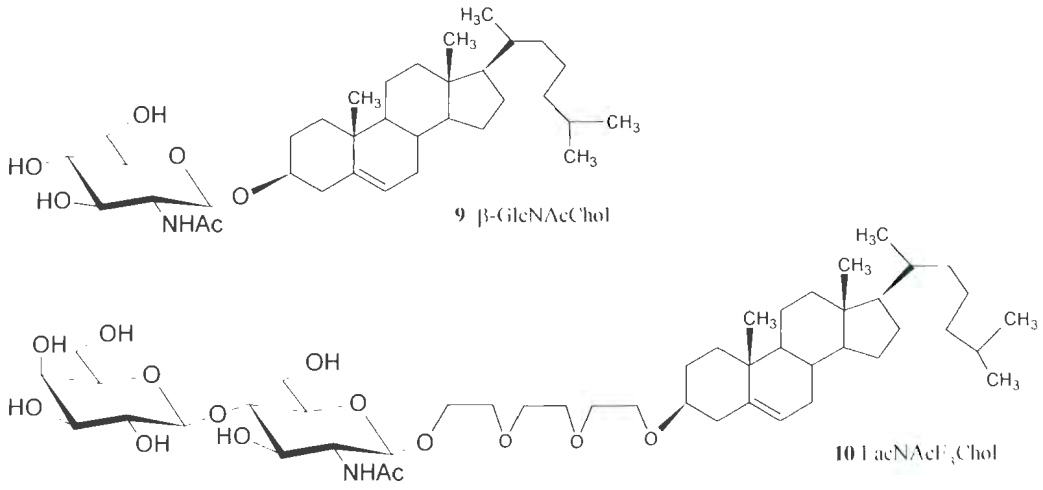

Figure 2.2: Structures of neoglycolypid cholesteryl derivatives 9-10

The neoglycolipids cholest-5-en-3-β-yl-2-acetamido-2-deoxy-β-D-glucopyranoside **9** (**Figure 2.2**) (β-GlcNAcChol) and 8-(cholest-5-en-3-β-yloxy)-3,6-dioxaoctyl-2-acetamido-2-deoxy-4-*O*-β-D-galactopyranosyl-β-D-glucopyranoside **10** **(Figure 2.2)** (LacNAcE$_3$Chol) were synthesized by Boullanger *et al* according to a previously reported procedure.[19, 45]

2.1.2. Synthesis of per-*O*-acetylated-2-acetamido-2-deoxy-D-glycopyranosyl neoglycolipids (5-6)

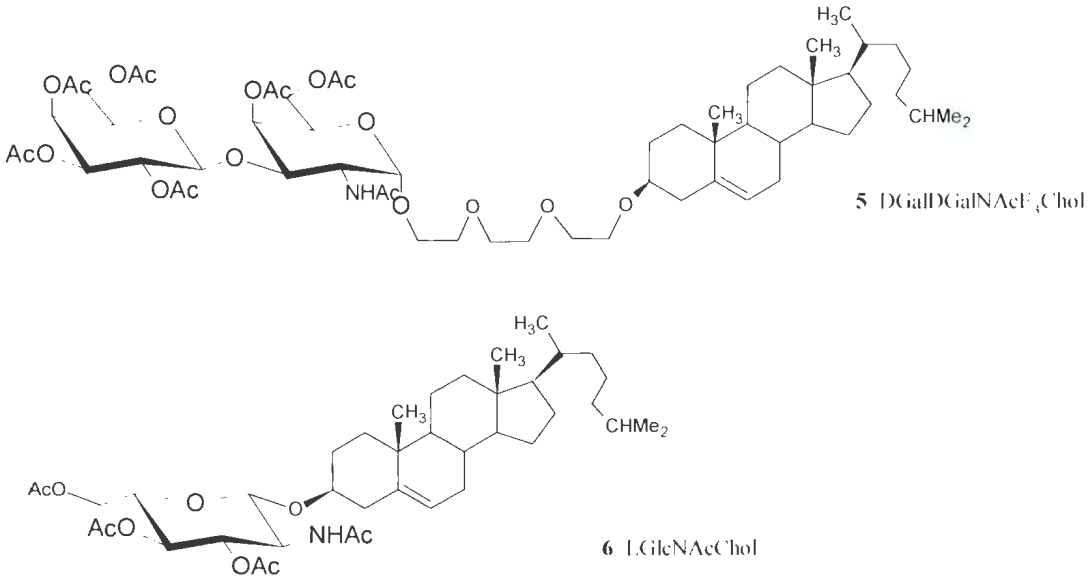

Figure 2.3: Structures of per-*O*-acetylated cholesteryl neoglycolipid derivatives 5 and 6

The synthesis of 8-(cholest-5-en-3-β-yloxy)-3,6-dioxaoctyl-2-acetamido-4,6-di-*O*-acetyl-3-*O*-(2,3,4,6-tetra-*O*-acetyl-β-D-galactopyranosyl)-2-deoxy-α-D-galactopyranoside (D-Gal-D-GalNAcE$_3$Chol) **5 (Figure 2.3)** and the cholest-5-en-3-β-yl-2-acetamido-3,4,6-tri-*O*-acetyl-2-deoxy-β-L-glucopyranoside (L-GlcNAcChol) **6 (Figure 2.3)** were achieved according to methods reported by Lafont *et al.*[45,47]

2.1.3. Synthesis of 2-azido-2-deoxy-β-D-galactopyranosyl neoglycolipids (7-8, 11-12)

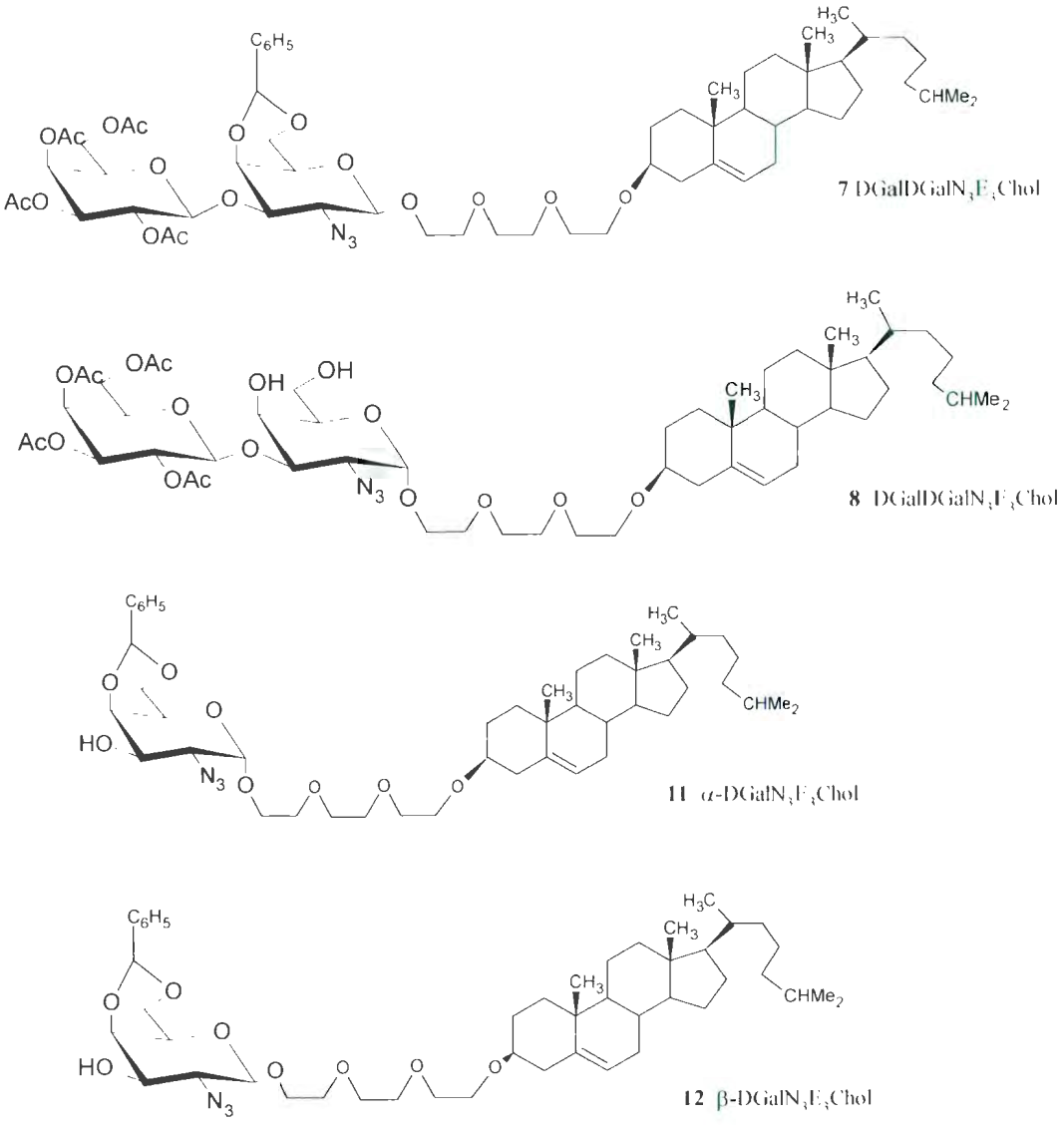

Figure 2.4: Structures of azido cholesteryl neoglycolipid derivatives 7, 8, 11 and 12

The 2-azido-2-deoxy-β-D-galactopyranosyl residue was attached to the neoglycolipids 8-(cholest-5-en-3-β-yloxy)-3,6-dioxaoctyl-3-*O*-(2,3,4,6-tetra-*O*-acetyl-β-D-galactopyranosyl)-2-azido-4,6-*O*-benzylidene-2-deoxy-β-D-galactopyranoside (D-Gal-D-GalN_3E_3Chol) **7** **(Figure 2.4)** and 8-(cholest-5-en-3-β-yloxy)-3,6-dioxaoctyl-3-*O*-(2,3,4,6-tetra-*O*-acetyl-β-D-galactopyranosyl)-2-azido-2-deoxy-α-D-galactopyranoside (D-Gal-D-GalN_3E_3Chol) **8** **(Figure 2.4)**, according to the method reported by Laurent *et al.*[14]

The molecules 8-(cholest-5-en-3-β-yloxy)-3,6-dioxaoctyl-2-azido-4,6-*O*-benzylidene-2-deoxy-α-D-galactopyranoside (α-D-GalN_3E_3Chol) **11** (**Figure 2.4**) and 8-(cholest-5-en-3-β-yloxy)-3,6-dioxaoctyl-2-azido-4,6-*O*-benzylidene-2-deoxy-β-D-galactopyranoside (β-D-GalN_3E_3Chol) **12** (**Figure 2.4**) were also reported previously, and were synthesized from a *N*-acetyl-α-D-galactosamine neoglycolipid.[14] These neoglycolipids contained the same saccharide (D-galactosamine-azido-D-galactosamine (DGalDGalN_3)). However, the presence of the 4,6-di-*O*-benzylidene group was present for **7** but not for **8**.

2.1.4. Synthesis of simple glycolipids (13-15)

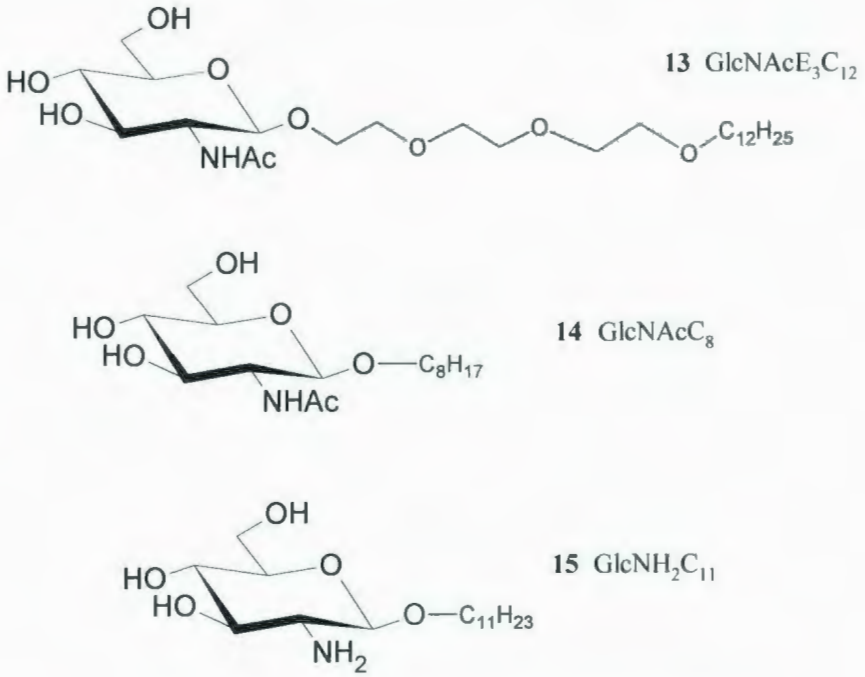

Figure 2.5: Structures of simple glycolipids 13-15

The synthesis of **13**, a 1-ethoxy-[2-2-ethoxy]-dodecanoxyl-2-*N*-acetyl-2-deoxy-β-D-glucopyranoside ($GlcNAcE_3C_{12}$) was accomplished by Boullanger *et al.*;[46] however, the cholesterol tosylate was replaced by an aliphatic alcohol. The synthesis of **14**, an octanoxyl-2-*N*-acetyl-2-deoxy-β-D-glucopyranoside ($GlcNAcC_8$) and **15**, a 1-undecyloxyl-2-amino-2-deoxy-β-D-glucopyranoside ($GlcNH_2C_{11}$) was consistently the same for the first step, according to Boullanger *et al.*[19] Compounds **13**, **14** and **15** are shown in **Figure 2.5**. The 1,3,4,6-tetra-*O*-acetyl-2-amino-2-deoxy-β-D-glucopyranose hydrochloride "**a**" **(Scheme 2.2)** was used for the synthesis of the 1,3,4,6-tetra-*O*-acetyl-2-deoxy-2-acetamido-β-D-glucopyranose "**b**" **(Scheme 2.2)** which was used as the glycosyl donor for the synthesis of the compound "**c**" **(Scheme 2.2)**.

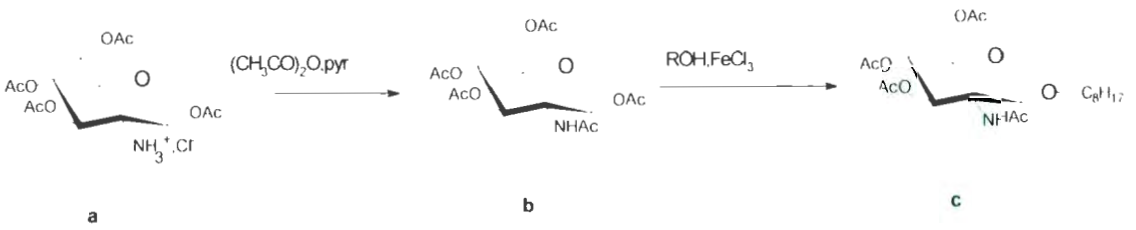

Scheme 2. 2: Scheme for the synthesis of molecules 13 to 15

Boullanger *et al.*[19] de-*O*-acetylated the amino glucolipid "**c**" to obtain the molecule **14 (Scheme 3)**. To obtain the molecule **15**, the same procedure was applied, followed by heating the amino glycolipid in a concentrated NaOH solution (**Scheme 2.3**).

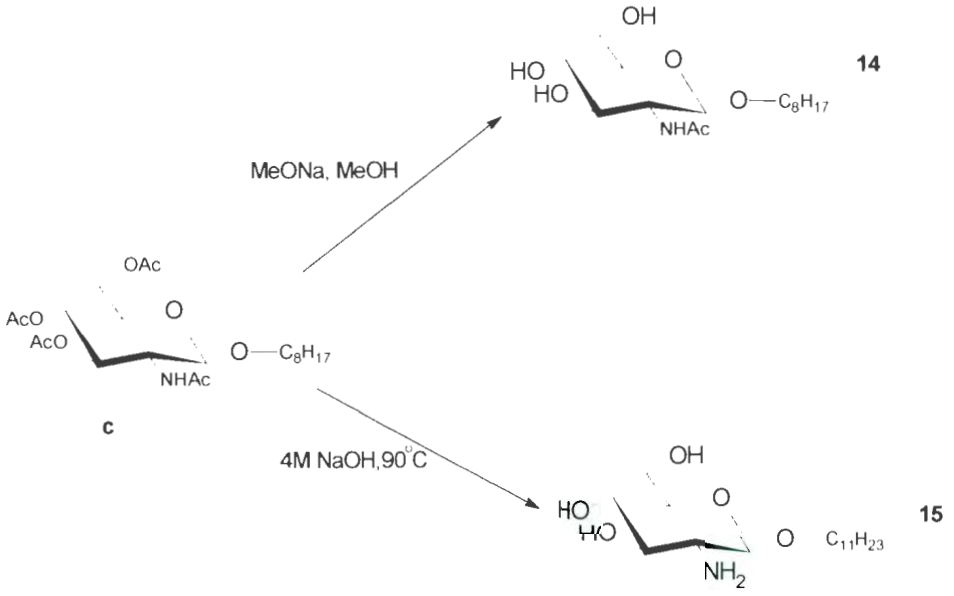

Scheme 2. 3: Deacylation of molecule 12

2.2. Instrument Methods

2.2.1. ESI mass spectrometry

The mass spectra of all neoglycolipids were acquired in the positive ion mode using an Applied Biosystems API-QSTAR XL quadrupole orthogonal time-of-flight (QqToF)-MS/MS hybrid tandem mass spectrometer (Applied Biosystems International-MDS Sciex, Foster City, California, USA). This instrument is capable of analyzing a mass range of *m/z* 5 to 40,000, with a resolution of 10,000 in the positive ion mode. ESI was performed with the Turbo Ionspray source operated at 5.5 kV and a temperature of 100°C. Each neoglycolipid was dissolved in 250 μL of methanol (MeOH) for the injection. The aliquots were infused into the mass spectrometer system using an integrated Harvard syringe pump (Quebec, Canada) at a rate of 5 μL/min. The ToF analyzer was calibrated using a Pep-Tyf protein which was dissolved in a 1:1 mixture of acetonitrile (ACN or CH_3CN)-water (H_2O) and checking for the exact masses of the $[M+H]^+$ at *m/z* 1638.8485 and $[M+H]^{2+}$ at *m/z* 819.9279 .

2.2.2. Low-energy CID-MS/MS

The product ions spectra were obtained from fragmentation in the radio-frequency (RF), linear acceleration pulsar high pressure (LINAC) equipped, quadrupole collision cell of the QqToF-MS/MS hybrid instrument. The collision gas used for MS/MS analyses was nitrogen. The collision energy (CE) and the CID gas conditions ensured that the precursor ion remained abundant. A series of second-generation ESI-CID-QqToF-

MS/MS experiments on the diagnostic product ions was conducted to re-confirm the various established fragmentation routes. These ESI-CID-QqTOF-MS/MS experiments were initiated by CID in the atmospheric pressure/vacuum interface using a higher declustering potential (DP). It was reported in previous research that increasing the DP influenced the ion count, by raising the "in-nozzle" fragmentation of the compound.[23,48,49] In that context, it is emphasized that low energy-collision-induced dissociation (CID) spectra are usually obtained by MS/MS: the parent ion is selected, collided with a neutral gas, and the fragment ion spectrum is recorded.

However, it was recognized very early that collisional dissociation could be induced in the electrospray source by increasing the different acceleration voltages. Different names for this process have been given by users and manufacturers: nozzle-skimmer fragmentation, cone-voltage fragmentation, skimmer-CID, etc.

In the present study, this will be referred to as ''source-CID.'' The disadvantage is that the parent ion is not selected. Rather, all ions emitted by the electrospray source undergo collisional activation, and all the fragments are collected in the same mass spectrum. Source-CID avoids any requirement for real-time data-dependent scanning software, as required for automated MS/MS. A simple ramp of voltages can be applied between the different skimmers and lenses to produce varying amounts of fragments during analyte elution.

2.2.3. Product ion scanning experiments

Tandem mass spectrometry analyses were conducted to determine the fragmentation pathways leading to the formation of the various product ions observed in the conventional mass spectra obtained from each neoglycolipid. These analyses were carried out under low-energy.

For the product ion scan analyses, the first quadrupole (Q_1) selected the corresponding precursor ion and it generated product ions by collision with N_2 gas in the (RF-only) quadrupole (Q_2). The third mass resolving time-of-flight analyzer (ToF) scanned the *m/z* values to determine the occurrence of particular product ions previously formed in the Q_2.

2.2.4. CID-MS^n or *quasi* MS^n analysis

The CID-MS/MS experiments were accomplished by selecting a precursor ion from the previous scan analysis. *Quasi* MS^n product ion scans are initiated by CID in the atmospheric pressure/vacuum interface using a higher declustering potential. It has been assumed that when a first generation product ion, formed by a conventional CID-MS/MS analysis, was selected for a product ion scan analysis, then the analysis of this selected ion was presumed to be a *quasi*-MS^3 analysis, which would be known as a second-generation CID-MS/MS analysis. In this thesis it has been shown, in fact, that a *quasi*-MS^3 or second generation product ion scan conducted with a QqToF-MS/MS hybrid

instrument is similar to a conventional MS^3 experiment conducted with a QIT-MS^n or FT-ICR-MS^n (**Chapter 5**).

2.3. ESI-MS and ESI-MS/MS analyses of the different series of neoglycolipids

2.3.1. Analysis of a new series of 2-acetamido-2-deoxyglycosyl-containing neoglycolipids (1-4)

The gas settings (GS1 and GS2) for the full scan analysis of 8-(cholest-5-en-3-β-yloxy)-3,6-dioxaoctyl-2-acetamido-2-deoxy-β-D-glucopyranoside "**1**" were kept constant at 30 (the flow conversion table is represented in **Appendix 1**), the declustering potential (DP) was 100 V and focusing potential (FP) was 150 V, and the low collision energy varied from 10 to 15 eV. In the case of the cholest-5-en-3-β-yl-2-acetamido-2-deoxy-β-L-glucopyranoside "**2**," the gas settings were the same as those used for **1**; however, the DP was changed to 300 V and the FP to 200 V. For the acquisition of the tandem mass spectrometry data, the DP was changed to 250 V, FP remained the same, and the collision energy was 15 eV.

The full scan settings used for 8-(cholest-5-en-3-β-yloxy)-3,6-dioxaoctyl-2-acetamido-2-deoxy-3-*O*-β-D-galactopyranosyl-α-D-galactopyranoside "**3**" were the same as "**1**," and the collision energy was kept constant at 15eV. Finally the settings used to analyze 11-(cholest-5-en-3-β-yloxy)-3,6,9-trioxaundecyl-α-L-fucopyranoside "**4**" were DP: 300 V, FP: 250 V and CE: 15 eV.

2.3.2. Analysis of a new series of 2-acetamido-2-deoxy-D-glycopyranosyl per-*O*-acetylated neoglycolipids (5-6)

The GS1 and GS2 settings were kept at 30 for both experiments; however, the declustering potential was kept at 100 V for the 8-(cholest-5-en-3-β-yloxy)-3,6-dioxaoctyl-2-acetamido-4,6-di-*O*-acetyl-3-*O*-(2,3,4,6-tetra-*O*-acetyl-β-D-galactopyranosyl)-2-deoxy-α-D-galactopyranoside "**5**" and at 200 V for the cholest-5-en-3-β-yl-2-acetamido-3,4,6-tri-*O*-acetyl-2-deoxy-β-L-glucopyranoside "**6**". The focusing potential was at 100 V for "**5**" and 150 V for "**6**". The collision energy parameters were 15 eV for molecule "**5**" and 10 eV for molecule "**6**".

2.3.3. Analysis of 2-azido-2-deoxy-β-D-galactopyranosyl neoglycolipids (7-8, 11-12)

The settings used to acquire the spectra of the 8-(cholest-5-en-3-β-yloxy)-3,6-dioxaoctyl-3-*O*-(2,3,4,6-tetra-*O*-acetyl-β-D-galactopyranosyl)-2-azido-4,6-*O*-benzylidene-2-deoxy-β-D-galactopyranoside "**7**" and the 8-(cholest-5-en-3-β-yloxy)-3,6-dioxaoctyl-3-*O*-(2,3,4,6-tetra-*O*-acetyl-β-D-galactopyranosyl)-2-azido-2-deoxy-α-D-galactopyranoside "**8**" were kept constant at DP: 100 V, FP: 150 V, DP2: 5 V (changed to 5 and 10, in the case of "**7**"), while CE varied from 10 eV for **8** to 20 eV for **7**. For "**11**" and "**12**", the cell collision energy varied between 10 eV and 15 eV.

2.3.4. Analysis of simple glycolipids (13-15)

The spectra of simple glycolipids **13** to **15** were acquired by keeping the GS1 and GS2 gas settings constant at 30, the temperature at 80°C, the DP at 100 V, FP at 50 V and the CE at 10 eV.

Chapter 3: Analysis of a series of new 2-acetamido-2-deoxy-glycosyl-containing neoglycolipids

Liposomes are often used for drug delivery and transformation or transfection of DNA due to their ability to target cancer cells. In this work, neoglycolipids were studied since they are stabilizing agents for cationic liposomes. The use of cationic liposomes for diagnostic and therapeutic purposes is a novel concept.[50]

Cationic liposomes are considered good gene carriers[51] and are often used in gene therapy for their powerful capacity to condense DNA and their high transgenic expression properties.[52] Although they present a low transfection efficiency[53,54], they have several advantages such as their effectiveness,[55,56] non-toxicity[54] and low immunogenicity.[54,55] There are also other fields that use cationic liposomes (agronomics, marine biotechnology).[57] Their use in cancer therapy has evolved to the second phase of clinical studies.[58,59]

3.1. Free neoglycolipids analysis results

The neoglycolipids in this study contain different mono or disaccharide moieties, namely: 2-acetamido-2-deoxy-3-*O*-β-D-galactopyranosyl-α-D-galactopyranoside in **3**, 2-acetamido-2-deoxy-β-D-glucopyranoside in **1**, 2-acetamido-2-deoxy-β-L-glucopyranoside in **2**, and α-L-fucopyranoside in **4**. The molecules discussed in this chapter are represented in **Figure 2.1**.

3.2. 8-(Cholest-5-en-3-β-yloxy)-3,6-dioxaoctyl-2-acetamido-2-deoxy-β-D-glucopyranoside (1)

In this study a solution of the highly purified neoglycolipid **1** mixed to methanol was introduced by injection into the electrospray ionization source, without any need for prior chromatographic separation. Accordingly, the protonated molecules $[M+H]^+$ and the major fragment ions (formed in-source) obtained with the high resolution QqToF-MS hybrid instrument, were free from any trace-level analytes eluting from an HPLC, together with a lot of matrix background that could give rise to mass multiplets.

3.2.1. QqTOF-MS analysis

The structure of the 8-(cholest-5-en-3-β-yloxy)-3,6-dioxaoctyl-2-acetamido-2-deoxy-β-D-glucopyranoside neoglycolipid allows the observation of fragment ions such as the sodiated $[M+Na]^+$ at *m/z* 744.4780, resulting from the protonated molecule $[M+H]^+$ at *m/z* 722.4983. Conventional analysis of the molecule "**1**" revealed the presence of the 1,2-cyclic sugar oxonium ion $[DGlcNAc]^+$ at *m/z* 204.0851. The cyclic sugar ion is an oxazolinium ion, with a positive charge delocalized on the N-C-O atoms. This sugar oxonium will be referred to as the sugar $[Oxonium]^+$ ion throughout the thesis.

Formation of the expected cholesteryl ion assigned as $[Cholestadiene+H]^+$ was observed at *m/z* 369.3399.

An additional elimination originating from the sugar oxonium ion, the [DGlcNAc-$2H_2O$-CH_3OH]$^+$ was observed *m/z* 138.0450. Eliminations from the protonated molecule were also observed and can be summarized as ions resulting from losses of molecules of water and methanol designated as [M+H-$2H_2O$-CH_3OH]$^+$ at *m/z* 138.0450. Subsequent elimination of molecules of water and ketene was observed for the fragment ion [M+H-$2H_2O$-CH_2CO]$^+$ at *m/z* 126.4294 (**Figure 3.1**). These losses can be either "concerted" or "consecutive" according to Banoub *et al.*[60] Likewise, it should be noted that, in that context, the "concerted" or "consecutive" losses from the different product ions in the MS/MS experiments, simply means that the molecules are both lost at the same time and within the same reaction region of the hybrid tandem mass spectrometer.

It has been presumed that the fragment at *m/z* 572.4106 is the suspected C-glycoside ion-species, which is formed by an ion-molecule complex reaction based on previous work.[5,23]

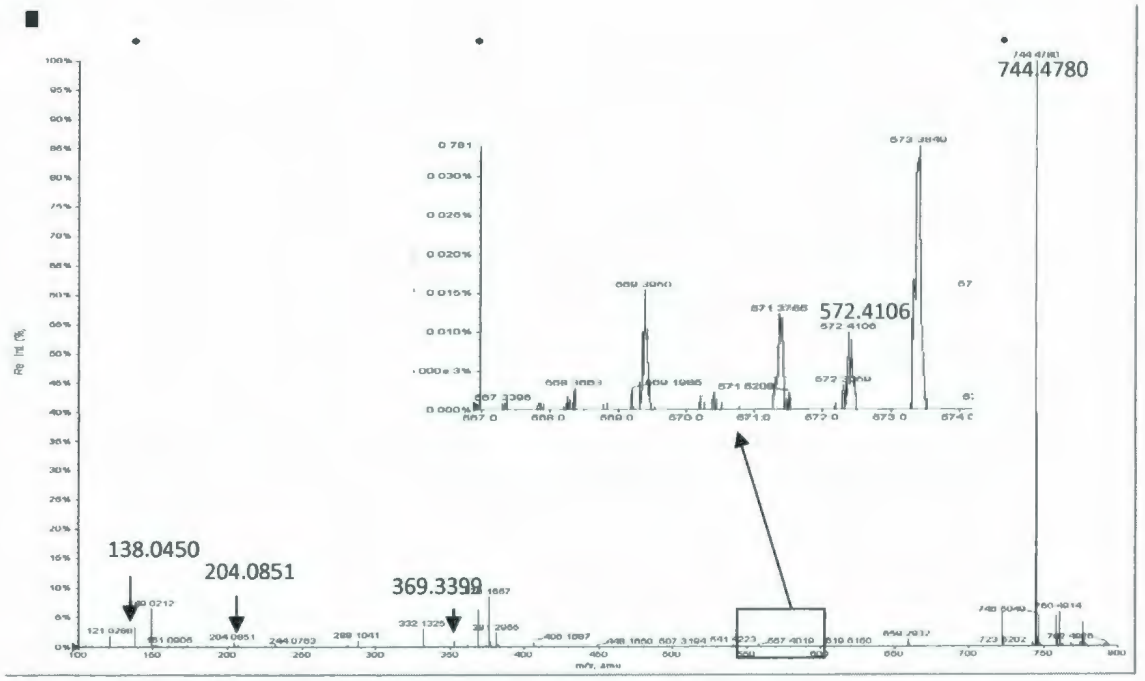

Figure 3.1: Full scan analysis of 8-(cholest-5-en-3-β-yloxy)-3,6-dioxaoctyl-2-acetamido-2-deoxy-β-D-glucopyranoside neoglycolipid-molecule " 1".

3.2.2. CID-MS/MS analysis of the protonated molecule

To confirm the gas-phase fragmentation pathway and the formation of these fragment ions, a low-energy collision tandem mass spectrometric analysis was first performed by selecting the precursor protonated molecule $[M+H]^+$. This MS/MS analysis yielded the expected product ions, which were observed during the full scan ESI-MS analysis (**Figure 3.1**). New product ions $[GlcNAc\text{-}H_2O]^+$ at *m/z* 186.46 and $[GlcNAc\text{-}2H_2O]^+$ at *m/z* 168.44 were observed. It was characterized as being formed by elimination of molecules of water from the GlcNAc oxonium. The *m/z* 288.47 fragment remains unidentified (**Figure 3.2**). The ion suspected to be a C-glycoside ion-species was observed at *m/z* 572.62 at 2.0779% (**Figure 3.2, Table 3.1**).

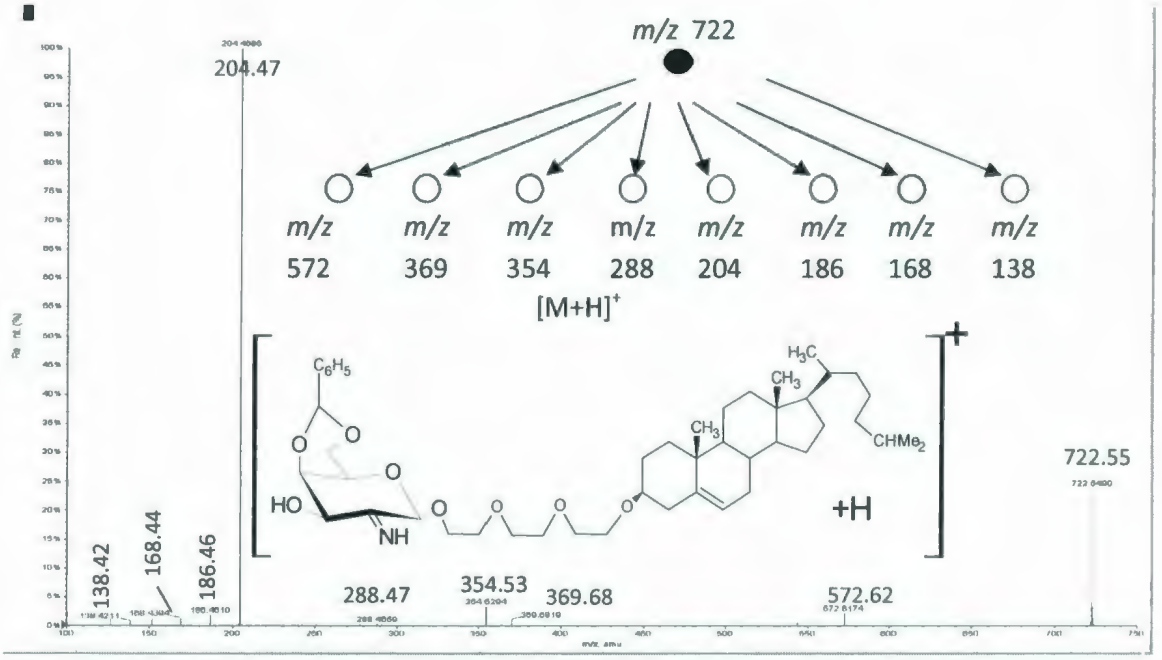

Figure 3.2: CID-MS/MS of the protonated molecule $[M+H]^+$ of (8-(cholest-5-en-3-β-yloxy)-3,6-dioxaoctyl 2-acetamido-2-deoxy-β-D-glucopyranoside), molecule "1", CE=15eV.

Table 3. 1: Relative intensity and *m/z* values obtained for each product ion from the product ion scan (CID-MS/MS) of the protonated molecule of $[M+H]^+$ "1".

Ion	Relative intensity (%)	*m/z*
$[M+H]^+$	23.90	722.55
$[C\text{-glycoside}+H]^+$	2.08	572.62
$[Cholestadiene+H]^+$	1.04	369.68
$[GlcNAcSpacer+H]^+$	3.38	354.53
$[DGlcNAc]^+$	100.00	204.47
$[GlcNAc-H_2O]^+$	1.82	186.46
$[GlcNAc-2H_2O]^+$	1.30	168.44
$[DGlcNAc-2H_2O-CH_3OH]^+$	0.78	138.42

The **Scheme 3.1** proposed a fragmentation pathway of the protonated molecule, issued from the results obtained during the full scan analysis, and the low-energy collision tandem mass spectrum.

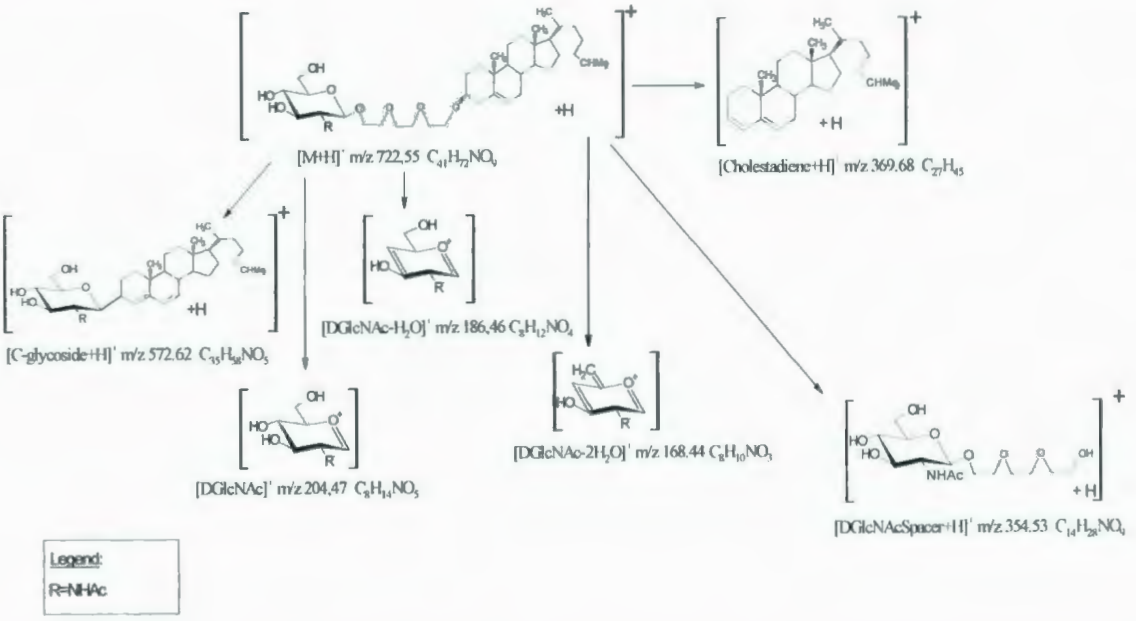

Scheme 3. 1: Proposed fragmentation pathway of 8-(cholest-5-en-3-β-yloxy)-3,6-dioxaoctyl 2-acetamido-2-deoxy-β-D-glucopyranoside, molecule "1"

3.2.3. Formation of a C-glycoside ion-species

The ion suspected to be a C-glycoside ion-species was observed during conventional scan analysis of **1**, as well as during the CID-MS/MS of the protonated molecule. Third-generation tandem mass spectrometry analysis (*quasi*-MS^4) of the ion at *m/z* 572.62 was performed to confirm the structure of this C-glycoside ion-species.

When the collision energy (CE) was set at 10 eV, two ions were observed. These were the $[Cholestadiene+H]^+$ and the $[Oxonium]^+$ ions. However, when the CE was increased to 15 eV, the presence of other ions, in addition to those cited above, were observed, confirming that adjusting the CE affects the abundance of the product ions. In fact, an ion was obtained at *m/z* 556.53, which was assigned as $[C\text{-}glycoside\text{-}CH_3]^+$. This CH_3 radical loss could arise from the NHAc (amino acetyl) group or directly from one of the methyl groups attached to the cholestadiene. The observation of further elimination from the C-glycoside ion-species is actually a new finding. The product ion $[DGlcNAc\text{-}H_2O]^+$, arising from the $[D\text{-}GlcNAc]^+$ by loss of a molecule of water, was noticed at *m/z* 186.47. Finally, ions observed at *m/z* 214.46 and *m/z* 408.41 were not identified (**Figure 3.3**).

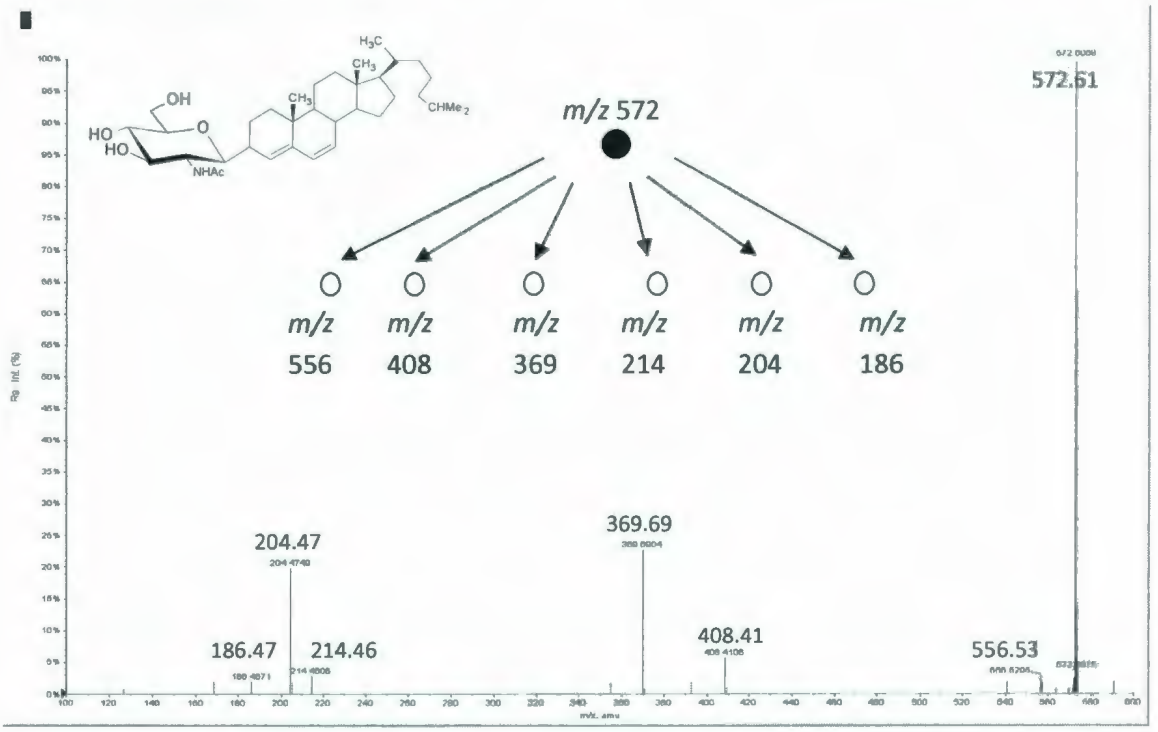

Figure 3.3: *Quasi*-MS^3 of the ion-species $[C\text{-}glycoside+H]^+$ arising from 8-(cholest-5-en-3-β-yloxy)-3,6-dioxaoctyl-2-acetamido-2-deoxy-β-D-glucopyranoside, molecule "1".

3.3. 8-(Cholest-5-en-3-β-yloxy)-3,6-dioxaoctyl-2-acetamido-2-deoxy-3-*O*-β-D-galactopyranosyl-α-D-galactopyranoside (3)

3.3.1. QqTOF-MS analysis

The sodiated molecule $[M+Na]^+$ at *m/z* 906.4690 was observed during the full scan analysis of the 8-(cholest-5-en-3-β-yloxy)-3,6-dioxaoctyl-2-acetamido-2-deoxy-3-*O*-β-D-galactopyranosyl-α-D-galactopyranoside. The $[M+H]^+$ at *m/z* 884.5172 and the $[M+H\text{-DGal}]^+$ at *m/z* 722.6374 were also observed, as were the disaccharide $[Sugar]^+$ moiety at *m/z* 366.5336 and the monosaccharide oxonium commonly known as $[DGalNAc]^+$ oxonium ion at *m/z* 204.5298 observed. The ion at *m/z* 572.6992 was suspected to be a $[C\text{-glycoside+H-DGal}]^+$ ion-species or a $[C\text{-glycoside}\mathbf{2}+H]^+$ ion-species (data not shown).

3.3.2. CID-MS/MS of the protonated molecule

The product ion scan of the $[M+H]^+$ ion confirmed the presence of the ions previously seen in the conventional full scan. Two product ions at *m/z* 330.53 and *m/z* 144.10 were observed and these were assigned as the $[Sugar\text{-}2H_2O]^+$ and $[DGalNAc\text{-}2H_2O\text{-MeOH}]^+$, respectively. These two product ions appeared also as fragment ions during the ESI-MS conventional scan analysis. The presence of the suspected $[C\text{-glycoside+H}]^+$ ion-species at *m/z* 734.61 and the $[C\text{-glycoside+H-DGal}]^+$ ion-species was noted (**Figure 3.4, Table 3.2**). It was realized that the eliminations of the neutrals from these product ions can be either "concerted" or "consecutive" as previously discussed.

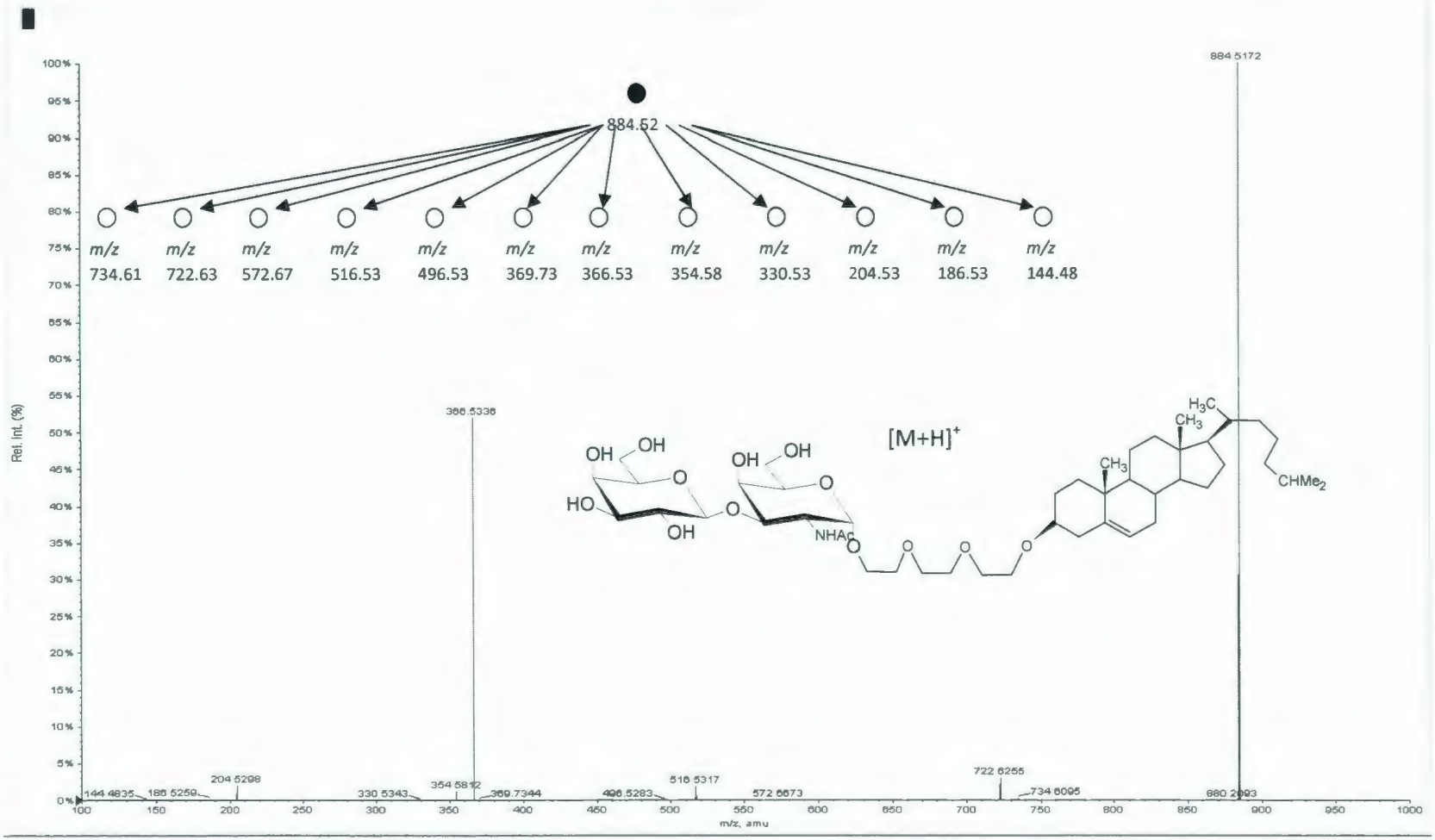

Figure 3.4: CID-MS/MS of the protonated molecule $[M+H]^+$ of the 8-(cholest-5-en-3-β-yloxy)-3,6-dioxaoctyl-2-acetamido-2-deoxy-3-*O*-β-D-galactopyranosyl-α-D-galactopyranoside, molecule"3".

Table 3. 2: Relative intensity and *m/z* values of the different product ions derived from the CID-MS/MS analysis of the 8-(cholest-5-en-3-β-yloxy)-3,6-dioxaoctyl-2-acetamido-2-deoxy-3-*O*-β-D-galactopyranosyl-α-D-galactopyranoside, molecule "3".

Ion	Relative intensity (%)	*m/z*
$[M+H]^+$	92.52	884.52
$[C\text{-glycoside}+H]^+$	2.49	734.61
$[M+H\text{-DGal}]^+$	6.73	722.63
$[C\text{-glycoside}+H\text{-DGal}]^+$	0.50	572.67
$[SugarSpacer]^+$	5.99	516.53
$[Cholestadiene+H]^+$	0.25	369.73
$[Sugar]^+$	100.00	366.53
$[OxoniumSpacer]^+$	3.99	354.58
$[Oxonium]^+$	7.23	204.53
$[Oxonium\text{-}H_2O]^+$	1.50	186.53

Scheme 3.2 below represents the possible fragmentation pathway of the protonated molecule $[M+H]^+$ focuses on the results obtained during the full scan analysis, as well as the results from the tandem mass spectrometry analysis.

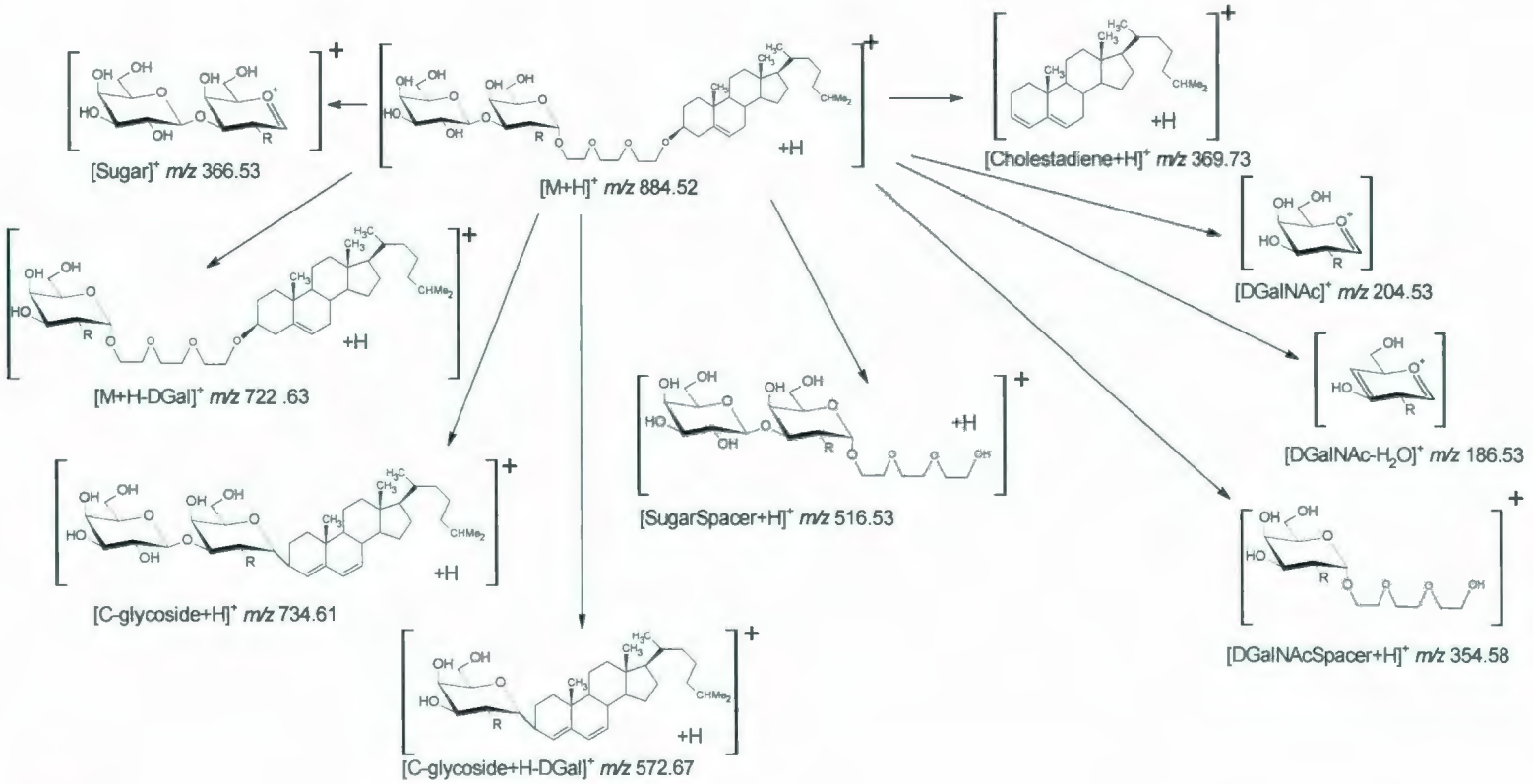

Legend :

R=NHAc

Scheme 3. 2: Proposed fragmentation pathway of the 8-(cholest-5-en-3-β-yloxy)-3,6-dioxaoctyl-2-acetamido-2-deoxy-3-*O*-β-D-galactopyranosyl-α-D-galactopyranoside, molecule "3".

3.3.3. Formation of the $[C\text{-glycoside}]^+$ and $[C\text{-glycoside+H-DGal}]^+$ ion-species

The second-generation tandem mass spectrometry analysis or *quasi*-MS^3 of the precursor $[C\text{-glycoside+H}]^+$ ion-species at m/z 734.61 was performed under the same conditions as the low-energy collision tandem mass spectrometry of the protonated molecule $[M+H]^+$. Therefore the precursor ion at m/z 734.61 produced the $[GlcNAc]^+$ oxonium at m/z 204.52 and the $[Cholestadiene+H]^+$ at m/z 369.74. An additional product ion was formed at m/z 186.51 resulting from the loss of water from the sugar oxonium ion at m/z 204.52. Additional eliminations from the sugar oxonium ion have been initially reported for another series of neoglycolipids.[23] Note that two other ions were also seen at m/z 375.64 and m/z 244.57. These were respectively assigned as $[Cholestadiene+CH_3]^+$ and $[DGalNAc+C_3H_3+H]^+$ ions (**Figure 3.5**).

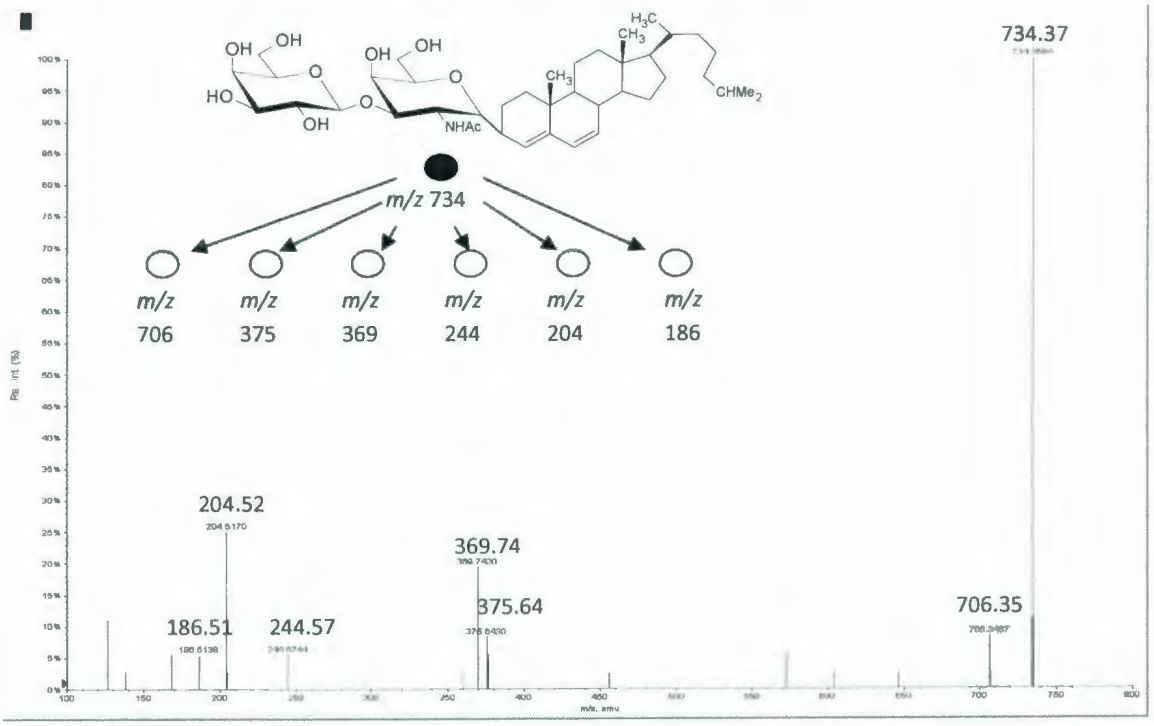

Figure 3.5: Second-generation tandem mass spectrometry or *quasi*-MS^3 of *m/z* 734.37, of the 8-(cholest-5-en-3-β-yloxy)-3,6-dioxaoctyl-2-acetamido-2-deoxy-3-*O*-β-D-galactopyranosyl-α-D-galactopyranoside, molecule "3".

It is interesting to note that another type of C-glycoside ion-species at *m/z* 572.67 was formed in this analysis. This was assigned as the new [C-glycoside+H-DGal]$^+$ ion-species, which was present during the conventional full scan and the CID-MS/MS of the protonated molecule. However, this ion was not present in the CID-MS/MS of the [C-glycoside]$^+$ ion-species.

The ion suspected to be a [C-glycoside+H-DGal]$^+$ ion-species, observed at *m/z* 572.67, was isolated in a second-generation, or *quasi*-MS^3 experiment, to observe its fragmentation and confirm its structure. Keeping the same parameters as before, it

fragmented to give the main product $[GlcNAc]^+$ oxonium ion at *m/z* 204.52 and also the $[Cholestadiene+H]^+$ product ion at *m/z* 369.75 (**Figure 3.6**).

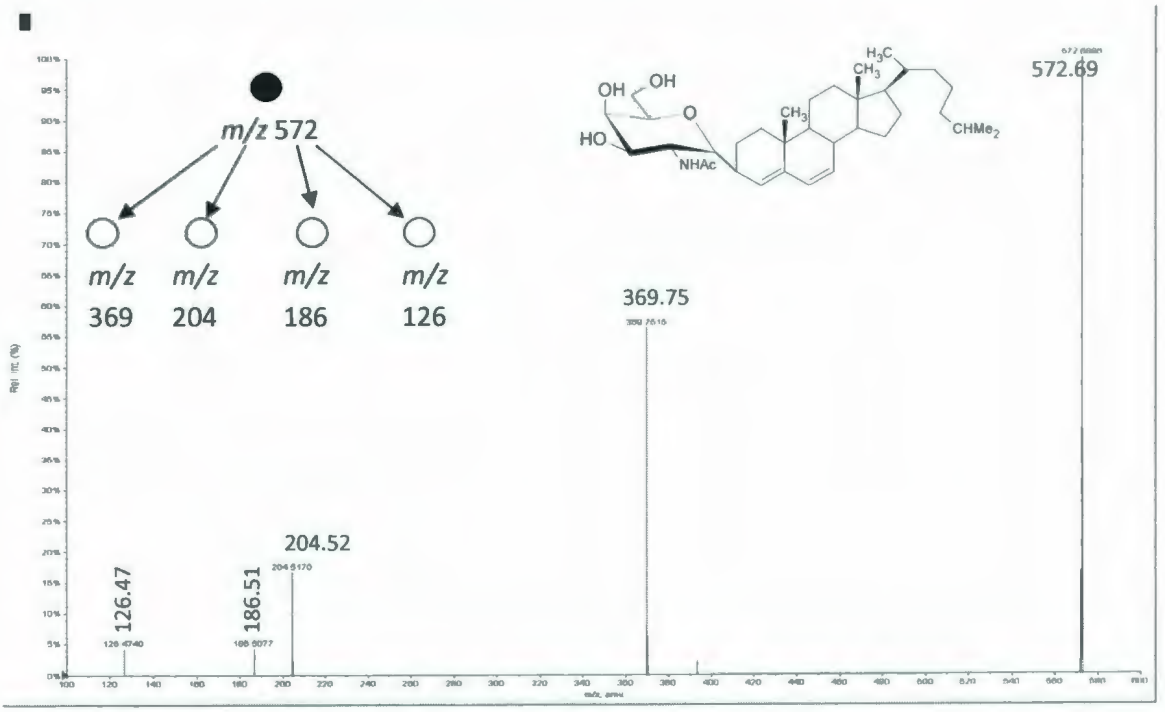

Figure 3.6: Second-generation mass spectrometry analysis or *quasi*-MS^3 of the *m/z* 572, product ion derived from the 8-(cholest-5-en-3-β-yloxy)-3,6-dioxaoctyl-2-acetamido-2-deoxy-3-*O*-β-D-galactopyranosyl-α-D-galactopyranoside, molecule "3".

Use of X_0 naming follows the work presented by Domon and Costello[61] represented in **Figure 3.7**.

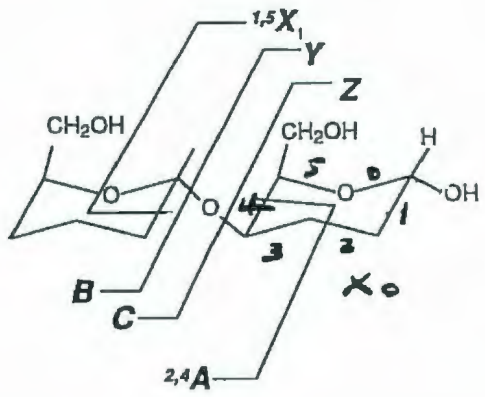

Figure 3.7: Probable fragmentations occurring for disaccharides[61]

Elimination from the product $[DGalNAc]^+$ oxonium ion, during the *quasi*-MS^3, gave the product ions $[DGalNAc\text{-}H_2O]^+$ at *m/z* 186.51 and $[DGalNAc\text{-}H_2O\text{-}^{2,4}X_0]^+$ at *m/z* 126.47 (**Figure 3.6**). This spectrum helped to confirm the structure of the [C-glycoside+H -DGal]$^+$ ion-species, which occurs due to an ion-molecule reaction occurring between the $[DGalNAc]^+$ oxonium and the $[Cholestadiene+H]^+$. The appearance of a second C-glycoside ion-species derived from a disaccharide neoglycolipid derivative was not previously observed.

The fact that the [C-glycoside+H-DGal]$^+$ ion-species was not observed in the second-generation tandem mass spectrometry analysis or *quasi*-MS^3 of the [C-glycoside+H]$^+$ ion-species, but was observed in the conventional scan and in the tandem mass spectrometry analysis of $[M+H]^+$ at *m/z* 884.52, suggests that the [C-glycoside+H-DGal]$^+$ ion-species might originate directly from the $[M+H]^+$ and $[M+H\text{-}DGal]^+$. It might be formed due to consecutive reactions occurring at the same time.

3.4. 11-(Cholest-5-en-3-β-yloxy)-3,6,9-trioxaundecyl-α-L-fucopyranoside (4)

Based on work previously done in this laboratory,[23] it was determined that the neoglycolipids that contain a fucosyl residue of the carbohydrate moiety were not able to form the $[C\text{-glycoside}+H]^+$ ion-species. In the novel series of free-neoglycolipids, there was indeed a fucosyl compound, namely 11-(cholest-5-en-3-β-yloxy)-3,6,9-trioxaundecyl-α-L-fucopyranoside. Tandem mass spectrometry of this molecule revealed the basic constituent product ions arising from the protonated molecule $[M+H]^+$ ion at *m/z* 709.0623 and no evidence of formation of the C-glycoside ion-species around *m/z* 576 **(Figure 3.8)**.

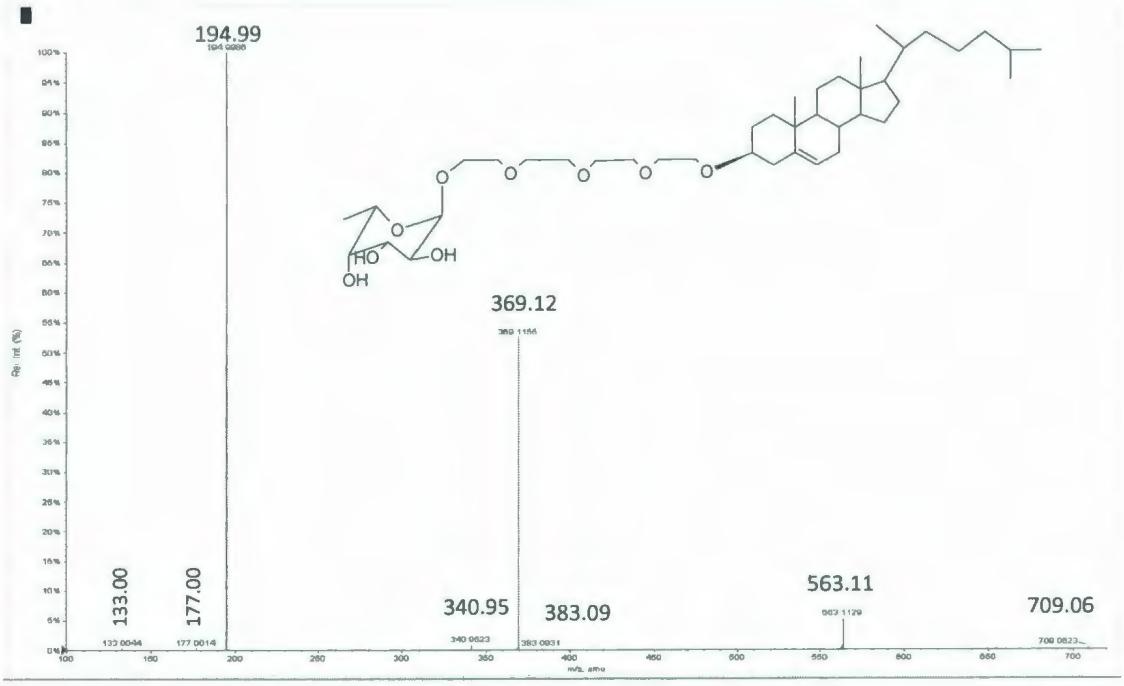

Figure 3.8: Tandem mass spectrum of the 11-(cholest-5-en-3-β-yloxy)-3,6,9-trioxaundecyl-α-L-fucopyranoside (molecule "4") protonated molecule $[M+H]^+$ at *m/z* 709.06 by ESI-QqTOF-MS/MS.

It should be noted that the sample was dissolved in MeOH, and formic acid was added to promote the formation of the protonated molecule at *m/z* 709.06 in the conventional ESI-QqTOF-MS. The presence of several fragment ions such as $[Cholestadiene+H]^+$ at *m/z* 369.12, and $[Fucose\text{-}CH_3OH]^+$ at *m/z* 133.00 were also noted. It should be noted that it is possible for the neoglycolipid to fragment at the spacer end producing the $[CholestadieneSpacer+H]^+$ ion at *m/z* 563.11 and the $[FucoseSpacer]^+$ ion at *m/z* 340.95. As expected, no $[C\text{-}glycoside+H]^+$ ion-species formation was observed at *m/z* 516, confirming the original hypothesis of a similar fucosyl containing neoglycolipid.[23] This confirms the original observation that any neoglycolipid cholesteryl possessing a free-carbohydrate lacking the 2-deoxy-2-acetamido or 2-deoxy-2-amino-group at position *C*-2, could not produce the $[C\text{-}glycoside]^+$ ion-species.[23] The following figure represents the ions obtained from the molecule after ionization (**Scheme 3.3**).

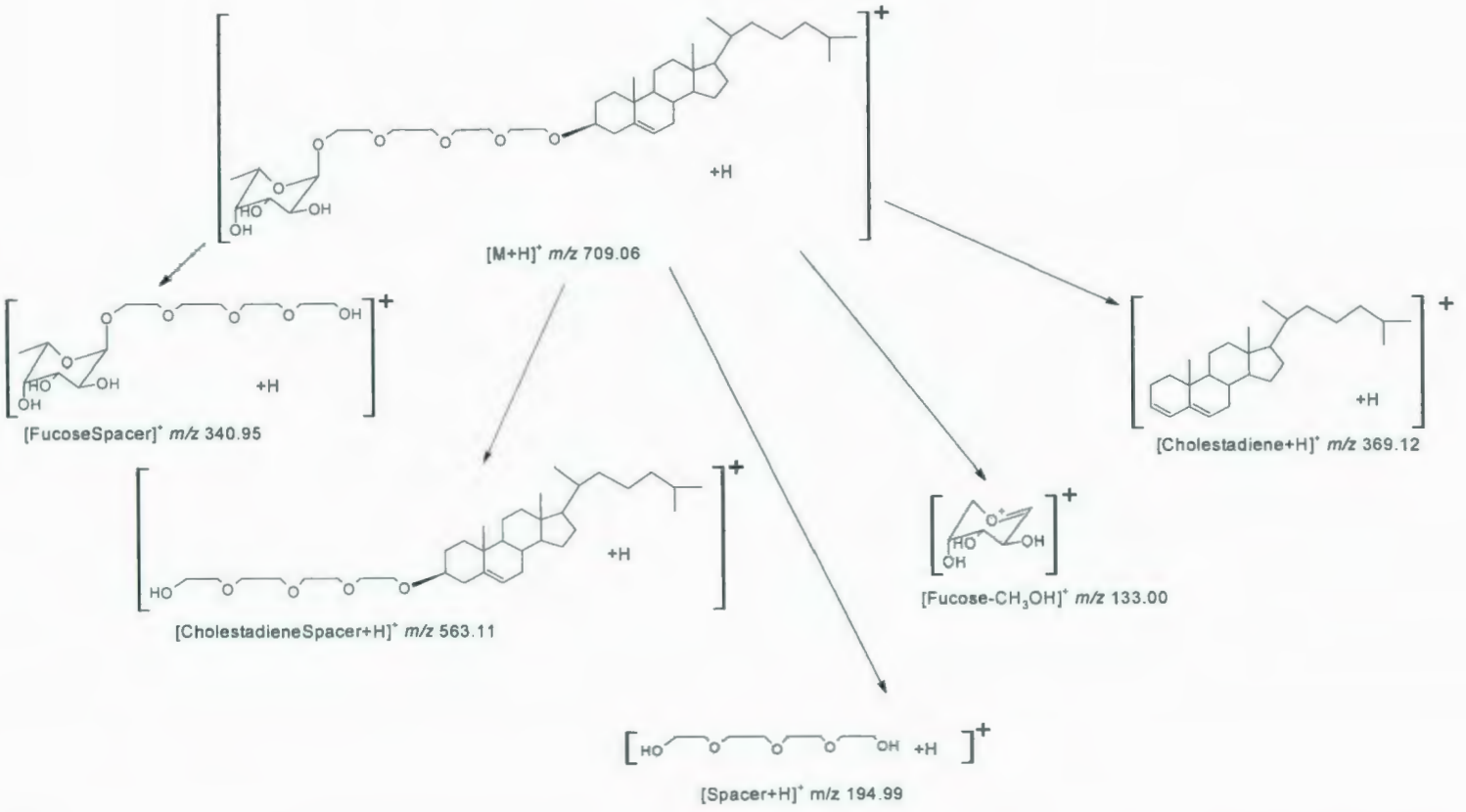

Scheme 3. 3: Ions resulting from the tandem mass spectrometry of the protonated molecule 11-(cholest-5-en-3-β-yloxy)-3,6,9-trioxaundecyl-α-L-fucopyranoside (molecule "4") $[M+H]^+$.

3.5. Discussion

In the conventional ESI-MS of compounds **1** and **3**, the formation of the corresponding protonated molecules was always observed, as well as the expected fragment ions produced from the protonated molecules. In addition, the formation of the $[C\text{-glycoside}+H]^+$ ion-species, the respective $[Oxonium]^+$ ion, and the $[Cholestadiene+H]^+$ ion were also observed.

The $[C\text{-glycoside}+H]^+$ ion-species was as well observed in the CID-MS/MS analyses during low-energy collision dissociation in the collision cell of the tandem mass spectrometer.

Its isolation by a *quasi*-MS^3 allowed its structure to be verified. The formation of both individual product ions: the 1,2-oxazolinium ion and the cholesta-3,5-diene ion was noted and confirmed the structure of the $[C\text{-glycoside}+H]^+$ ion-species formed by an intramolecular ion-molecule complex reaction . This dual formation can be explained by the fact that during the CID-MS/MS process, two competitive mechanisms occur, as described in **Chapter 1**.

Therefore for a short period of time, these product ions and neutral molecules are all present in the collision cell as part of the complex transition state, which breaks down by an intramolecular mechanism to form the $[C\text{-glycoside}+H]^+$ ion-species .

Molecular modeling based on thermodynamic parameters (proton affinities) is normally used to determine which type of complexation can happen, prior to the CID-

fragmentation. In this case, such modeling between the 1,2-oxazolinium and the neutral cholesta-3,5-diene was not performed. However, even if theoretical thermodynamic calculations (such as the multiconfigurational self-consistent field theory, coupled cluster theory and two density-functional theory-based methods)[62] were used, the results obtained compared to the theoretical calculations should conclude that the breakdown of the activated ion molecule complex break down by an internal 'intramechanism" with consecutive elimination of the spacer molecule.[63,64]

Nevertheless, it has been postulated that the sugar oxazolinium ion is thermodynamically favored for the protonation site[64] over the cholestadiene. This oxazolinium ion can form a pseudo ionic bond with the neutral conjugated cholesta-3,5-diene, which results in the complexation. It should be further noted that the occurrence of such complexation has been identified using other samples and various mass spectrometers such as CI-MS/MS,[64] ESI-MS/MS,[65,66] ion trap-MS/MS[67] and triple quadrupole-MS/MS.[65]

The formation of the $[C\text{-glycoside}]^+$ ion-species appears to be dependent on the concentration of the sample, the declustering potential and the focusing potential. Previous research shows that the ion-molecule reaction can also be influenced by the temperature.[67]

In conclusion, it is tentatively presumed that the ion-molecule reaction can occur by intramolecular mechanism between the positively charged $[1,2\text{-cyclic oxazolinium}]^+$

and the neutral molecule of cholesta-3,5-diene as part of the activated ion-molecule complex.

In this case study, it was interesting to note the formation of two types of related $[C\text{-glycoside}+H]^+$ ion-species for the disaccharide compound 8-(cholest-5-en-3-β-yloxy)-3,6-dioxaoctyl-2-acetamido-2-deoxy-3-*O*-β-D-galactopyranosyl-α-D-galactopyranoside **3**. The disaccharide $[C\text{-glycoside}+H]^+$ ion-species was formed, as expected, between the 1,2-oxazolinium ion and the neutral cholesta-3,5-diene. It also showed a complex fragmentation, where some product ions have not been determined yet, but could result from direct elimination from the C-glycoside ion-species. In addition, the $[C\text{-glycoside}+H\text{-DGal}]^+$ ion-species was also formed by elimination of the non-reducing end galactopyranosyl moiety from the disaccharide glycosyl portion of the protonated molecule $[M+H]^+$. The formation of this $[C\text{-glycoside-DGal}+H]^+$ ion-species rationalized from an ion-molecule reaction between the $[GalNAc]^+$ monosaccharide 1,2-oxazolinium and the neutral cholesta-3,5-diene. The monosaccharide $[GalNAc]^+$ 1,2-oxazolinium ion is formed by cleavage of a β-D-galactopyranosyl residue from the disaccharide portion.

Therefore, the CID-MS/MS of the protonated molecule **3** allows the structural elucidation of the disaccharide neoglycolipid into two different ions species such as the $[C\text{-glycoside}+H]^+$ and the $[C\text{-glycoside-DGal}]^+$ (**Scheme 3.4**).

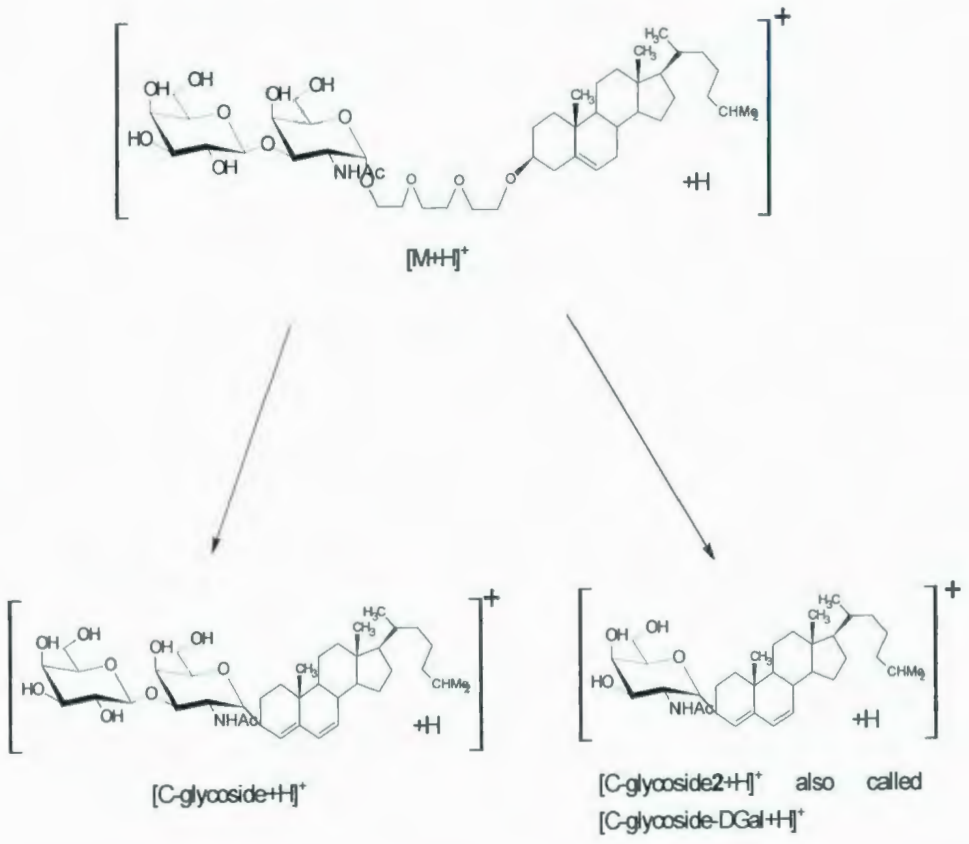

Scheme 3. 4: Representation of the two different [C-glycoside]$^+$ ion-species issued from the protonated molecule 8-(cholest-5-en-3-β-yloxy)-3,6-dioxaoctyl-2-acetamido-2-deoxy-3-*O*-β-D-galactopyranosyl-α-D-galactopyranoside (molecule"3").

Note that the ions species [C-glycoside+H]$^+$ and [C-glycoside+H-DGal]$^+$ were produced from the disaccharide protonated molecule. However, the ion-species [C-glycoside+H-DGal]$^+$ was also formed from the *quasi*-MS^3 of the [M+H-DGal]$^+$ ion. Finally, this discovery was new in the field of neoglycolipid studies forming a potential C-glycoside ion-species.

Previous work has shown that the fucose glycolipid cannot rearrange after fragmentation, to give a [C-glycoside+H]$^+$ ion-species.[23] This was proven to be correct

for the ESI-QqTOF-MS and CID-QqTOF-MS/MS of the compound 11-(cholest-5-en-3-β-yloxy)-3,6,9-trioxaundecyl-α-L-fucopyranoside **4**.

In conclusion, the ESI-MS and MS/MS studies of the fucose glycolipid **4** and the series of the mono- or disaccharides containing the 2-*N*-acetamido or 2-amino-2-deoxy sugars allowed the verification of the requirement of the *N*-acetyl group or the amino group portion of the analyzed glycolipid, to allow the reaction between the neutral cholesta-3,5-diene and the 1,2-cyclic-oxazolinium ion to produce an ion-species such as $[C\text{-glycoside+H}]^+$.

Chapter 4: 2-Acetamido-2-deoxy-D-glycopyranosyl per-O-acetylated neoglycolipids

A new series of per-*O*-acetylated compounds (**Figure 2.3**) containing the α-D-glycopyranosyl and disaccharide containing the GlcNAc residue was used to confirm by ESI-QqToF-MS/MS analyses, that these per-*O*-acetylated neoglycolipids did not form the $[C\text{-glycoside}+H]^+$ ion-species during the fragmentation of the precursor protonated molecules obtained, as indicated earlier,[5,23] and in **Chapter 3**.

4.1. Mass spectrometric analyses of the 2-acetamido-2-deoxy-D-glycopyranosyl per-*O*-acetylated neoglycolipids

4.2. 8-(Cholest-5-en-3-β-yloxy)-3,6-dioxaoctyl-2-acetamido-4,6-di-*O*-acetyl-3-*O*-(2,3,4,6-tetra-*O*-acetyl-β-D-galactopyranosyl)-2-deoxy-α-D-galactopyranose (5)

4.2.1. Qq-TOF analysis

The full scan ESI-MS analysis of the molecule **5** gave the $[M+H]^+$ ion at *m/z* 1136.2500, the fragment $[DGalDGalNAcSpacer]^+$ ion at *m/z* 768.3224, the disaccharide [Gal1→GlcNAc4] oxonium ion at *m/z* 618.3637, the $[Cholestadiene+H]^+$ ion at *m/z* 369.6991 and the monosaccharide $[DGal]^+$ oxonium ion at *m/z* 331.4733. Additional eliminations from the $[DGal]^+$ oxonium ion were observed at *m/z* 169.4484 and *m/z* 150.4247. They were assigned as $[DGal\text{-}2AcOH\text{-}CH_2CO]^+$ and $[DGalNAc\text{-}H_2O\text{-}2AcOH]^+$, respectively resulting from consecutive losses of acetic acid and ketene

(CH_2CO) molecules or by the losses of water and acetic acid. Such acetic acid and ketene losses were previously reported[60] with carbohydrates present in lipid A obtained from a lipopolysaccharide. Interestingly, the monosaccharide oxonium ion $[DGalNAc]^+$ derived from the dissacharide was noticed at *m/z* 288.4927, which suggests a few possibilities for the fragment ion at *m/z* 169.4484, which could also be a $[DGalNAc+H-2AcOH]^+$ obtained from elimination of acetic acid. It appears that for the per-*O*-acetylated neoglycolipids, the elimination of the molecules of acetic acid and ketene more likely blocks the formation of the 1,2-cyclic oxonium ion (**Figure 4.1**), which in that case is not formed and hence fails to react with the cholestadiene.

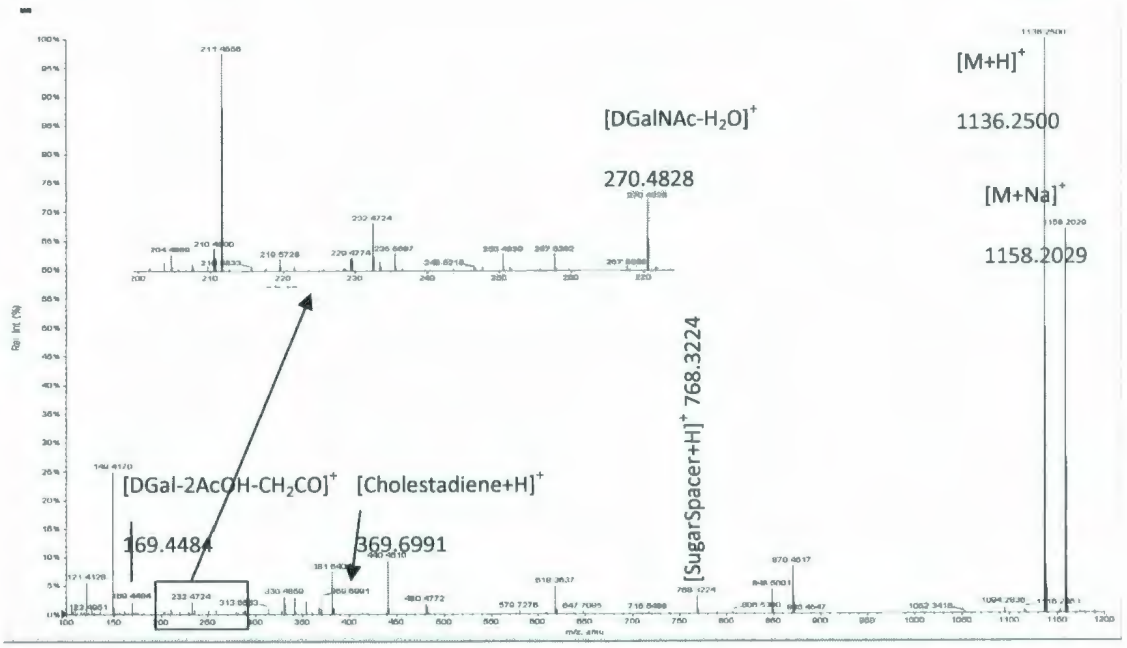

Figure 4.1: Full scan spectrum of 8-(cholest-5-en-3-β-yloxy)-3,6-dioxaoctyl 2-acetamido-4,6-di-*O*-acetyl-3-*O*-(2,3,4,6-tetra-*O*-acetyl-β-D-galactopyranosyl)-2-deoxy-α-D-galactopyranose, molecule "5".

There was no ion observed at *m/z* 985.5999, whereas there would have been if a $[C\text{-glycoside+H}]^+$ ion-species had been present.

4.2.2. CID-MS/MS analysis of the protonated molecule

A CID-MS/MS of the $[M+H]^+$ precursor ion at *m/z* 1136.25 was performed, and indicated that the protonated molecule $[M+H]^+$ at *m/z* 1136.27 generates, as expected, the product ion $[DGalDGalNAcSpacer+H]^+$ at *m/z* 768.32, the $[DGalDGalNAc]^+$ at *m/z* 618.36 and also the $[Cholestadiene+H]^+$ at *m/z* 369.69. The monosaccharide non-reducing end oxonium $[DGal]^+$ at *m/z* 331.47 and the reducing end of the disaccharide $[DGalNAc]^+$ at *m/z* 288.48 were also noticed (**Figure 4.2**).

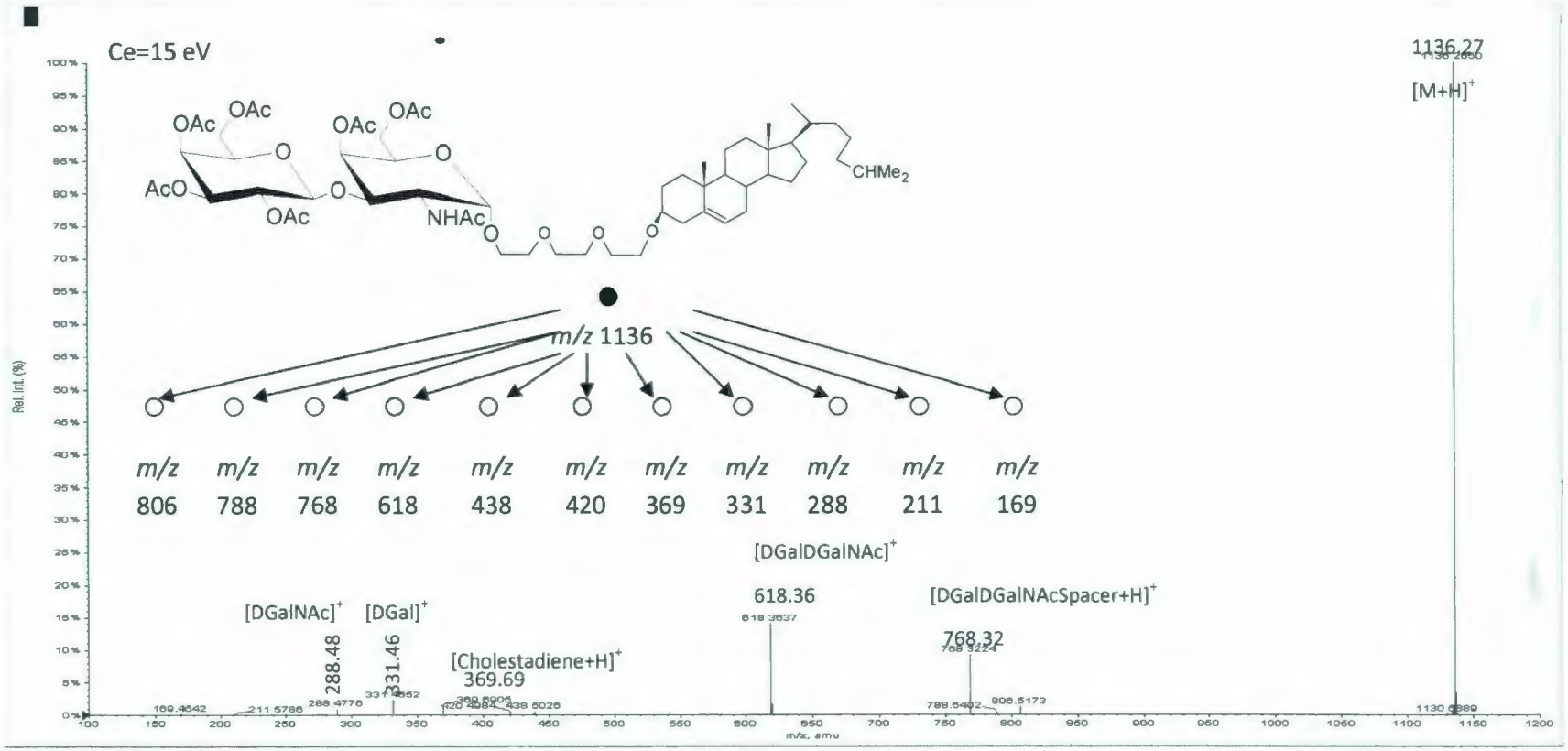

Figure 4.2: CID-MS/MS of the protonated molecule 8-(cholest-5-en-3-β-yloxy)-3,6-dioxaoctyl 2-acetamido-4,6-di-*O*-acetyl-3-*O*-(2,3,4,6-tetra-*O*-acetyl-β-D-galactopyranosyl)-2-deoxy-α-D-galactopyranose $[M+H]^+$ at *m/z* 1136.27, molecule "5".

4.2.3. CID-MS/MS of the sugar-spacer and the sugar

The CID-MS/MS of the ions $[DGalDGalNAcSpacer]^+$ at *m/z* 768.32 and the $[DGalDGalNAc]^+$ at *m/z* 618.36 were performed using second-generation product ion scans (data not shown). The product ion $[DGalNAc\text{-}H_2O]^+$ at *m/z* 270.49, for both preselected analyzed ions could be observed. The $[DGalNAc\text{-}H_2O\text{-}AcOH]^+$ product ion at *m/z* 210.47 and the $[DGalNAc\text{-}2AcOH\text{-}H_2O]^+$ product ion at *m/z* 150.47 were also noticed during the *quasi*-MS^3 of the $[DGalDGalNAc]^+$ oxonium ion. It was previously found that product ions arising from consecutive or concerted losses of acetic acid and water, happened at the same time and in same region of reaction in a hybrid tandem mass spectrometer.[60] During the CID-MS/MS analysis of the $[DGalDGalNAc]^+$ oxonium ion, elimination of the two product oxonium ions $[DGal]^+$ and $[DGalNAc]^+$ was observed. The CID-MS/MS analyses of the sugar moiety permitted us to obtain a precise fingerprint of molecule **5**. In fact, it was observed, during the acquisition of the full scan that two possible ions could be issued from both saccharides at *m/z* 169. This ion was also present during the CID-MS/MS of $[M+H]^+$. In addition, it was observed that the *O*-acetylated groups protect the molecule and appeared to be difficult to break in one step. This phenomenon is applicable to the protonated molecule as well as for the carbohydrate moieties. **Scheme 4.1** represents all the conclusions derived from the results obtained during conventional, CID-MS/MS analyses of the 8-(cholest-5-en-3-β-yloxy)-3,6-dioxaoctyl-2-acetamido-4,6-di-*O*-acetyl-3-*O*-(2,3,4,6-tetra-*O*-acetyl-β-D-galactopyranosyl)-2-deoxy-α-D-galactopyranose (**5**) and CID-MS/MS analyses of its product ions.

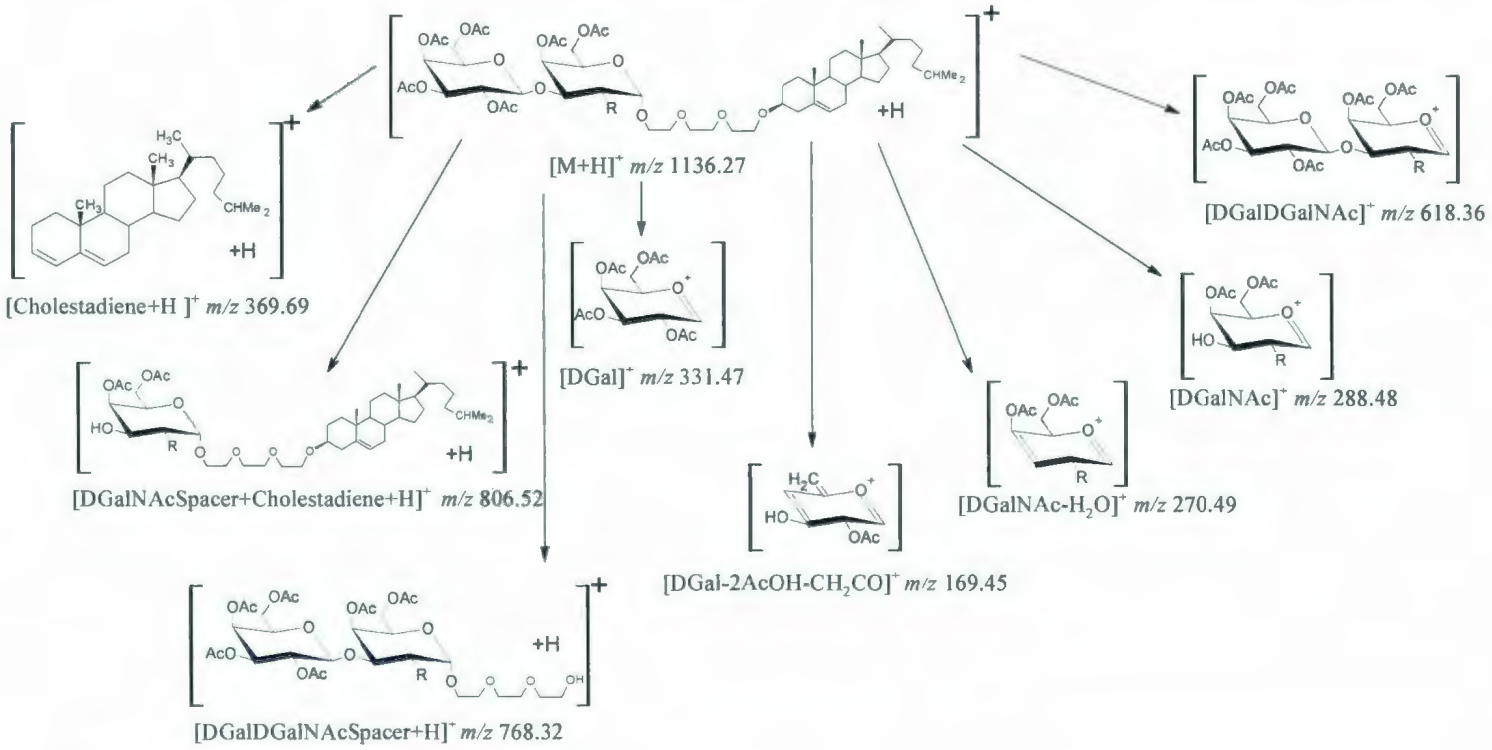

Scheme 4. 1: Proposed fragmentation pathway of 8-(cholest-5-en-3-β-yloxy)-3,6-dioxaoctyl-2-acetamido-4,6-di-*O*-acetyl-3-*O*-(2,3,4,6-tetra-*O*-acetyl-β-D-galactopyranosyl)-2-deoxy-α-D-galactopyranose, molecule "5".

4.3. Cholest-5-en-3-β-yl-2-acetamido-3,4,6-tri-*O*-acetyl-2-deoxy-β-L-glucopyranoside (6)

4.3.1. QqTOF-MS analysis

In the conventional full scan ESI-MS analysis, the presence of the sodiated molecule $[M+Na]^+$ at *m/z* 738.5098 and also the presence of the protonated molecule $[M+H]^+$ at *m/z* 716.5520 was found, in addition to the fragment ion **A** $[Cholestadiene+H]^+$ at *m/z* 369.7110, and the $\mathbf{B_1}$ $[LGlcNAc]^+$, or $[Oxonium]^+$ ion at *m/z* 330.4962, and its derivatives (**Figure 4.3**).

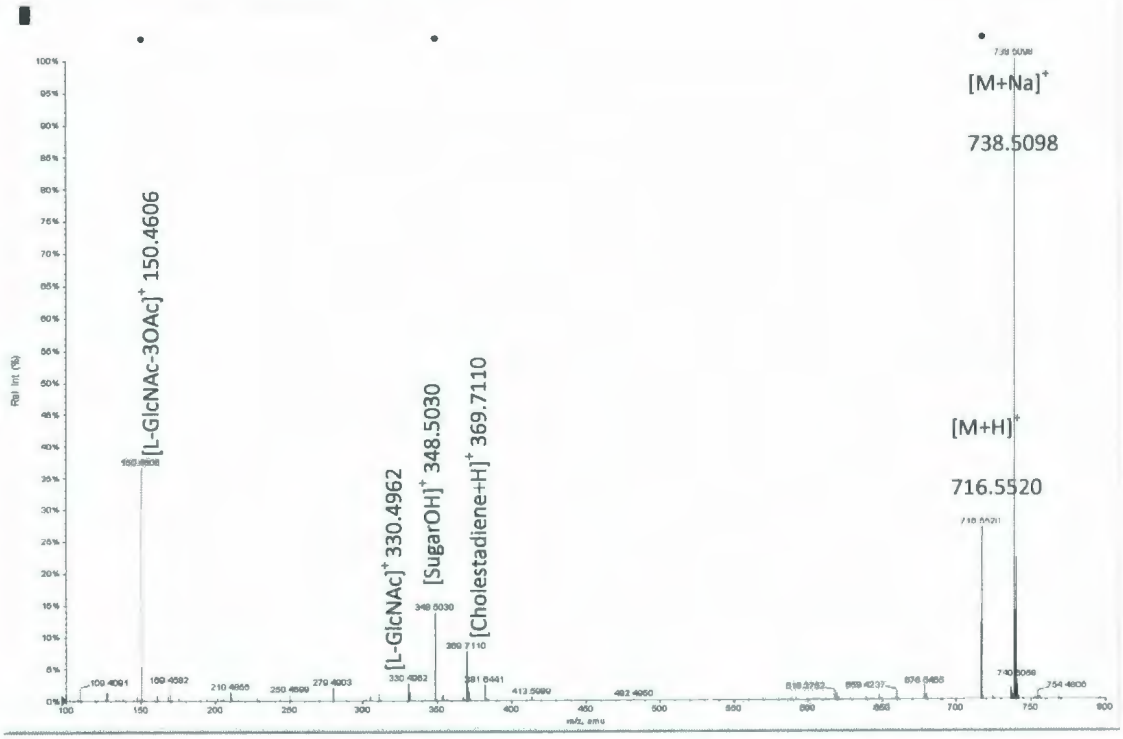

Figure 4.3: ESI-MS of the cholest-5-en-3-β-yl-2-acetamido-3,4,6-tri-*O*-acetyl-2-deoxy-β-L-glucopyranoside, molecule "6".

4.3.2. CID-MS/MS analysis of the protonated molecule

The low-energy CID-QqToF-MS/MS of the selected product ion $[M+H]^+$ at *m/z* 716.55 resulted in the formation of the product ions: $[Cholestadiene+H]^+$ **A** at *m/z* 369.72, the $[SugarOH]^+$ **B** (also called the $[Oxonium+H_2O]^+$ ion), at *m/z* 348.49; and the oxonium $[L\text{-}GlcNAc]^+$ $\mathbf{B_1}$ at *m/z* 330.50. The *O*-acetylated product oxonium ion $[L\text{-}GlcNAc]^+$ $\mathbf{B_1}$ fragmented into the product ions $[Oxonium\text{-}AcOH]^+$ $\mathbf{B_3}$ at *m/z* 270.51, $[Oxonium\text{-}2AcOH]^+$ $\mathbf{B_5}$ at *m/z* 210.49, or $[Oxonium\text{-}3AcOH]^+$ $\mathbf{B_7}$ at *m/z* 150.45 from the product ion $[M+H]^+$. By changing the collision energy from 10 to 15 eV during the CID-MS/MS of the protonated molecule $[M+H]^+$, two new product ions could be detected, presumably that of $[M+H\text{-}2AcOH]^+$ at *m/z* 596.60 and $[Oxonium\text{-}CH_2CO]^+$ $\mathbf{B_2}$ at *m/z* 288.51 (**Figure 4.4**). As previously stated, raising the collision energy results in the formation of more product ions.

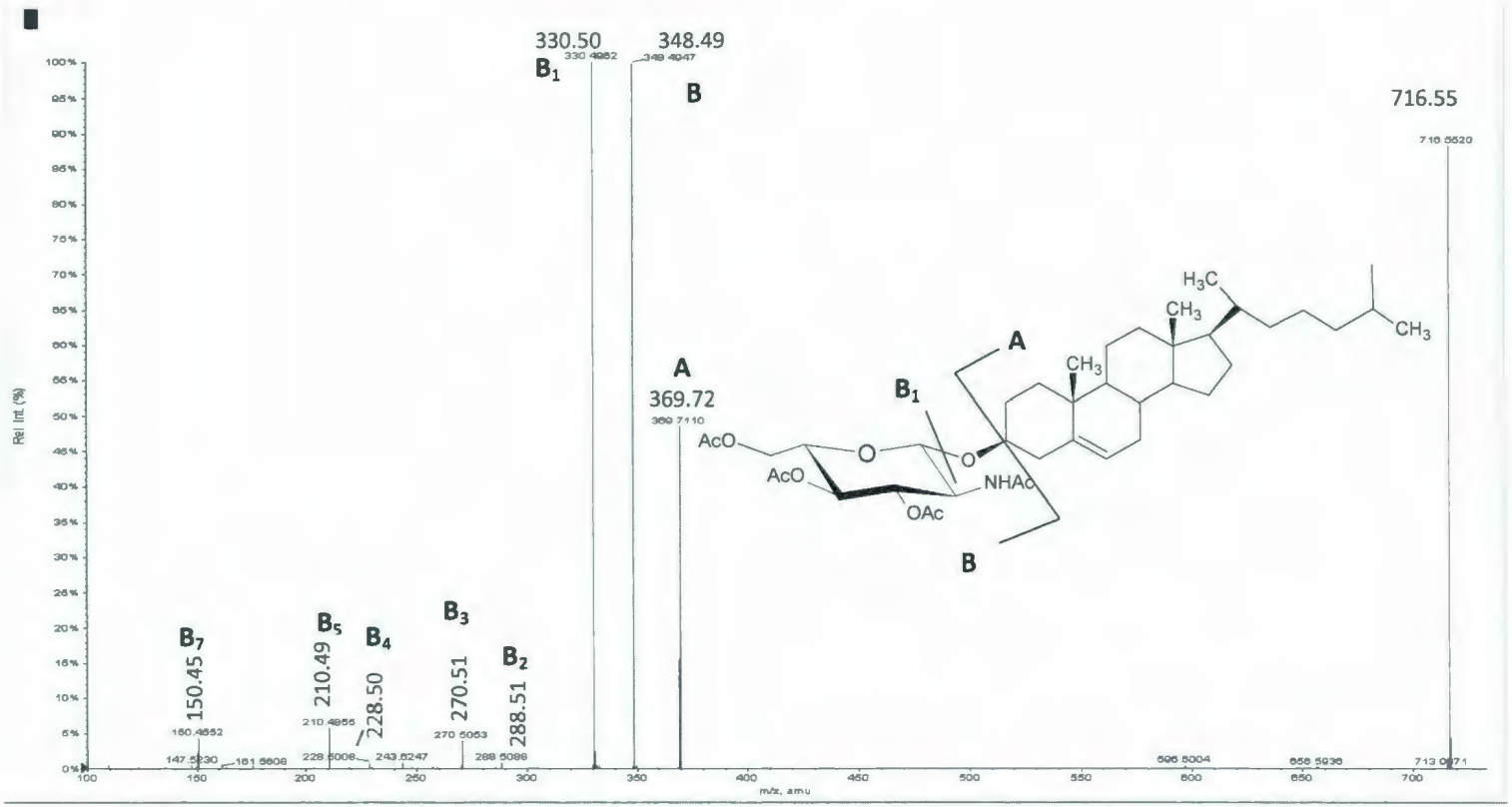

Figure 4.4: Tandem mass spectrometry analysis of the precursor ion $[M+H]^+$ at *m/z* 716.55, molecule "6".

4.3.3. CID-MS/MS of the [SugarOH]$^+$ B

The second-generation product ion scan (*quasi*-MS^3) of the fully acetylated [SugarOH]$^+$ **B** precursor oxonium ion at *m/z* 348.49 was performed with a CE of 10 eV (**Figure 4.5**).

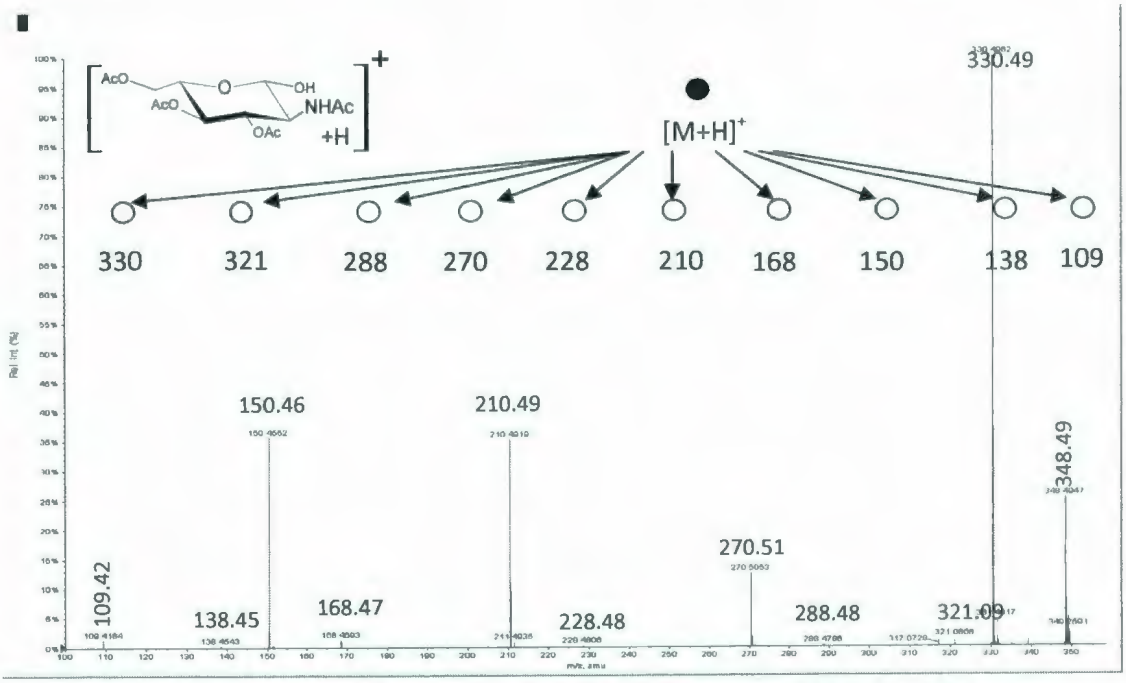

Figure 4.5: Second-generation tandem mass spectrometry of the [SugarOH]$^+$ also called [L-GlcNAcOH]$^+$, molecule "6".

The product ions issued from **B** were similar to the ones obtained during the conventional scan analysis and the CID-MS/MS of the protonated molecule. The elimination of acid acetic and ketene molecules was observed and confirmed. Additional elimination was observed at *m/z* 168.47 assigned as a [LGlcNAc-2AcOH-CH_2CO]$^+$ $\mathbf{B_6}$. The ion observed at *m/z* 109.42 was not identified.

Scheme 4.2 represents a tentative representation of the fragmentation pathway of the protonated molecule $[M+H]^+$. It focuses on the monosaccharide product ions. In fact, the protonated molecule breaks down into the $[L\text{-}GlcNAcOH+H]^+$ ion "**B**" at *m/z* 348.13 and the $[Cholestadiene+H]^+$ ion "**A**" at *m/z* 369.35. This $[M+H]^+$ ion is also able to fragment into the $[L\text{-}GlcNAc]^+$ oxonium ion " $\mathbf{B_1}$"at *m/z* 330.12. The data obtained from the second-generation tandem mass spectrometry analysis of **B** permitted the determination of the fingerprint of the sugar moiety of the per-*O*-acetylated neoglycolipid **6**.

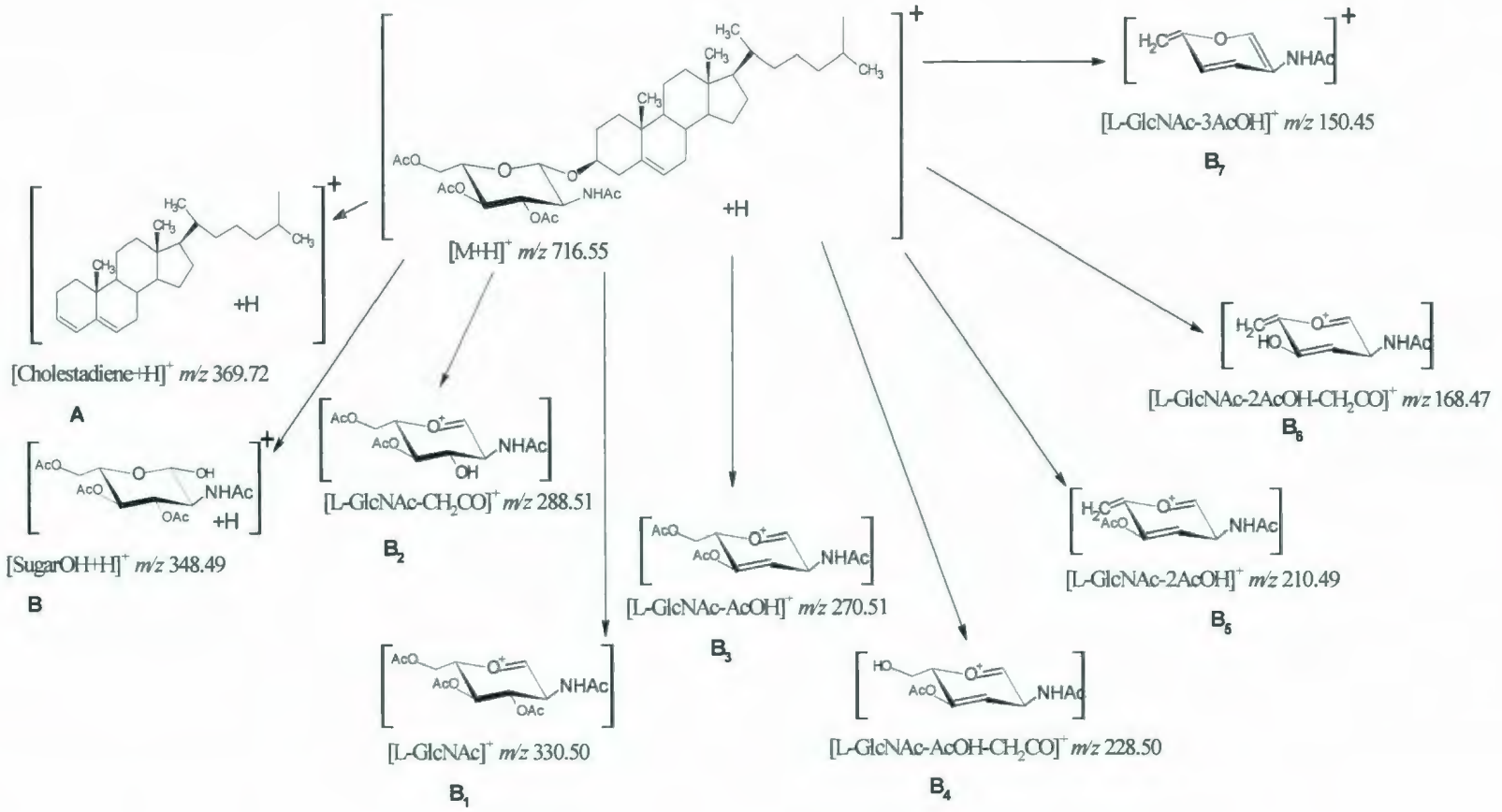

Scheme 4. 2: Proposed fragmentation pathway for the molecule cholest-5-en-3-β-yl-2-acetamido-3,4,6-tri-*O*-acetyl-2-deoxy-β-L-glucopyranoside, molecule "6".

4.4. Discussion

The analyses of the molecules **5** and **6** permitted us to confirm previous research[5,23] regarding per-*O*-acetylated neoglycolipid fragmentation. Consecutive or concerted elimination of acetic acid and ketene molecules prevents the possible production of an unprotected oxonium ion such as a deacetylated oxonium ion. It was found earlier that the oxonium ions are extremely reactive and will preferentially eliminate molecules of acetic acid and ketene, by concerted mechanisms and by destabilizing the 1,2-cyclic oxazolinium ion. Therefore, this oxazolinium ion does not have the time to form the cyclic reactive species that can react with the electrophilic cholesta-3,5-diene molecule found in the collision cell."[5] This "*O*-acetylated effect" likely prevents the formation of the $[C\text{-glycoside}+H]^+$ ion-species, as well as the overall reactivity of the per-*O*-acetylated-sugar oxonium ions in the series of per-*O*-acetylated neoglycolipids containing the D-GlcNAc and/or L-GlcNAc residues. Needless to say, as the unprotected $[GlcNAc]^+$ oxonium is not formed, it is not possible to have an ion-molecule interaction with the cholestadiene molecule, even with the presence of an acetamido on the *C*-2 of the carbohydrate. In fact, as stated in **Chapter 3**, the presence of an amido or acetamido group is needed to permit an ion-molecule reaction between oxonium and cholestadiene. However, the protection of the neoglycolipid by the acetylated group prevents this formation.

During fragmentation of the free underivatized and per-O-acetylated neoglycolipids, the products ions such as cholestadiene and other secondary product ions, derived from the different saccharide moieties, are similar. However, in the case of the

per-*O*-acetylated neoglycolipids, the main difference remains in the number of elimination reactions producing acetic acid and ketene. During this work, it was found that these eliminations were favored over the formation of the 1,2-cyclic oxonium ion. Therefore, **Scheme 4.3** presents the tentative rationale for the absence of the [C-glycoside+H]$^+$ ion-species.

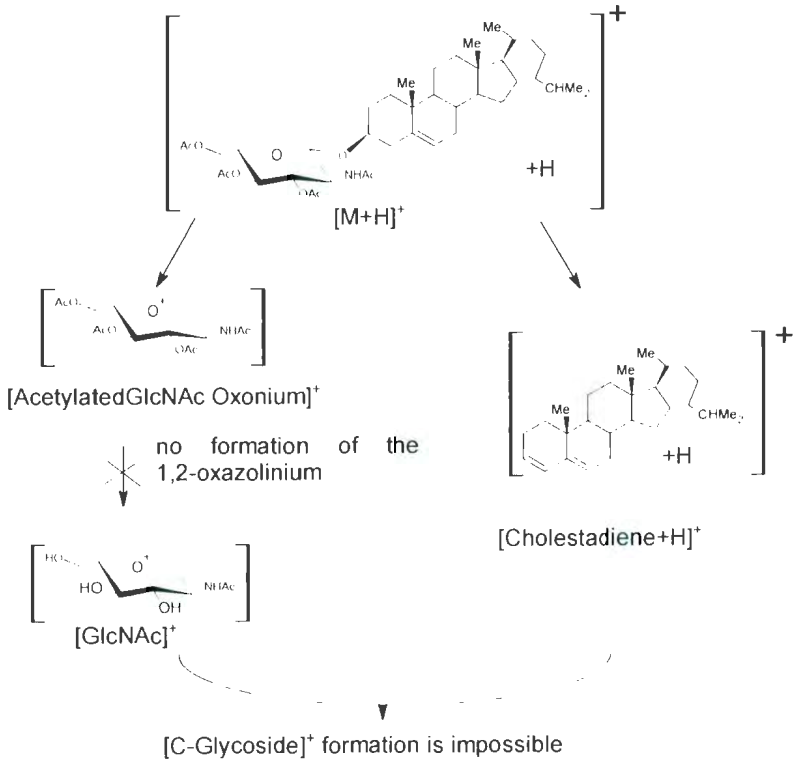

Scheme 4. 3: Lack of [C-glycoside+H]$^+$ formation from *O*-acetylated neoglycolipid cholesteryl derivatives.

Chapter 5: The formation of a new C-glycoside ion-species from a new neoglycolipid series containing the 2-azido-2-deoxy-β-D-galactopyranosyl residue moiety

A novel series of synthetic neoglycoconjugates, presented in **Figure 2.4**, containing the 2-azido-2-deoxy-β-D-glucopyranosyl unit was subjected to electrospray ionization mass spectrometry analysis using the hybrid QqTOF-MS/MS instrument to investigate the formation of the corresponding $[C\text{-glycoside}+H]^+$ ion-species inside the collision cell during tandem mass spectrometry.

The neoglycoconjugates of this novel series formed a new type of $[C\text{-glycoside}+H\text{-}N_2]^+$ ion-species . This latter product ion was presumed to be formed from a result of three consecutive reactions which take place in the collision cell of the hybrid QqToF-MS/MS instrument. These internal consecutive reactions were classified as follows: i) the excision of the polyethoxy chain; ii) the elimination of a N_2 molecule from the oxonium ion, followed by; iii) the formation of the $[C\text{-glycoside}+H\text{-}N_2]^+$ ion-species by an intramolecular mechanism (**Scheme 5.1**). It is suggested that the internal elimination of the spacer and the N_2 molecules, in addition to the intramolecular association between the sugar ion and the neutral cholestadiene molecule, occurs in the gas-phase and within the activated transition ion-molecule complex. As previously mentioned, it is not possible to assess now with certainty whether the $[C\text{-glycoside}+H\text{-}N_2]^+$ ion-species is held by strong electrostatic forces or by a true covalent bond.

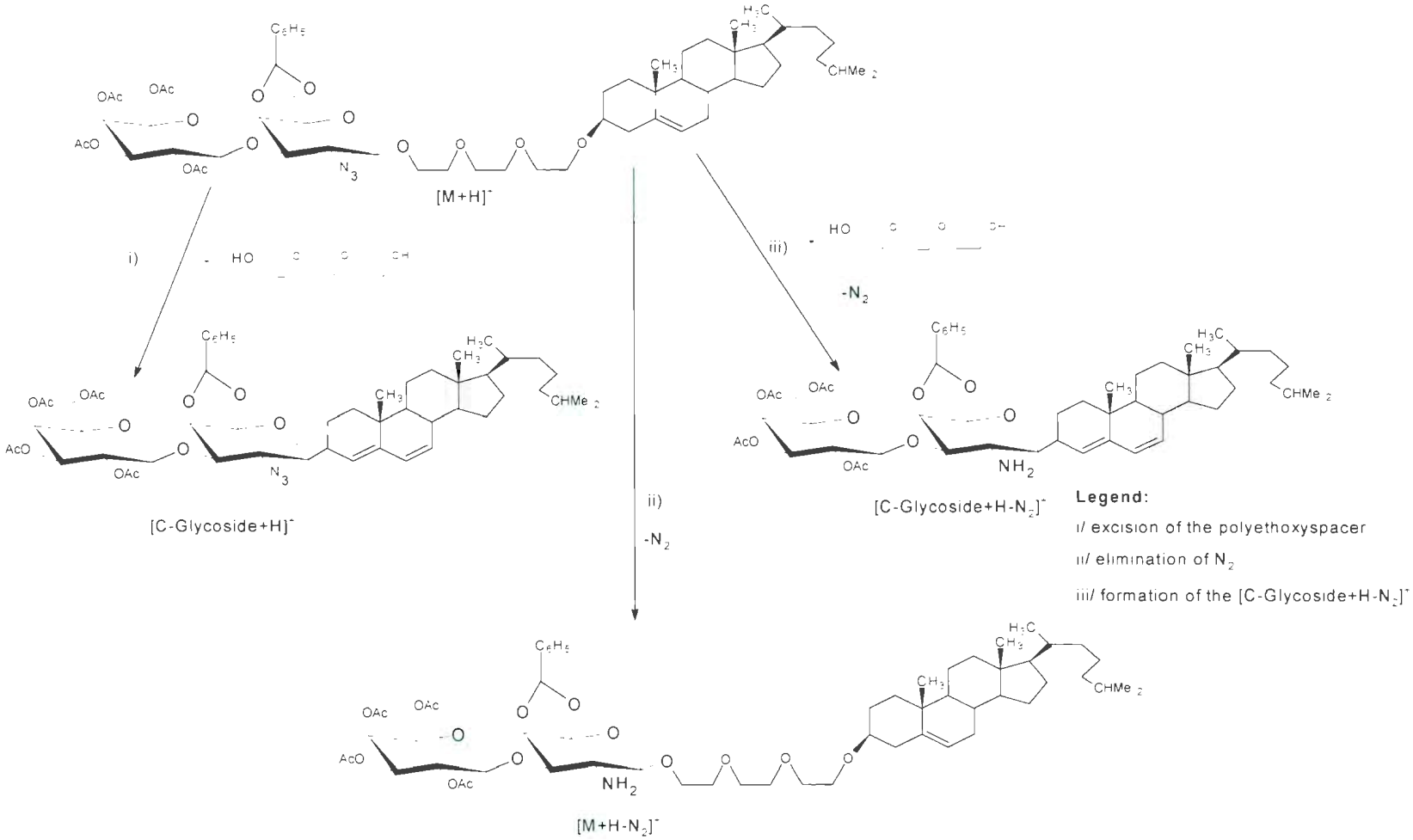

Scheme 5. 1: Consecutive reactions occurring in the collision cell.

5.1. Mass spectrometric analyses

5.2. Partially *O*-acetylated galacto azido neoglycolipid

5.2.1. 8-(Cholest-5-en-3-β-yloxy)-3,6-dioxaoctyl-3-*O*-(2,3,4,6-tetra-*O*-acetyl-β-D-galactopyranosyl)-2-azido-4,6-*O*-benzylidene-2-deoxy-β-D-galactopyranoside (7)

In the preceding analyses (**Chapter 4**), and also in previous research,[5,23] it was postulated that no [C-glycoside+H]$^+$ ion-species could be obtained if the *O*-acetylated group were present on the reducing end of the carbohydrate moiety. Thus, it was of interest to try to use a disaccharide neoglycolipid formed from a 2-azido-2-deoxy-β-D-glucopyranosyl moiety, in which the non-reducing end group of the disaccharide was a per-acetylated galactopyranosyl derivative, and its reducing end contained a 4,6 di-*O*-benzylidene non-participating group. This reasoning was chosen in order to show that the absence of the *O*-acetyl groups on the reducing end 2-azido-2-deoxy-β-D-glucopyranosyl moiety will not interfere with the formation of the [C-glycoside+H]$^+$ ion-species.

5.2.1.1. QqToF analysis

The ESI-MS in **Figures 5.1** and **5.2** show the expected sodiated molecule [M+Na]$^+$ at *m/z* 1146.2319 and the protonated [M+H]$^+$ molecule at *m/z* 1124.3180. It should be noted that the DP2 in these ESI-MS was increased to 10 V, which enhanced the "in-nozzle" fragmentation of the molecule **7**.

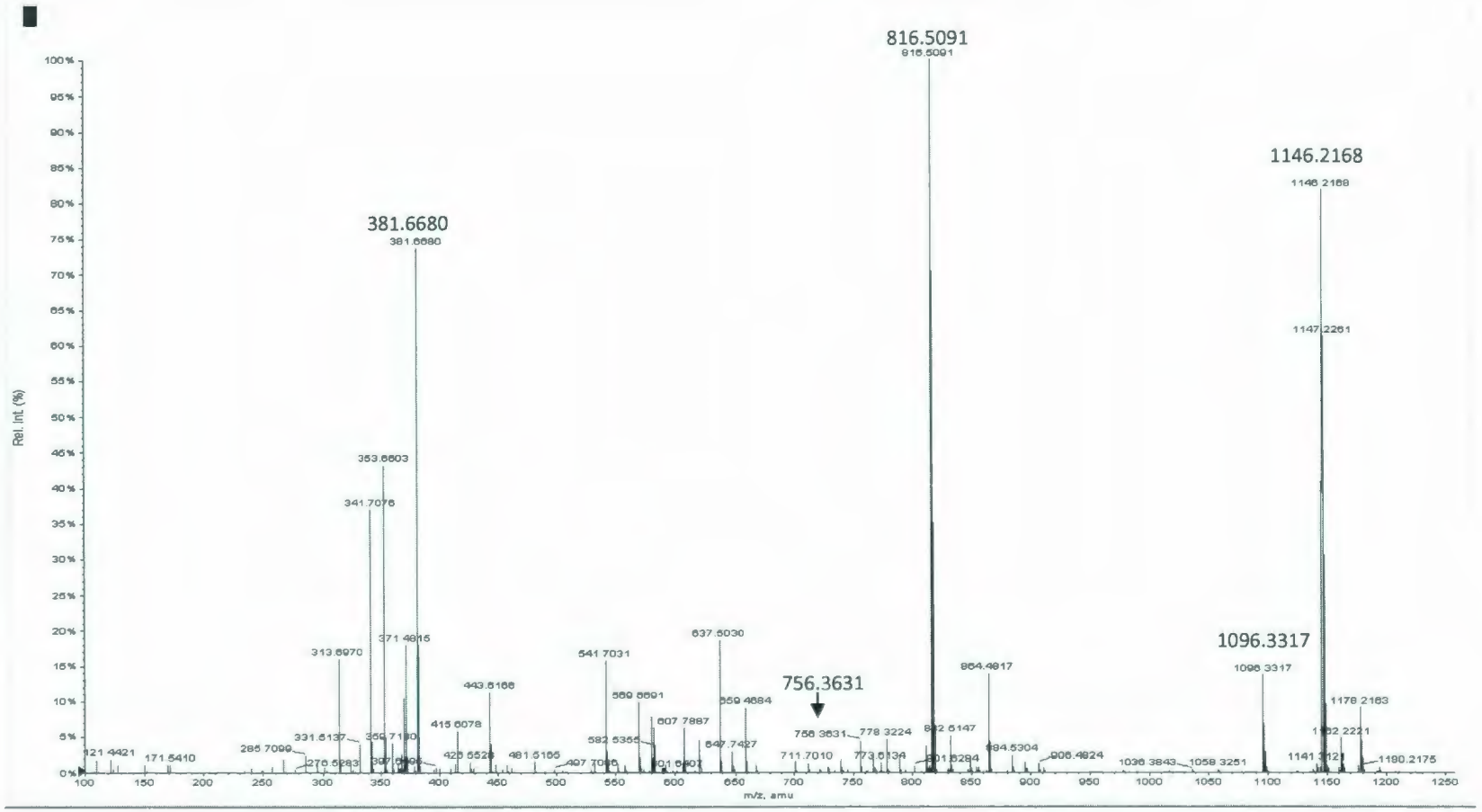

Figure 5.1: Full scan ESI-MS analysis of 8-(cholest-5-en-3-β-yloxy)-3,6-dioxaoctyl-3-*O*-(2,3,4,6-tetra-*O*-acetyl-β-D-galactopyranosyl)-2-azido-4,6-*O*-benzylidene-2-deoxy-β-D-galactopyranoside, molecule "7". DP 100V FP 150V DP2 5V

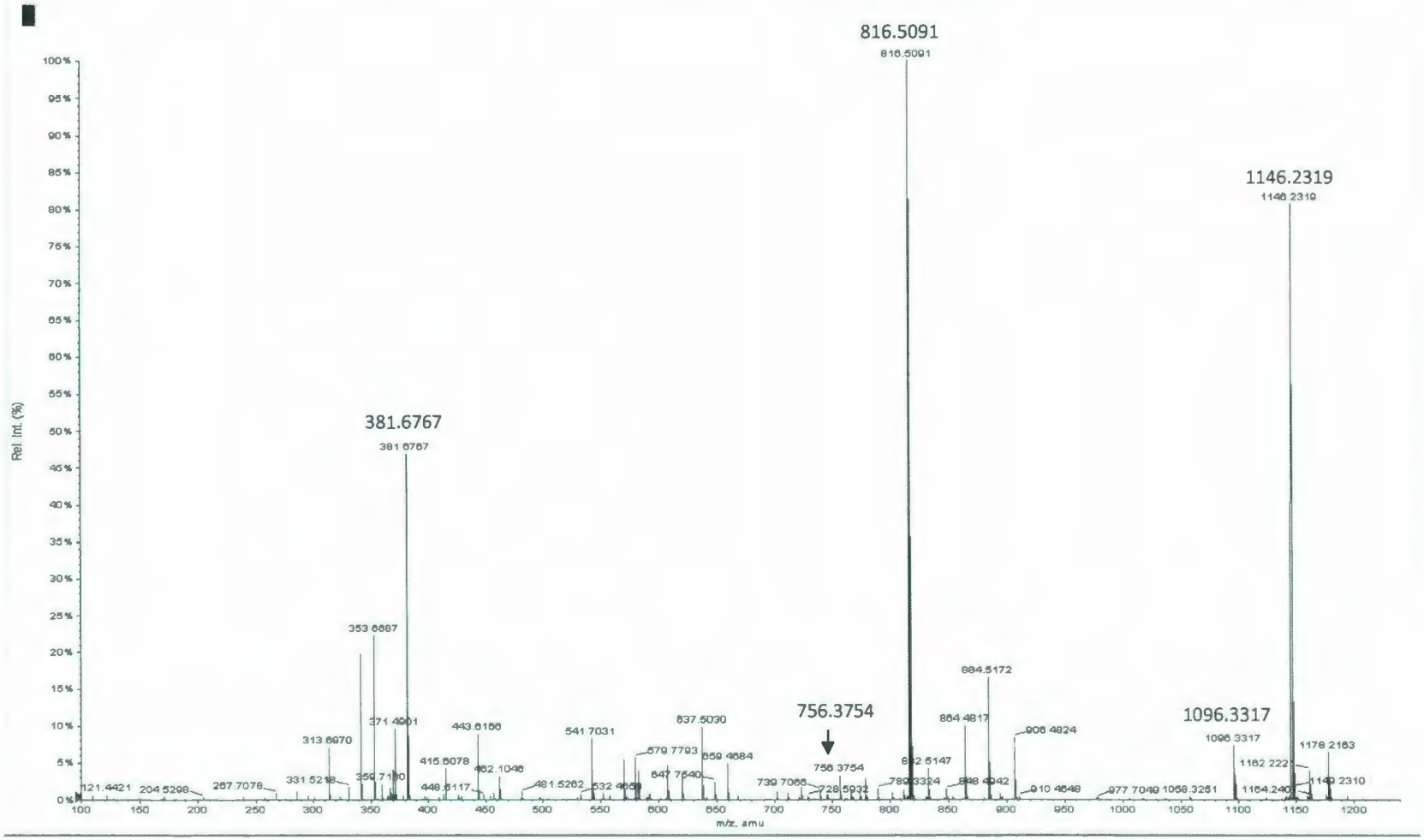

Figure 5.2: Full scan ESI-MS analysis of 8-(cholest-5-en-3-β-yloxy)-3,6-dioxaoctyl-3-*O*-(2,3,4,6-tetra-*O*-acetyl-β-D-galactopyranosyl)-2-azido-4,6-*O*-benzylidene-2-deoxy-β-D-galactopyranoside, molecule "7". DP 100V FP 150V DP2 10V

The presence of the product ion $[M+H-N_2]^+$ at *m/z* 1096.3317 could be detected. It has been shown in the literature that 2-azido-2-deoxy-pyranoside MALDI-ToF-MS analyses indicated that the azido group excised a molecule of N_2, converting the azido group into a free–NH_2 amino group.[68] Other researchers have also noticed the loss of N_2 in different azido sugar compounds analyzed by electron ionization (EI), chemical ionization (CI), mass-analyzed ion kinetic energy (MIKE) and fast atom bombardment (FAB).[69,70]

The ESI-MS also showed the formation of the $[SugarSpacer]^+$ fragment ion at *m/z* 756.3754 and the $[Cholestadiene+H]^+$ fragment ion at *m/z* 369.7430. Other fragment ions were also noted and were assigned to the non-reducing end of the disaccharide portion $[DGal]^+$ oxonium moiety or $[DGalN_3]^+$ oxonium reducing end of the disaccharide moiety. Finally, a low intensity fragment was noticed at *m/z* 947.3147, which was assigned as the $[C\text{-glycoside-}N_2+H]^+$ ion-species. The ESI-MS spectrum in **Figure 5.2** is actually similar to that in **Figure 5.1**, the only difference being in the abundance of the ions, mainly due to the DP applied.

5.2.1.2. CID-MS/MS of the protonated molecule

The CID-tandem mass spectrum of the $[M+H]^+$ protonated molecule, is a source of quantitative information regarding the products ions obtained. The product ion scan of the protonated molecule **7** was divided in several sections, in order to explain the structure of all the product ions formed (**Figure 5.3**).

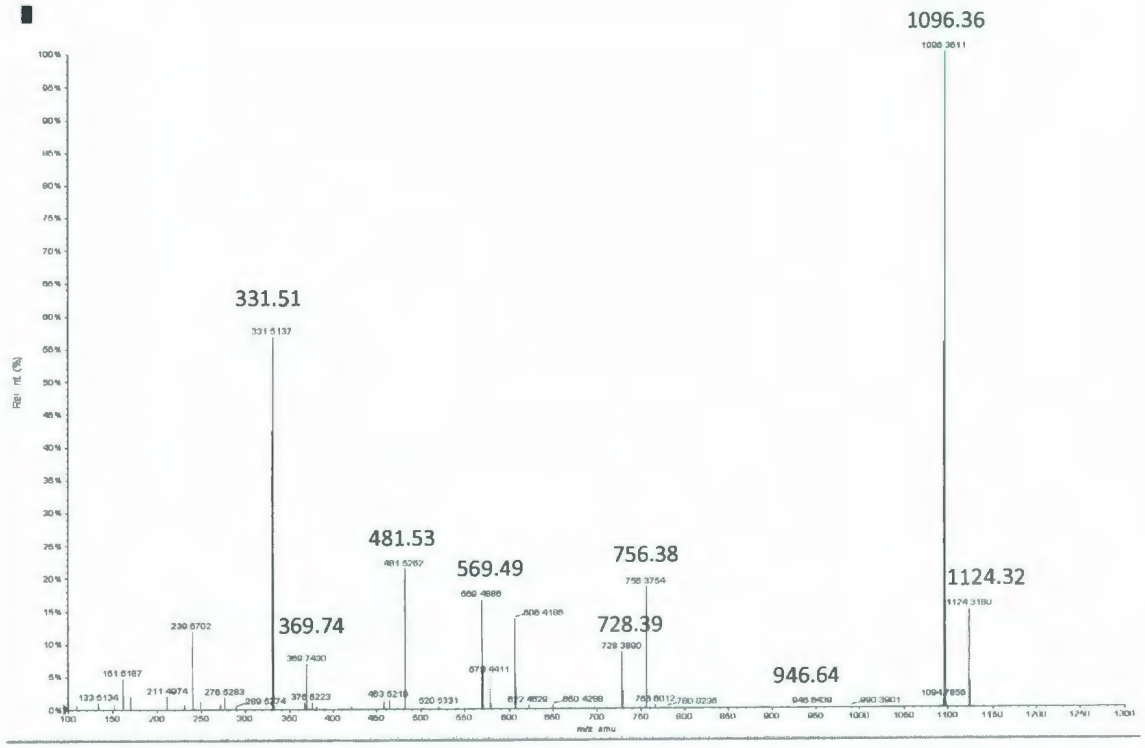

Figure 5.3: CID-MS/MS scan of the protonated molecule 8-(cholest-5-en-3-β-yloxy)-3,6-dioxaoctyl-3-*O*-(2,3,4,6-tetra-*O*-acetyl-β-D-galactopyranosyl)-2-azido-4,6-*O*-benzylidene-2-deoxy-β-D-galactopyranoside (molecule 7) at *m/z* 1124.32.

The CID-MS/MS of the disaccharide 8-(cholest-5-en-3-β-yloxy)-3,6-dioxaoctyl-3-*O*-(2,3,4,6-tetra-*O*-acetyl-β-D-galactopyranosyl)-2-azido-4,6-*O*-benzylidene-2-deoxy-β-D-galactopyranoside **7** protonated molecule $[M+H]^+$ at *m/z* 1124.32 gave the $[M+H-N_2]^+$ product ion at *m/z* 1096.36 (Base peak). The other expected product ions were also detected such as the $[SugarSpacer+H]^+$ at *m/z* 756.38, the $[Sugar-N_2-AcOH-CH_2CO+H]^+$ product ion at *m/z* 481.53, the $[Cholestadiene+H]^+$ product ion at *m/z* 369.74 and the $[DGal]^+$ product oxonium ion at *m/z* 331.51. Finally, the formation of the product ion of the $[\beta\text{-D-Gal}\ (1\rightarrow3)\ \beta\text{-D-GalNAc-}N_2]^+$ C-glycoside at *m/z* 946.64 could also be detected.

The molecule **7** is characterized by three main components: i) the presence of the 2-azido group on the 2-azido-2-deoxy-amino sugar; ii) the presence of the non-participating 4,6-di-*O*-benzylidene group on the reducing end of the disaccharide portion; and iii) the presence of the fully per-*O*-acetylated-D-galactopyranosyl non-reducing end of the disaccharide portion of the neoglycolipid. Therefore, it has been deemed that the presence of the 2-azido-2-deoxy group allows the formation of the $[M+H-N_2]^+$ molecule and these variations can also be the source of the novel C-glycoside ion-species assigned as a $[C\text{-glycoside}+H-N_2]^+$ ion species formed during the CID-MS/MS analysis of the protonated molecule $[M+H]^+$. It has been established previously in the literature that the N_2 elimination occurs by a spontaneous reaction.[71]

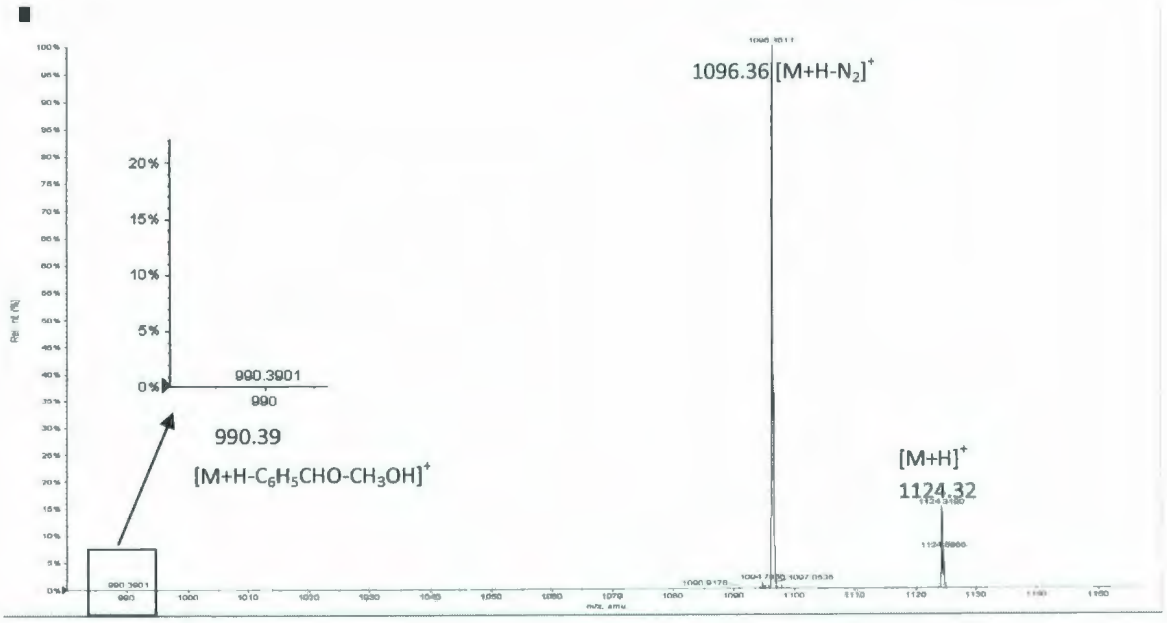

Figure 5.4: CID-MS/MS spectrum region from *m/z* 990 to 1130 of the 8-(cholest-5-en-3-β-yloxy)-3,6-dioxaoctyl-3-*O*-(2,3,4,6-tetra-*O*-acetyl-β-D-galactopyranosyl)-2-azido-4,6-*O*-benzylidene-2-deoxy-β-D-galactopyranoside, molecule "7".

A new fragment was revealed at *m/z* 990.39 (**Figure 5.4**). A possible product ion was found for this ion, which can occur by loss of the 4,6-benzylidene group in the form of a molecule of benzaldehyde (C_6H_5CHO) followed by a loss of methanol from the protonated $[M+H]^+$.

Figure 5.5 shows the presence of the $[C\text{-glycoside}+H\text{-}N_2]^+$ ion-species at *m/z* 946.64 and the $[SugarSpacer+H]^+$ product ion at *m/z* 756.38. The characterized product ions formed by the loss of the non-reducing per-*O*-acetylated galactopyranosyl unit (331 Da) at *m/z* 780.03 and *m/z* 766.60 were also noted.

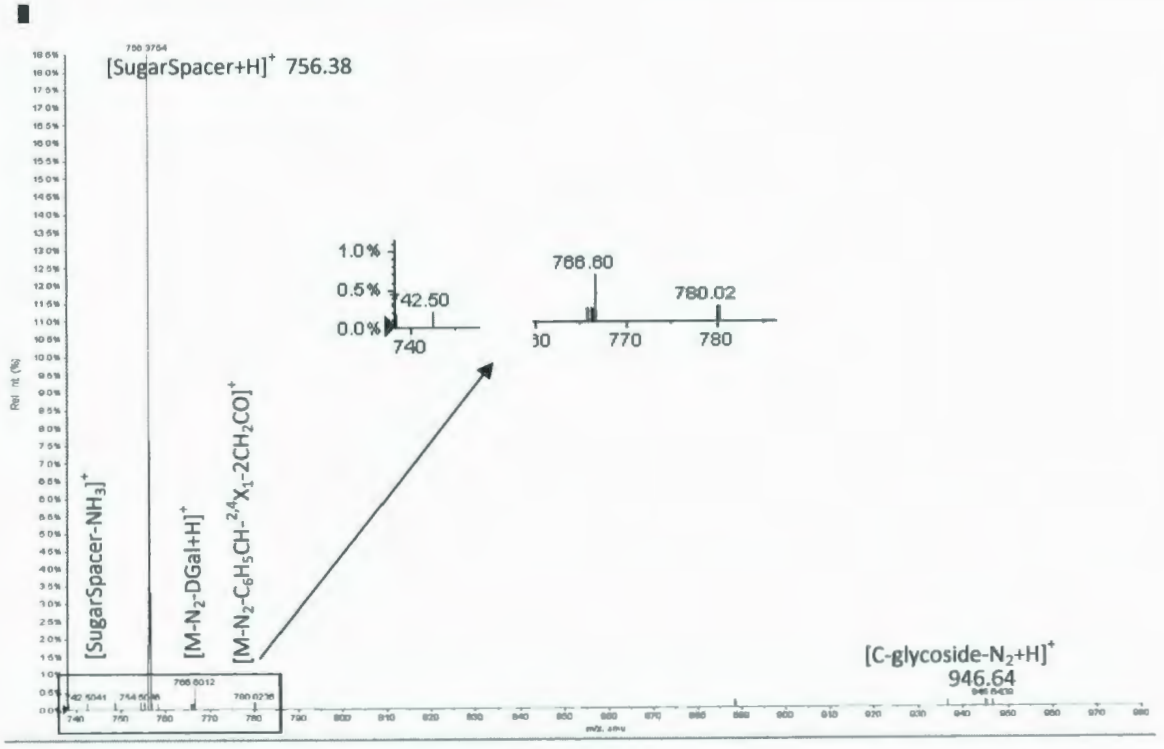

Figure 5.5: CID-MS/MS spectrum region from *m/z* 740 to 980 of the 8-(cholest-5-en-3-β-yloxy)-3,6-dioxaoctyl-3-*O*-(2,3,4,6-tetra-*O*-acetyl-β-D-galactopyranosyl)-2-azido-4,6-*O*-benzylidene-2-deoxy-β-D-galactopyranoside, molecule "7".

The product ion at *m/z* 780.02 could be obtained by loss of benzaldehyde, a methyl group, and the non-reducing galactopyranoside. The figure below represents its possible eventual structure (**Figure 5.6**).

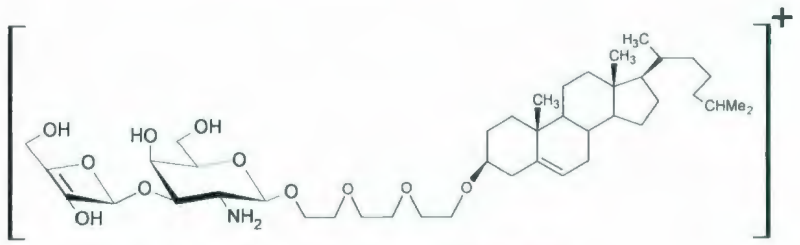

$[M\text{-}N_2\text{-}C_6H_5CH\text{-}^{2,4}X_1\text{-}2CH_2CO]^+$ *m/z* 780.02

Figure 5.6: Possible structure of the *m/z* 780.02 ion

The following figure represents the possible structure of the product ion found at *m/z* 766.60 (**Figure 5.7**).

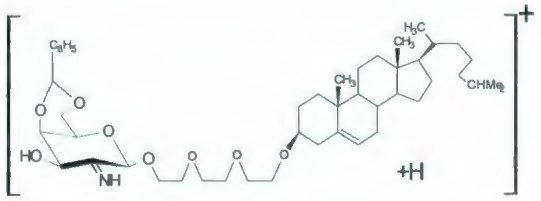

$[M+H\text{-}N_2\text{-}DGal]^+$ m/z 766.60

Figure 5.7: Possible ion for *m/z* 766.60

Figure 5.8 is based on the *m/z* region from 560 to 760 and reveals several product ions that appear to be derived from the $[SugarSpacer+H]^+$ ion. The $[SugarSpacer+H\text{-}N_2]^+$ product ion was assigned as *m/z* 728.39. The product ion at *m/z* 622.46 was assigned as the $[DGal1\rightarrow3DGlcNAc+H]^+$, and the one at *m/z* 578.44 as a $[DGal1\rightarrow3DGlcNAc\text{-}N_2]^+$ ion.

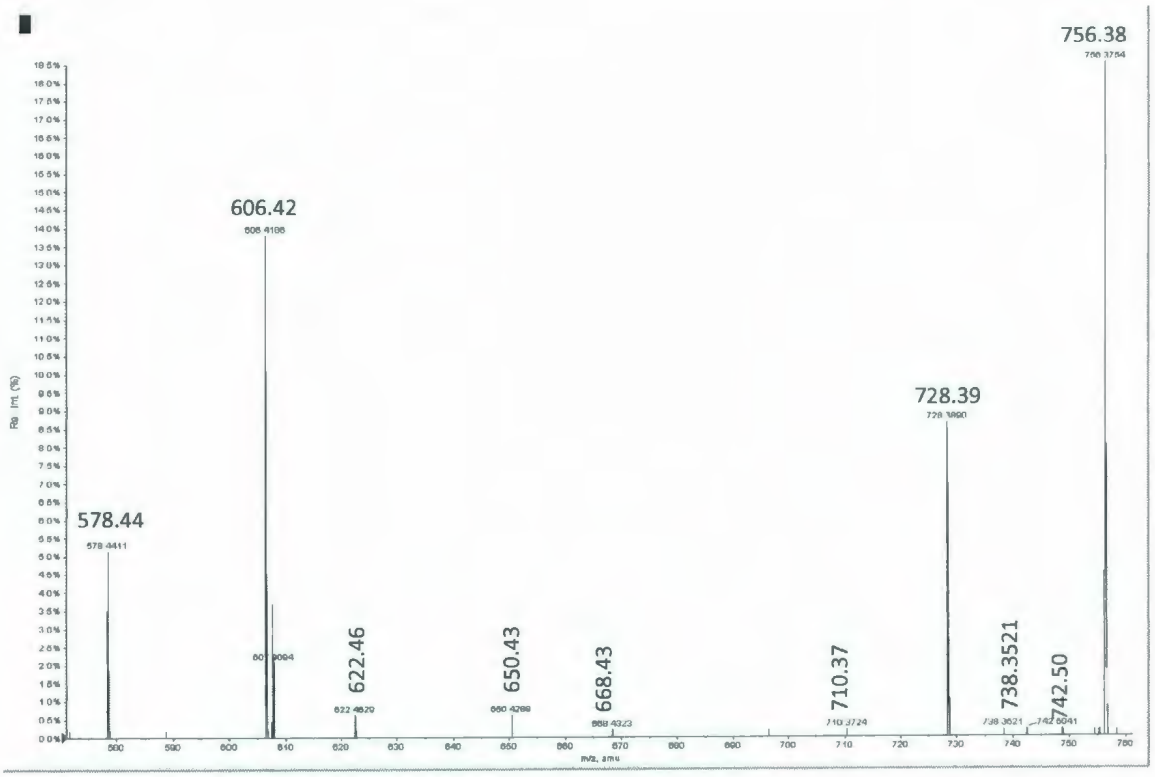

Figure 5.8: CID-MS/MS spectrum region from *m/z* 560 to 760 of the 8-(cholest-5-en-3-β-yloxy)-3,6-dioxaoctyl-3-*O*-(2,3,4,6-tetra-*O*-acetyl-β-D-galactopyranosyl)-2-azido-4,6-*O*-benzylidene-2-deoxy-β-D-galactopyranoside, molecule "7".

Figure 5.9 represents the possible ions present in the spectrum in **Figure 5.8**. The product ion at *m/z* 742.50 was assigned as the $[SugarSpacer\text{-}NH_3]^+$ ion; the product ion at *m/z* 668.43 was assigned as the $[SugarSpacer+H\text{-}N_2\text{-}AcOH]^+$ ion.

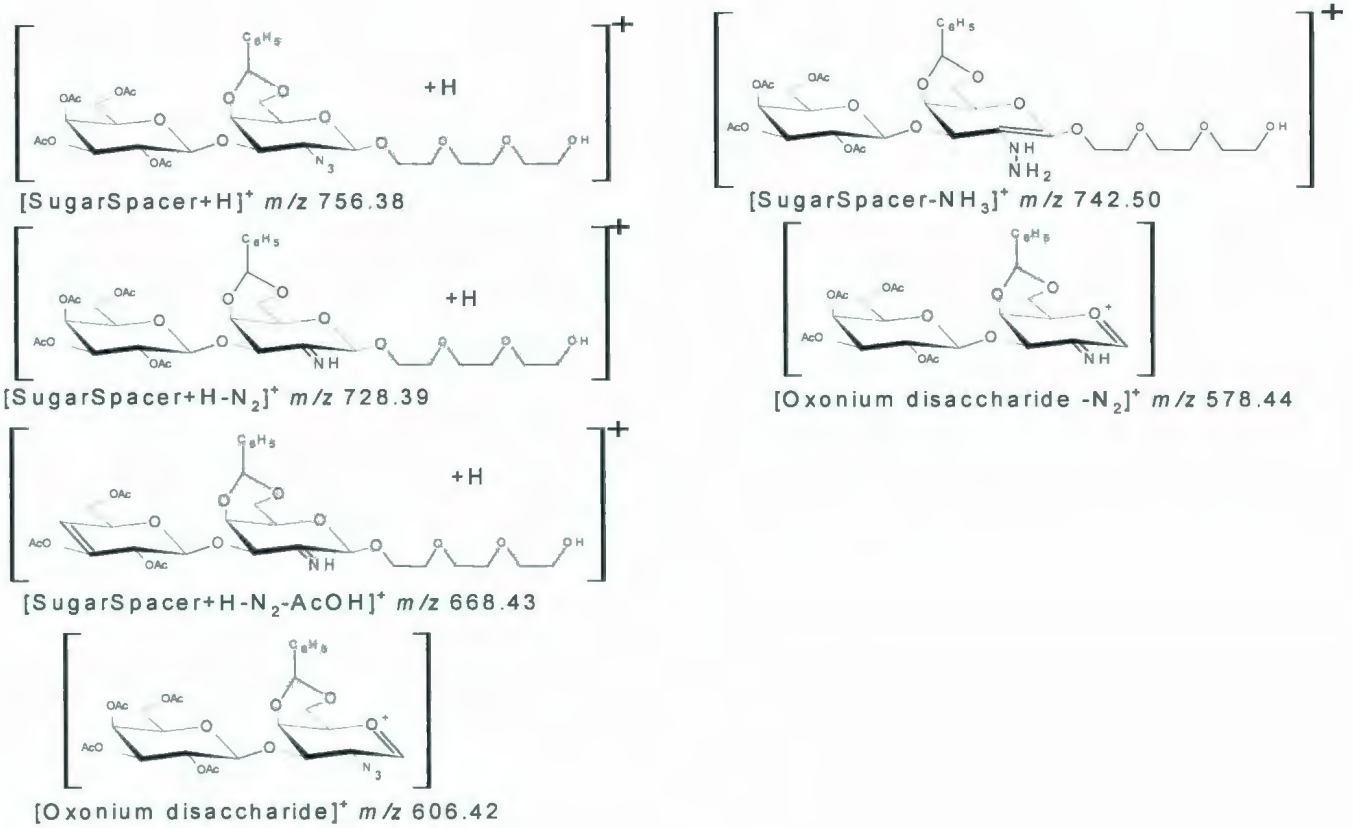

Figure 5.9: Possible ion structures from the section *m/z* 560-760

The spectrum in **Figure 5.10** shows the product ions from *m/z* 300 to 580.

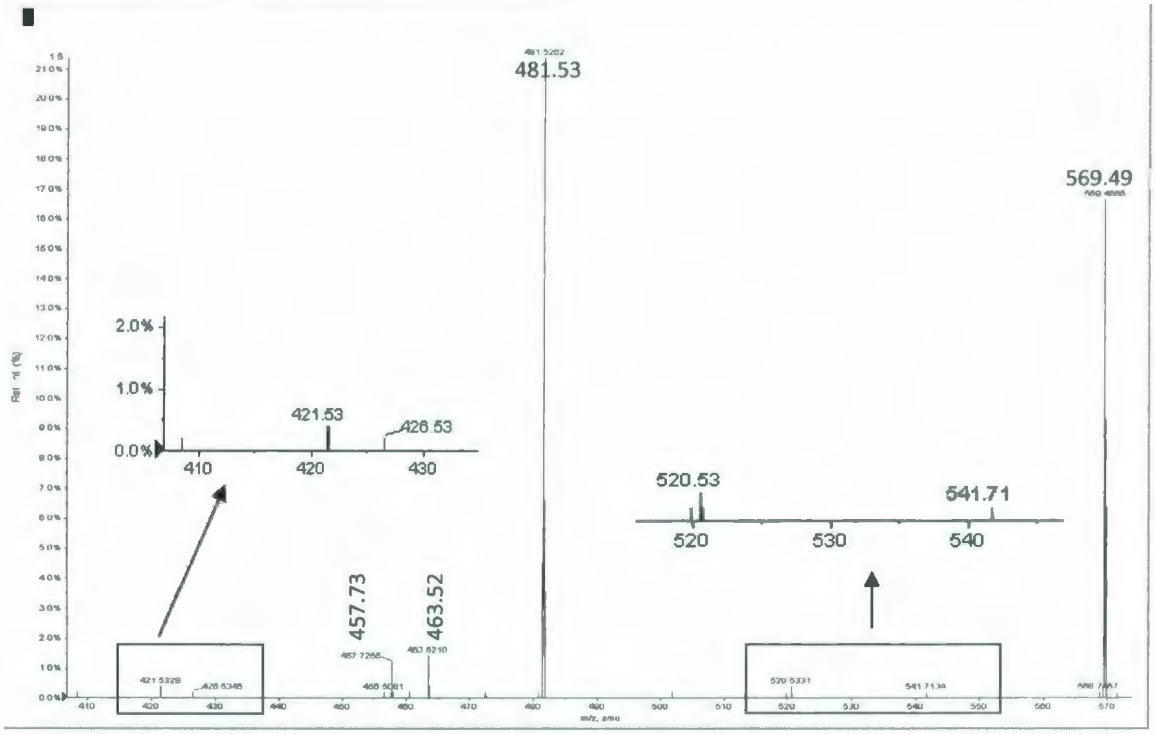

Figure 5.10: CID-MS/MS spectrum from *m/z* 410 to 570 of the 8-(cholest-5-en-3-β-yloxy)-3,6-dioxaoctyl-3-*O*-(2,3,4,6-tetra-*O*-acetyl-β-D-galactopyranosyl)-2-azido-4,6-*O*-benzylidene-2-deoxy-β-D-galactopyranoside, molecule "7".

Elimination of acid acetic and ketene was observed with the product ion at *m/z* 481.53 assigned as the $[Sugar+H-N_2-2AcOH-CH_2CO]^+$ ion. The product ion at *m/z* 569.49 was abundant in this section of the spectra (**Figure 5.10**); however, no plausible assignment could be made. Elimination of the benzaldehyde molecule was observed at *m/z* 520.53 and assigned as the $[Sugar+H-C_6H_5CHO]^+$ ion. Elimination of a consecutive or concerted N_2 molecule, in addition to the per-*O*-acetylated groups and a molecule of acetic acid were observed at *m/z* 463.52 and *m/z* 421.53. The product ion at *m/z* 457.73 was assigned as the $[Sugar-C_6H_5CH-AcOH]^+$ ion (**Figure 5.11**).

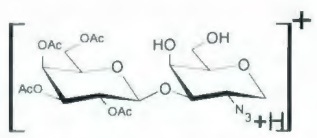

[Sugar-C_6H_5CHO+H]$^+$ *m/z* 520.53

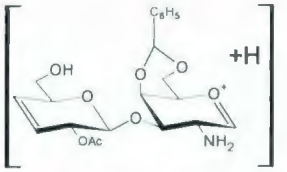

[Sugar-N_2-2AcOH-CH_2CO+H]$^+$ *m/z* 421.53

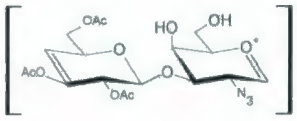

[Sugar-C_6H_5CH-AcOH]$^+$ *m/z* 457.73

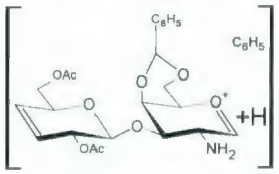

[Sugar-N_2-2AcOH+H]$^+$ *m/z* 463.52

Legend:

Sugar= β-D-Gal(1-3)-β-D-Gal

Figure 5.11: Different possibilities for the *m/z* ions found from 300 to 570

The *m/z* region from 240 to 400 (**Figure 5.12**), reveals less fragmentation. The main product [Cholestadiene+H]$^+$ ion at *m/z* 369.74 and the [DGal]$^+$ product ion moiety at *m/z* 331.51 were found. Furthermore the product ion [$DGalN_3$-N_2]$^+$ was characterized at *m/z* 248.52. By looking at the different ions present in this region of the mass spectrum, the presence of the product ion [DGal-CH_2CO]$^+$ at *m/z* 289.52 could be discerned. The presence of the product ion at *m/z* 276.53, which was characterized as the reducing end of the disaccharide moiety [$DGalN_3$]$^+$, was also observed. This provides evidence that the product [$DGalN_3$-N_2]$^+$ ion formed at *m/z* 248.52 indeed originates from the precursor ion [$DGalN_3$]$^+$ at *m/z* 276.53. Finally, a low-intensity product ion was observed at *m/z* 375.52, which was assigned as the [Oxonium disaccharide-$^{2,4}X_1$-CH_2CO]$^+$ ion, since its calculated value is equal to *m/z* 376.14.

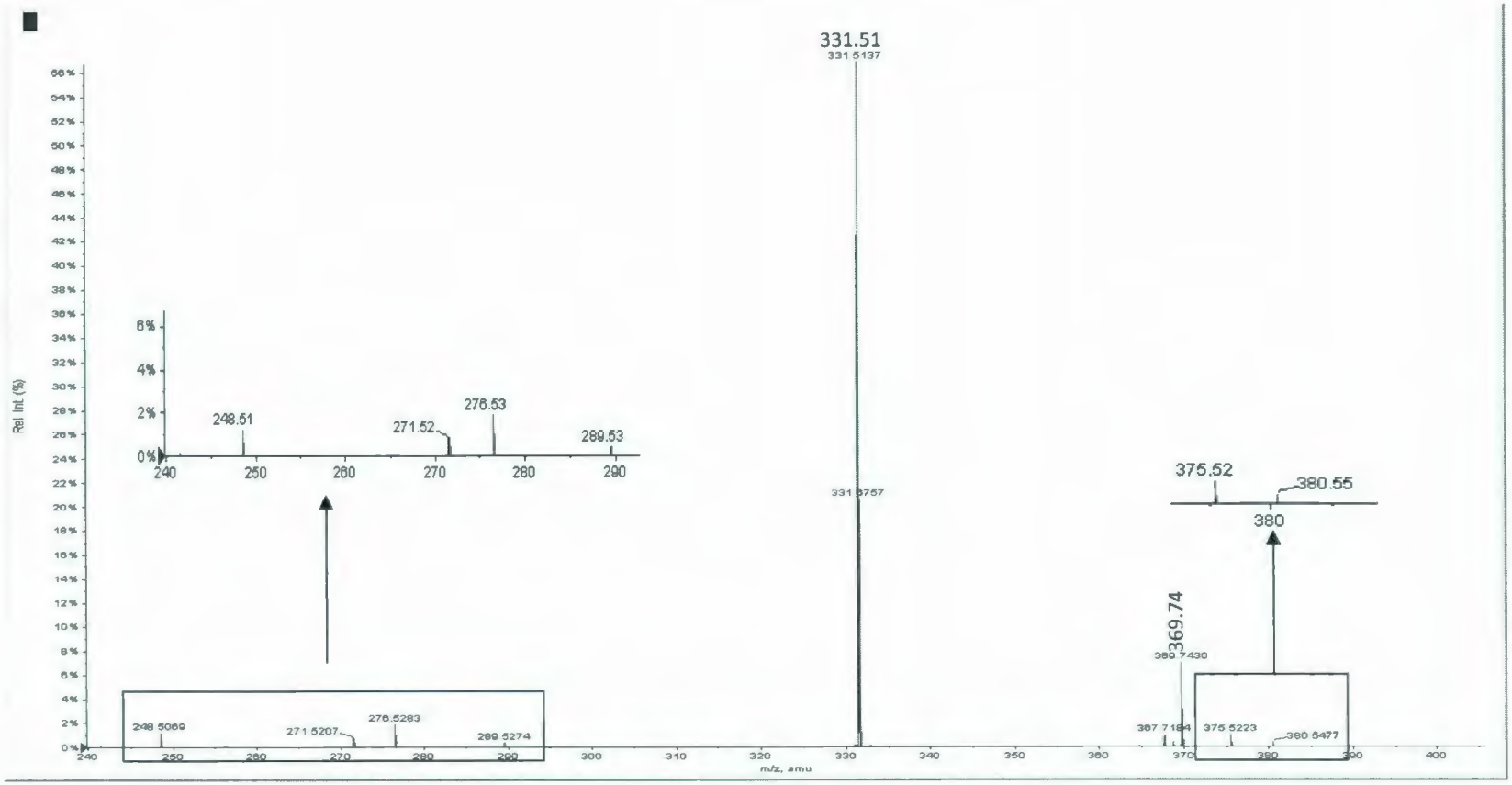

Figure 5.12: CID-MS/MS spectrum region from *m/z* 240 to 400 of the 8-(cholest-5-en-3-β-yloxy)-3,6-dioxaoctyl-3-*O*-(2,3,4,6-tetra-*O*-acetyl-β-D-galactopyranosyl)-2-azido-4,6-*O*-benzylidene-2-deoxy-β-D-galactopyranoside, molecule "7".

The key product ions observed in the **Figure 5.12** are represented in the following figure (**Figure 5.13**).

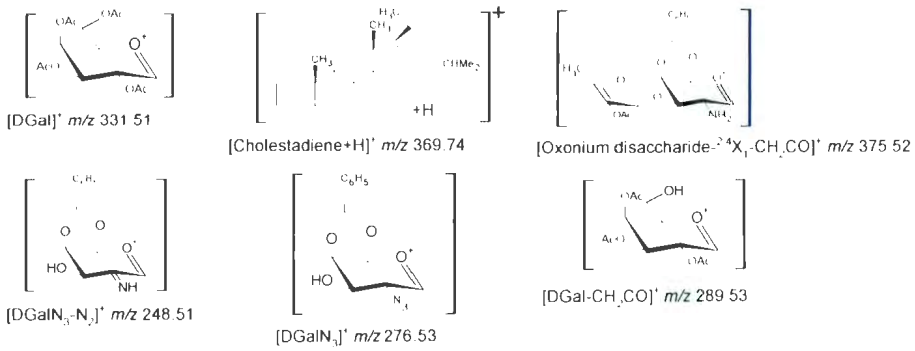

Figure 5.13: Tentative structure of the product ions from *m/z* 240 to 400

Figure 5.14 appears to show the product ions derived from both the product oxonium and the 4,6-di-benzylidene-D-GalN_3. In fact, their respective theoretical *m z* are almost the same (*m/z* 230.07782 for the $[DGal\text{-}AcOH\text{-}CH_2CO+H]^+$ and *m/z* 230.0812 for the $[DGalN_3\text{-}N_2\text{-}H_2O]^+$).

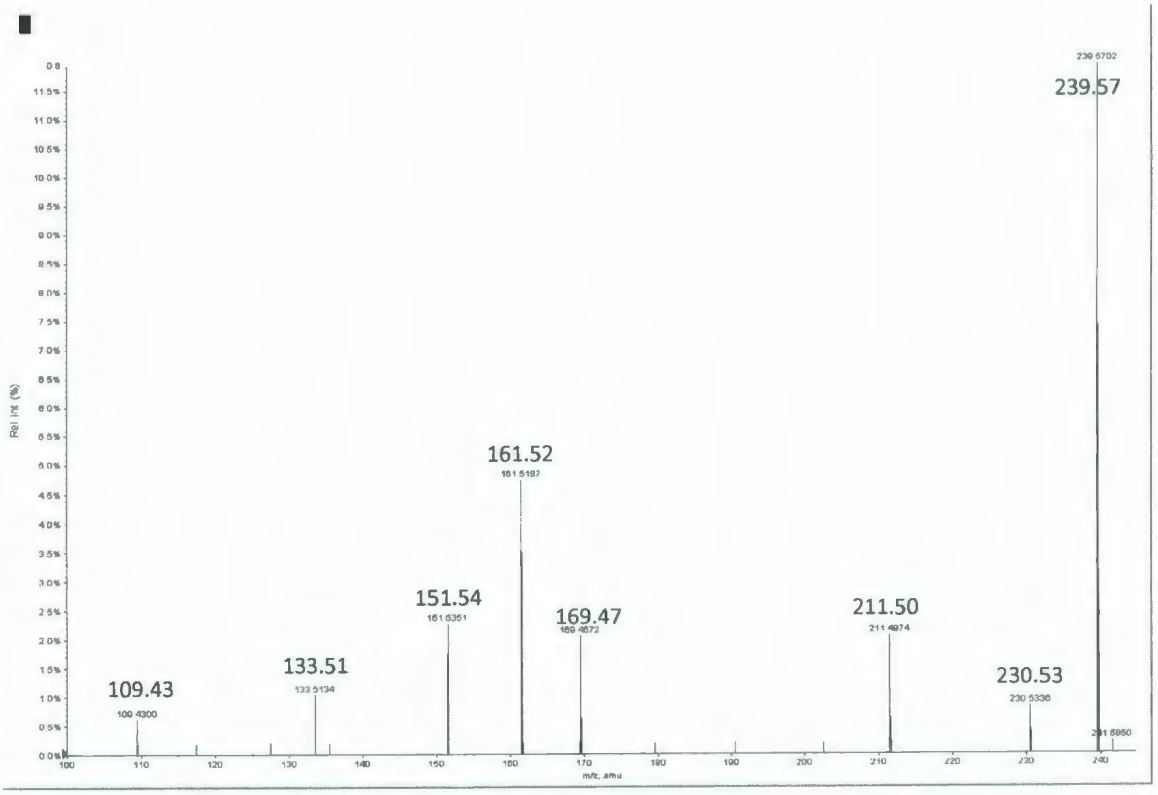

Figure 5.14: CID-MS/MS spectrum region from *m/z* 100 to 240 of the 8-(cholest-5-en-3-β-yloxy)-3,6-dioxaoctyl-3-*O*-(2,3,4,6-tetra-*O*-acetyl-β-D-galactopyranosyl)-2-azido-4,6-*O*-benzylidene-2-deoxy-β-D-galactopyranoside, molecule "7".

The product ion at *m/z* 230.53 occurs by losses of acetic acid followed by ketene from the $[DGal]^+$. The product ions at *m/z* 211.50, *m/z* 169.47 and *m/z* 161.52 are derived from the per-*O*-acetylated non-reducing galactopyranosyl moiety. The chemical structure of the *O*-acetylated product ions derived from the fully acetylated carbohydrate DGal moiety are indicated in **Figure 5.15**.

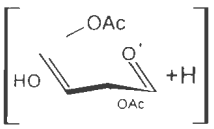

[DGal-AcOH-CH_2CO+H]$^+$ *m/z* 230.53

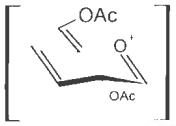

[DGal-2AcOH]$^+$ *m/z* 211.50

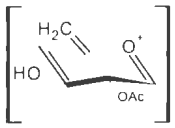

[DGal-2AcOH-CH_2CO]$^+$*m/z* 169.47

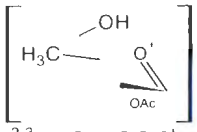

[DGal-$^{2\ 3}X_0$-CH_2CO-]$^+$ *m/z* 161.52

Figure 5.15: Possible ions from [DGal]$^+$

The product ion [$DGalN_3$]$^+$ yields the product ion [$DGalN_3$+H-N_2-H_2O-C_6H_5-CHO]$^+$ at *m/z* 133.51. It should be noted that the product ion can be derived from the 4,6-benzylidene group and is present at *m/z* 109.43, which is mostly a [1-*O*-methyl-hex-1,3,5-ene+H]$^+$ ion (**Figure 5.16**).

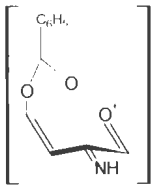

[$DGalN_3$-N_2-H_2O]$^+$*m/z* 230.53

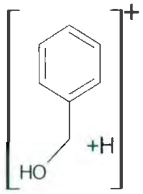

[1 O-Methyl-hex-1,3,5-ene+H]$^+$ *m/z* 109.43

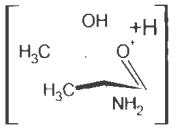

[$DGalN_3$-N_2-H_2O-C_6H_5-CHO+H]$^+$ *m/z* 133.51

Figure 5.16: Possible ions from both oxonium and benzene ring

The second generation tandem mass spectrometric analysis of the carbohydrate moiety was not performed, but would have been of interest to determine the fragmentation pathway.

The reconfirmation of the various gas-phase fragmentation routes of the [C-glycoside+H-N_2]$^+$ ion-species at *m/z* 946.64 was also performed. However, the product ion was impossible to isolate or to fragment. The protection of the neoglycolipids by the presence of the per-*O*-acetylated group could be a reason for this.

5.2.2. 8-(Cholest-5-en-3-β-yloxy)-3,6-dioxaoctyl 3-*O*-(2,3,4,6-tetra-*O*-acetyl-β-D-galactopyranosyl)-2-azido-2-deoxy-α-D-galactopyranoside (8)

5.2.2.1. QqToF analysis

Molecule **8** differs from **7**, as it does not have the 4,6-benzylidene group on the azido-D-galactosamine carbohydrate. The ESI-MS conventional scan analysis of **8** demonstrated the presence of the sodiated molecule [M+Na]$^+$ at *m/z* 1058.2729, and the protonated molecule [M+H]$^+$ was noticed in low abundance at *m/z* 1036.3515. Evidence for the 2-azido influence was provided by the presence of [M+H-N_2]$^+$ at *m/z* 1008.3860 and the [C-glycoside+H-N_2]$^+$ ion-species at *m/z* 859.4893 (4.9296e^{-3}%). The common diagnostic fragment ions derived from the protonated molecule were also observed: the [Cholestadiene+H]$^+$ fragment ion at *m/z* 369.7377, the [DGal]$^+$ at *m/z* 331.5020 and its acetylated derivatives, the fragment ion at *m/z* 169.4869 formed by the loss of two acetic acid and one ketene molecules, and the fragment ion at *m/z* 151.5269 formed by the loss

three acetic acid molecules. The disaccharide was observed at *m/z* 519.3950 and with the polyethoxyspacer at *m/z* 668.4015 (data not shown).

5.2.2.2. CID-MS/MS analyses of the protonated molecule

In order to confirm the fragmentation pathway of molecule **8**, and also to check the possibility of the creation "in situ" of the $[C\text{-glycoside}+H]^+$ and $[C\text{-glycoside}+H\text{-}N_2]^+$ ions species, low-collision energy tandem mass spectrometry analysis of the protonated molecule $[M+H]^+$ was performed (**Figure 5.17**). This indicated the presence of the expected product ions: $[M+H\text{-}N_2]^+$ at *m/z* 1008.35, $[SugarSpacer+H]^+$ at *m/z* 668.41 and $[Cholestadiene+H]^+$ at *m/z* 369.74. Other product ions such as the $[Sugar\text{-}N_2]^+$ at *m/z* 490.49, and two monosaccharides derived from the oxonium dissacharide structure $[DGal]^+$ at *m/z* 331.49 were detected. The ion at *m/z* 151.53 was deduced to be formed from the loss of three acetic acid molecules from the $[DGal]^+$. The $[C\text{-glycoside}+H]^+$ ion-species at *m/z* 886 was not observed.

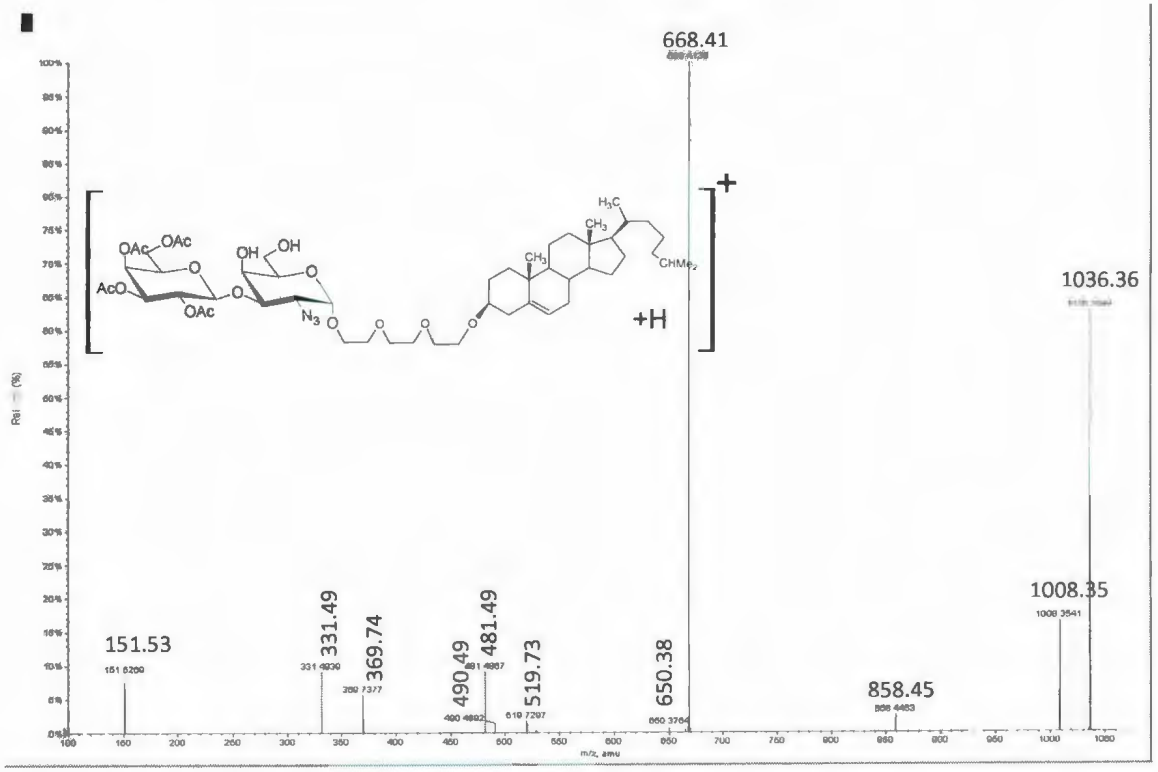

Figure 5.17: CID-MS/MS spectrum of the protonated molecule 8-(cholest-5-en-3-β-yloxy)-3,6-dioxaoctyl 3-*O*-(2,3,4,6-tetra-*O*-acetyl-β-D-galactopyranosyl)-2-azido-2-deoxy-α-D-galactopyranoside (molecule "8") $[M+H]^+$ at *m/z* 1036.36.

It was also assumed that the $[SugarSpacer+H]^+$ product ion gave rise to the ion at *m/z* 519.73, resulting from the excision of the spacer chain and was assigned as $[Sugar+H]^+$ (spectra not shown).

Scheme 5.2 represents the eventual fragmentation pathway of molecule **8**.

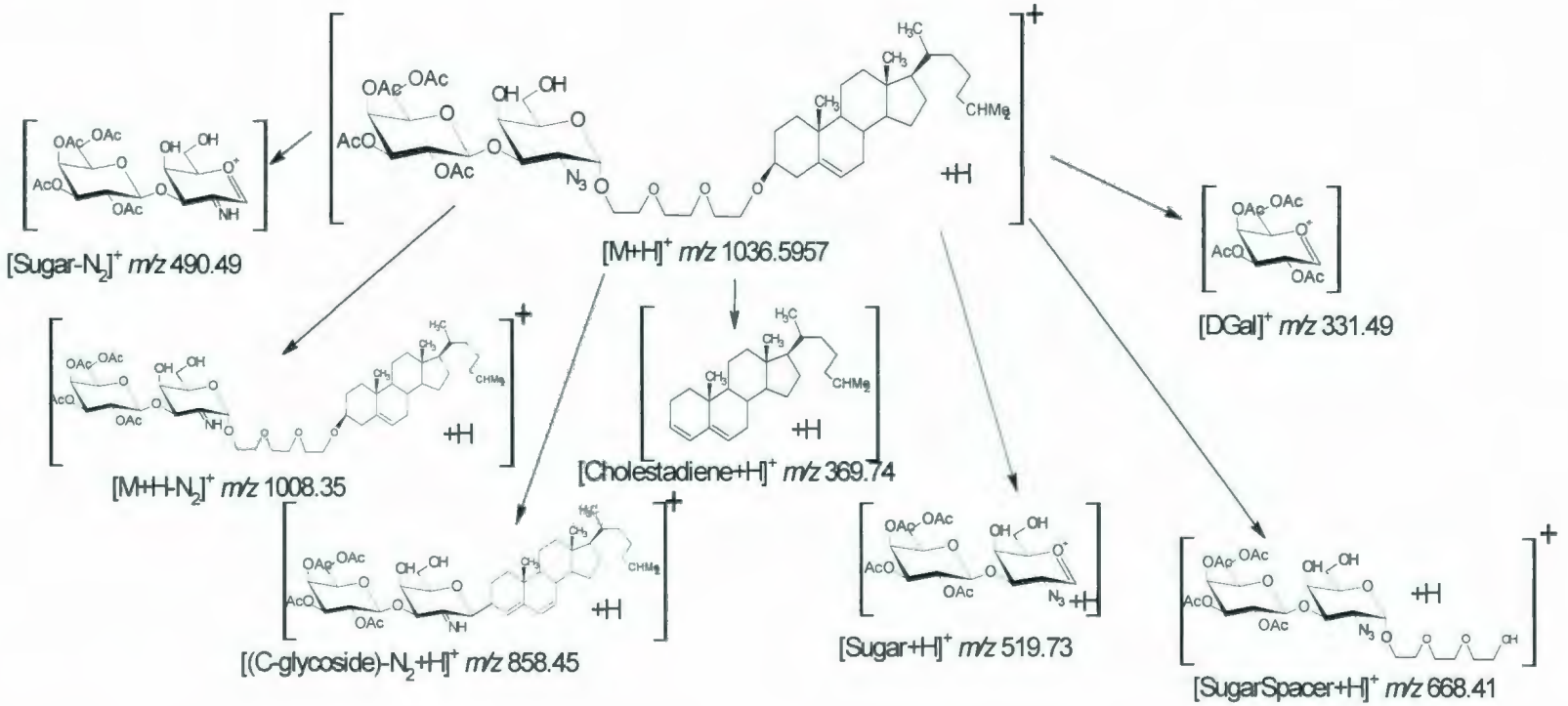

Scheme 5. 2: A possible fragmentation scheme obtained from the isolation of 8-(cholest-5-en-3-β-yloxy)-3,6-dioxaoctyl 3-*O*-(2,3,4,6-tetra-*O*-acetyl-β-D-galactopyranosyl)-2-azido-2-deoxy-α-D-galactopyranoside, molecule "8", protonated molecule $[M+H]^+$ from CID-MS/MS of *m/z* 1036.36

5.2.2.3. CID-MS/MS of the $[M+H-N_2]^+$ ion

The product ion scan of $[M+H-N_2]^+$ was performed to look for the formation of the expected $[Oxonium-N_2]^+$ product ion and also the $[C\text{-}glycoside+H-N_2]^+$ ion-species. The precursor $[M+H-N_2]^+$ ion fragmented into three product ions; unfortunately these were not the one expected. In fact, the $[Cholesta\text{-}3\text{-}ene]^+$ product ion at *m/z* 371.46, and two other fragments were noted: a product ion at *m/z* 648.72, which was assigned as the $[M+H-N_2-DGal-CH_3OH]^+$ ion, and another at *m/z* 617.40 which might be a $[M+H-N_2-DGal-3H_2O]^+$ ion. These ions are represented in **Scheme 5.3**.

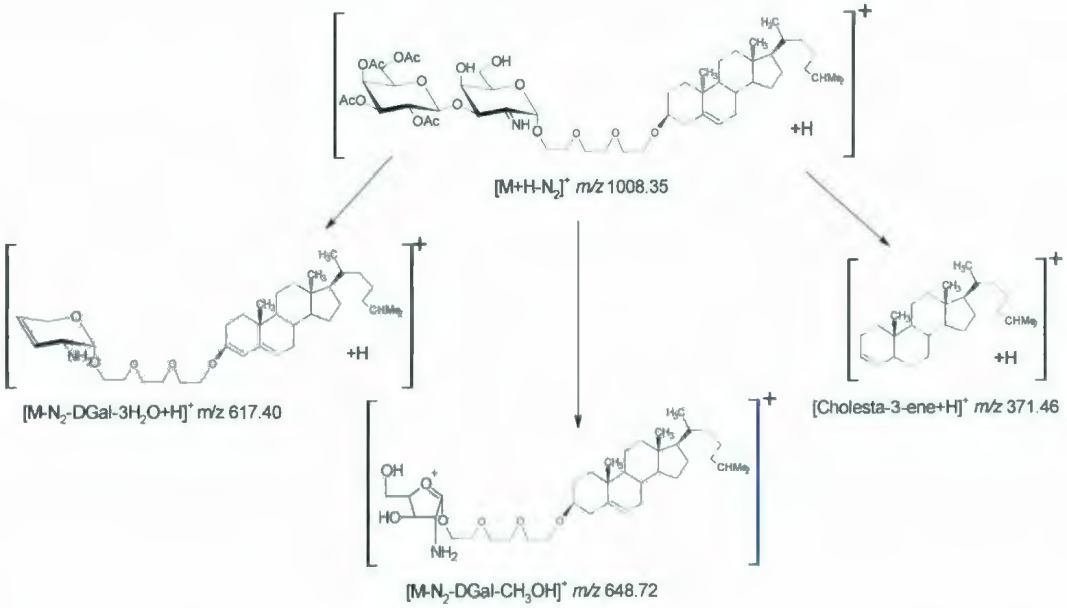

Scheme 5. 3: Proposed fragmentation pathway derived from the second generation tandem mass spectrum of the $[M+H-N_2]^+$ ion, molecule "8".

Scheme 5.3 actually may hint to a remote deactivation from the non-reducing end group to the reducing end group, hence preventing the formation of the expected [C-

glycoside+H-N_2]$^+$ ion-species and the fragmentation of this protonated disaccharide molecule. This demonstrates that there are three competing reactions: the losses of the acetyl groups from the per-*O*-acetylated D-galactose, losses of methanol, and the consecutive elimination of water from the 2-azido-2-deoxy-D-galactosamine.

5.2.2.4. CID-MS/MS of the [SugarSpacer]$^+$ ion

The second-generation CID-MS/MS of the [SugarSpacer]$^+$ at *m/z* 668.57 was conducted to confirm the fragmentation routes of this product ion, and to attempt to observe the two constituent monosaccharides of the disaccharide. It was also anticipated that it would be possible to observe, what is now termed the "azido effect" (namely loss of a N_2 molecule), on the fragmentation of this precursor ion. The fragmentation route for the [Amino-D-GalSpacer]$^+$ ion at *m/z* 668.57 is represented in **Scheme 5.4** and **Figure 5.18**.

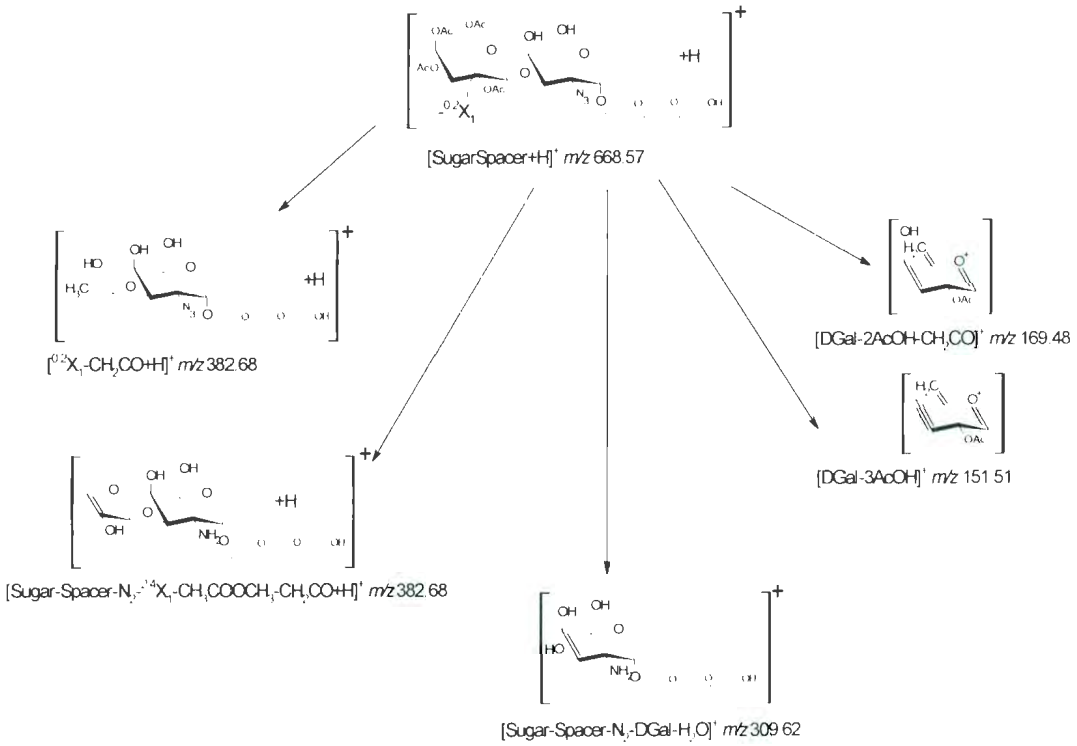

Scheme 5. 4: Proposed fragmentation pathway derived from the tandem mass spectrum of the [SugarSpacer]$^+$ ion at *m/z* 668.57, molecule "8".

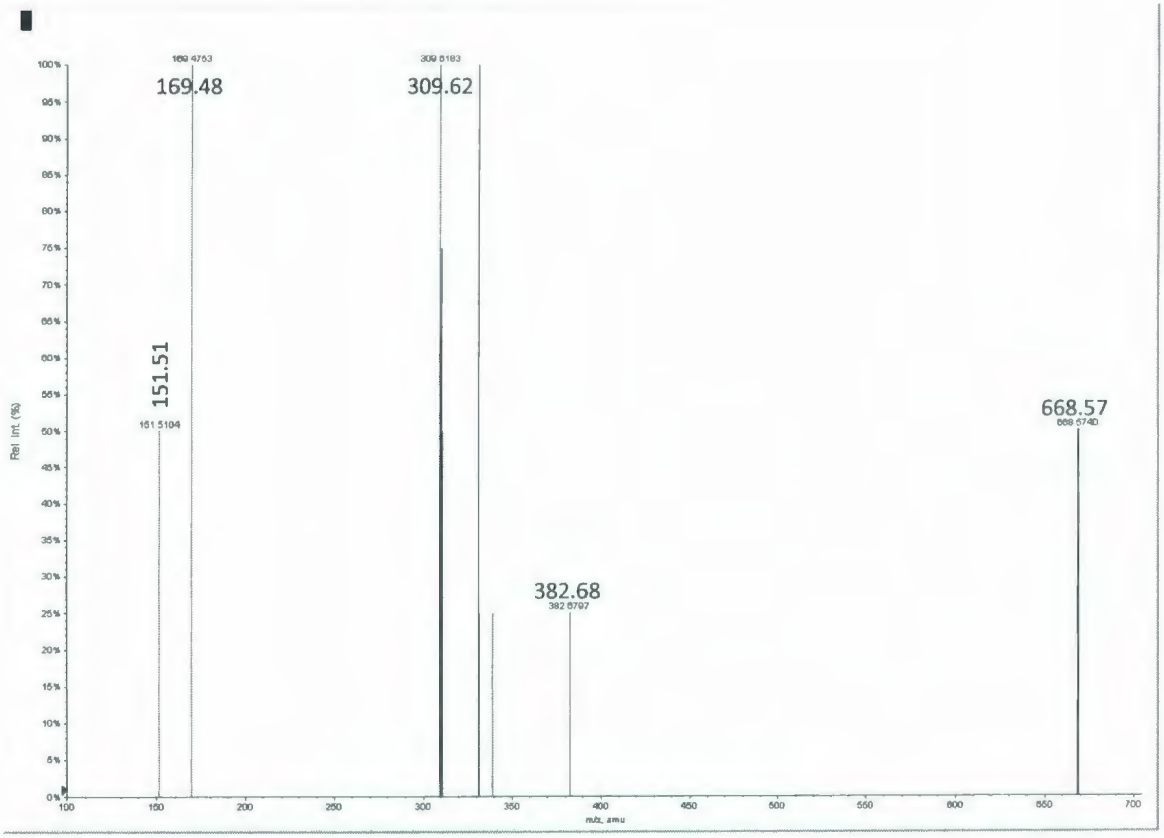

Figure 5.18: CID-MS/MS of the [SugarSpacer+H]$^+$ ion at *m/z* 668.57 issued from the molecule of 8-(cholest-5-en-3-β-yloxy)-3,6-dioxaoctyl 3-*O*-(2,3,4,6-tetra-*O*-acetyl-β-D-galactopyranosyl)-2-azido-2-deoxy-α-D-galactopyranoside (molecule "8")

This MS^2 spectrum shown in **Figure 5.18** demonstrates that the precursor disaccharide ion fragments into its two monomer product ions. The product ion at *m/z* 382.68 was assigned as the [SugarSpacer-$^{2,4}X_1$-CH_3OCOCH_3-N_2+H]$^+$, formed by the elimination of nitrogen and methyl acetate molecules. The second product ion at *m/z* 309.62 occurs by the loss of the per-acetylated galactopyranosyl non-reducing end from the precursor ion.

5.2.2.5. CID-MS/MS of the $[C\text{-glycoside}+H\text{-}N_2]^+$ ion-species

The product ion scan of the $[C\text{-glycoside}+H\text{-}N_2]^+$ ion-species at *m/z* 858.45 was isolated from the CID-MS/MS spectrum of the protonated molecule **8**, and the same conclusions were made as for compound **7**. It was possible to isolate the $[C\text{-glycoside}+H\text{-}N_2]^+$ ion-species, however, no fragments were obtained, which might be due to the per-*O*-acetylated presence on the non-reducing end carbohydrate moiety. In fact, the per-*O*-acetylated groups protect the neoglycolipid and inhibit fragmentation. Another reason could be that the bond connecting the oxonium to the cholestadiene is a strong covalent bond.

5.3. Discussion

In the case of 8-(cholest-5-en-3-β-yloxy)-3,6-dioxaoctyl-3-*O*-(2,3,4,6-tetra-*O*-acetyl-β-D-galactopyranosyl)-2-azido-4,6-*O*-benzylidene-2-deoxy-β-D-galactopyranoside **7**, it was evident that three structural substituents seemed to interfere with the fragmentation routes: i) the presence of the 2-azido group, ii) the partial *O*-acetylation of the non-reducing carbohydrate end moiety and iii) the presence of the 4,6-*O*-benzylidene group on the azido D-galactosamine section. The presence of a possible $[C\text{-glycoside}+H\text{-}N_2]^+$ ion-species was observed, and while it could be isolated, it could not be fragmented. This ion was present during the conventional scan analysis and ClD-MS/MS analysis of the protonated molecule of the respective studied neoglycolipid **7** or **8**. It is hypothesized that this phenomenon could be due to either the low concentration of the sample injected,

or to the presence of the *O*-acetylated non-reducing carbohydrate moiety, which appears to protect the disaccharide molecule from further fragmentation.

In the case of 8-(cholest-5-en-3-β-yloxy)-3,6-dioxaoctyl-3-*O*-(2,3,4,6-tetra-*O*-acetyl-β-D-galactopyranosyl)-2-azido-2-deoxy-α-D-galactopyranoside **8**, it was noted that the ESI-QqTOF-MS was very similar to the one obtained for compound **7**. The ESI-MS afforded the protonated molecule $[M+H]^+$ at *m/z* 1036, the sodiated molecule $[M+Na]^+$ at *m/z* 1058, the $[M+H-N_2]^+$ at *m/z* 1008, the $[C\text{-glycoside}+H-N_2]^+$ ion-species at *m/z* 859, the $[Cholestadiene+H]^+$ at *m/z* 369 and the $[DGal]^+$ at *m/z* 331. The CID-MS/MS of the protonated molecule **8** afforded the $[M+H-N_2]^+$, the $[SugarSpacer+H]^+$ at *m/z* 668, the $[Cholestadiene]^+$ and the $[DGal]^+$ among other ions. It became apparent that as predicted, compound **8** behaves exactly as compound **7** under the same ESI-MS and MS/MS conditions. Therefore three consecutive reactions govern the fragmentation of these compounds. The first one is the creation of the $[C\text{-glycoside}+H-N_2]^+$ ion-species obtained from the reaction occurring between $[Oxonium-N_2]^+$ and the neutral cholestadiene. which occurs in the activated transition ion-molecule complex by an intramolecular mechanism, the second is the spontaneous elimination of a N_2 molecule permitting the change of the 2-azido to a 2-amino group,[73] while the last concerns the partial *O*-acetylation of the non-reducing carbohydrate end moiety.

It is interesting to note that Giorgi's group, at the University of Siena, Italy, analyzed these 2-azido partially per-*O*-acetylated molecules using an ion trap tandem mass spectrometer, and they observed that the $[C\text{-glycoside}+H-N_2]^+$ ion-species was present during conventional scan analysis and also CID-MS/MS of the protonated

molecule. He showed that the abundant $[C\text{-glycoside}+H\text{-}N_2]^+$ ion-species formed could not fragment by MS^3 experiment in agreement with the ESI-QqToF-MS and MS/MS findings. In addition, Amster's group, at the University of Georgia, USA, conducted the same experiments with an FT-ICR-MS^n instrument. In their case the $[C\text{-glycoside}+H\text{-}N_2]^+$ ion-species was obtained in higher relative abundance than the protonated molecule and they were able to isolate it, but it also did not fragment by an MS^3 experiment.

The $[C\text{-glycoside}+H\text{-}N_2]^+$ ion-species formation *in situ* in a cell collision can result from both the $[M+H]^+$ and $[M+H\text{-}N_2]^+$ precursor ions. These findings allowed the proposal of the possible fragmentation pathways of these two precursor ions, which both formed the $[C\text{-glycoside}+H\text{-}N_2]^+$ ion-species. The latter was proposed to be created (as described earlier in **Chapters 1** and **3**) by an intramolecular mechanism.

Even though, the $[C\text{-glycoside}+H\text{-}N_2]^+$ ion-species could not be fragmented, it is believed that the 2-deoxy-2-azido protonated molecule can spontaneously change into a protonated 2-deoxy-2-amino molecule, by loss of a molecule of nitrogen. This newly formed protonated amino molecule would then permit the formation of the $[C\text{-glycoside}+H\text{-}N_2]^+$ ion-species, which is formed by intramolecular reaction between the $[Oxonium\text{-}N_2]^+$ ion and the cholestadiene molecule in the activated ion-molecule complex.

Based on the ESI-MS, CID-MS^2 and MS^3 scans and the proposed fragmentation pathways for **7** and **8**, it has been concluded that the benzylidene group could influence

the fragmentation route as well as the presence of the acetyl-group in the β– or α-D-galactopyranosyl residue of the non-reducing end of the disaccharide group.

Even though, the resistance to fragmentation of the $[C\text{-glycoside}+H\text{-}N_2]^+$ ion-species cannot be fully explained in this chapter, the analyses carried out in **Chapter 6** with molecules **11** and **12** demonstrate that the $[C\text{-glycoside}+H\text{-}N_2]^+$ ion-species can be isolated, if no *O*-acetylated group is present on the saccharide moiety.

Chapter 6: Differentiation of anomers and constitutional isomers of some neoglycolipids

Cholest-5-en-3-β-yl-2-acetamido-2-deoxy-β-D-glucopyranoside (**9**), and 8-(cholest-5-en-3-β-yloxy)-3,6-dioxaoctyl-2-acetamido-2-deoxy-4-*O*-β-D-galactopyranosyl-β-D-glucopyranoside (**10**) are neoglycolipids that have already been analyzed using ESI-CID-MS/MS.[23]

The molecule 8-(cholest-5-en-3-β-yloxy)-3,6-dioxaoctyl-2-acetamido-2-deoxy-3-*O*-β-D-galactopyranosyl-α-D-galactopyranoside **3**, which was studied earlier (**Chapter 3**), is similar to 8-(cholest-5-en-3-β-yloxy)-3,6-dioxaoctyl-2-acetamido-2-deoxy-4-*O*-β-D-galactopyranosyl-α-D-glucopyranoside (**10**), and the cholest-5-en-3-β-yl-2-acetamido-2-deoxy-β-L-glucopyranoside **2** is similar to cholest-5-en-3-β-yl-2-acetamido-2-deoxy-β-D-glucopyranoside **9**. The molecules **3** and **10** are constitutional isomers, whereas **2** and **9** are anomeric diastereoisomers. Furthermore, two azido neoglycolipids numbered **11** (8-(cholest-5-en-3-β-yloxy)-3,6-dioxaoctyl-2-azido-4,6-*O*-benzylidene-2-deoxy-α-D-galactopyranoside) and **12** (8-(cholest-5-en-3-β-yloxy)-3,6-dioxaoctyl-2-azido-4,6-*O*-benzylidene-2-deoxy-β-D-galactopyranoside), which are both anomeric diastereoisomers were analyzed.

In this chapter, some differences are noted in the low-energy CID-MS/MS fragmentation pathways (presence of more diagnostic, higher intensity product ions) according to the changes associated with the anomeric or isomeric effect and the diastereoisomeric difference, due to the change in the chemical structures of some distinct neoglycolipids.

6.1. Differentiation of diastereoisomeric anomers

6.1.1. 8-(Cholest-5-en-3-β-yloxy)-3,6-dioxaoctyl-2-azido-4,6-*O*-benzylidene-2-deoxy-α-D-galactopyranoside (11) vs 8-(cholest-5-en-3-β-yloxy)-3,6-dioxaoctyl-2-azido-4,6-*O*-benzylidene-2-deoxy-β-D-galactopyranoside (12)

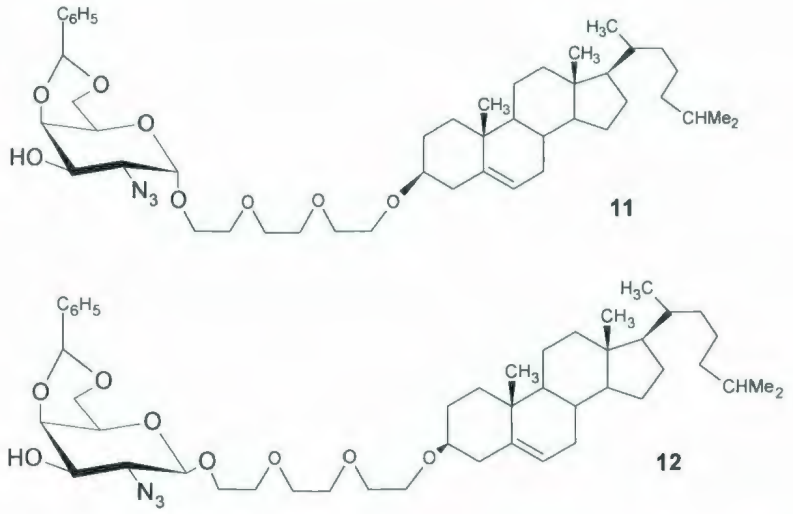

Figure 6.1: Representation of the molecules 11 and 12

It can be observed that the structures of **11** and **12** (**Figure 6.1**) have similarities to those of **7** and **8** as shown previously in **Figure 2.4**. The former are monosaccharides, while the latter are disaccharides. The common point is that both pairs of galactosamine-spacer-cholesteryl compounds possessing a 2-deoxy-2-azido-group, containing a 4,6-*O*-benzylidene group. Compounds **7** and **12** have β-glycosidic linkages and compounds **8** and **11** have α-glycosidic linkages to the cholesterol.

6.1.2. 8-(Cholest-5-en-3-β-yloxy)-3,6-dioxaoctyl-2-azido-4,6-*O*-benzylidene-2-deoxy-α-D-galactopyranoside (11)

The CID-tandem mass spectrum of the protonated molecule $[M+H]^+$ at *m/z* 794.49 isolated from compound **11** gave a similar intensity for the molecular ion (73.64%) and the $[M+H-N_2]^+$ at *m/z* 766.54 (74.55%). According to the structure of **11**, the main expected product ions were the [Cholestadiene+H]$^+$ observed at *m/z* 369.68 and the azido carbohydrate moiety $[DGalN_3]^+$ at *m/z* 276.47, which created the product ion $[DGalN_3-N_2]^+$ at *m/z* 248.49 (**Figure 6.2**).

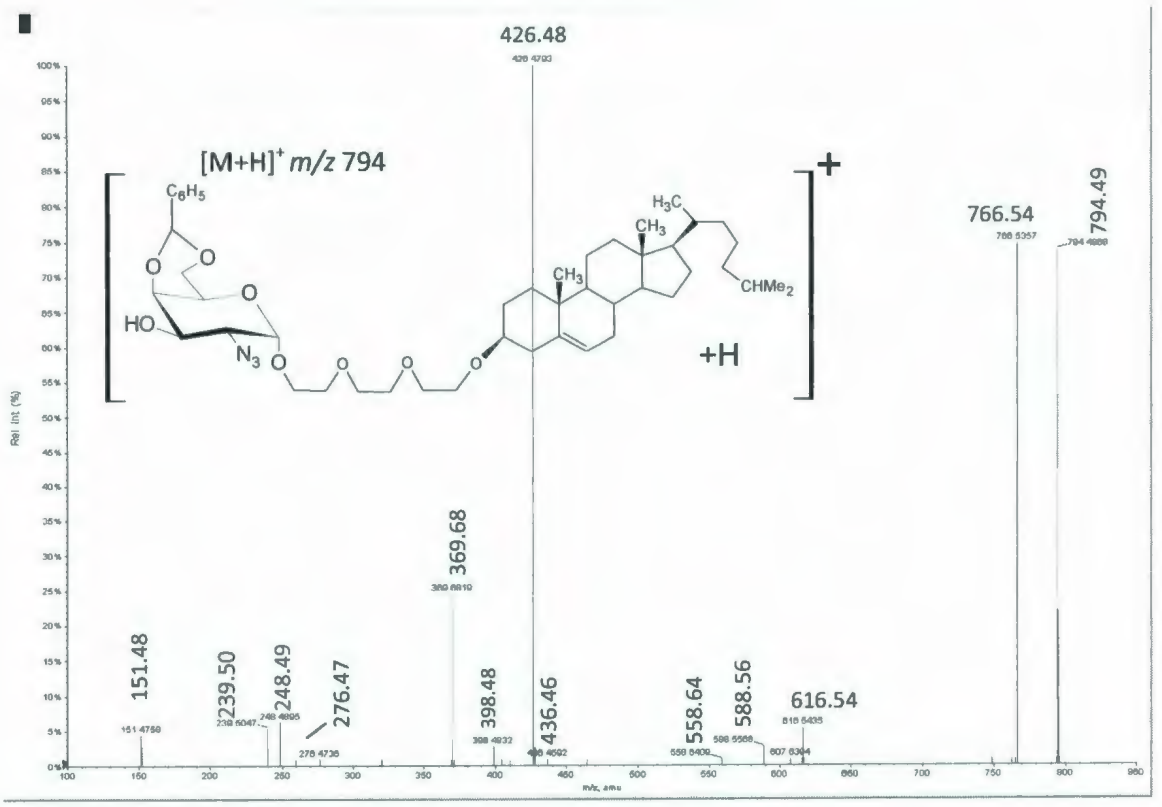

Figure 6.2: Tandem mass spectrum of the protonated molecule $[M+H]^+$ of the compound 8-(cholest-5-en-3-β-yloxy)-3,6-dioxaoctyl-2-azido-4,6-*O*-benzylidene-2-deoxy-α-D-galactopyranoside, molecule "11".

The product ion formed by the polyethoxy spacer linked to the azido carbohydrate (100%) $[\alpha\text{-D-GalN}_3\text{Spacer+H}]^+$ at *m/z* 426.48 was observed. The presence of the product ion at *m/z* 616.54 was noted and was assigned as a $[\text{C-glycoside+H-N}_2]^+$ ion-species (**Figure 6.3**). The product ion at *m/z* 588.56 was assigned as $[\text{M-N}_2\text{-}^{2,4}\text{X}_0]^+$ (**Figures 6.4-6.5**).

Some other ions were also noticed in low abundance. The proposed fragmentation pathways of ions derived from the protonated molecule $[\text{M+H}]^+$ are presented in **Figures 6.4** to **6.5**.

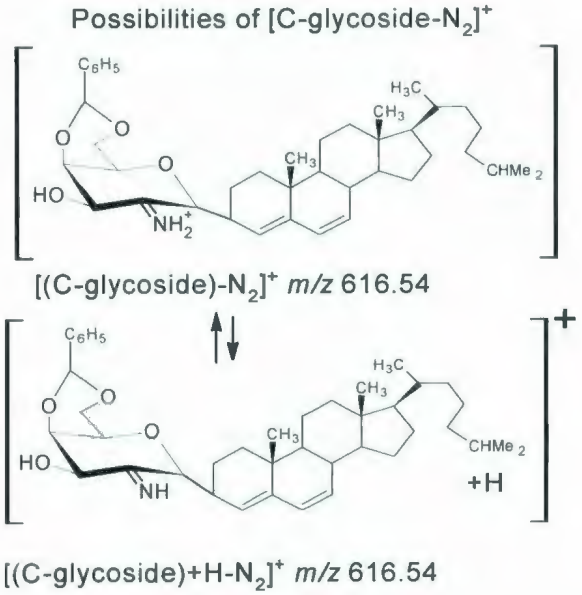

Figure 6.3: Possible structures for the product ion at *m/z* 616 obtained during the CID-MS/MS of the $[\text{M+H}]^+$ protonated molecule, molecule "11".

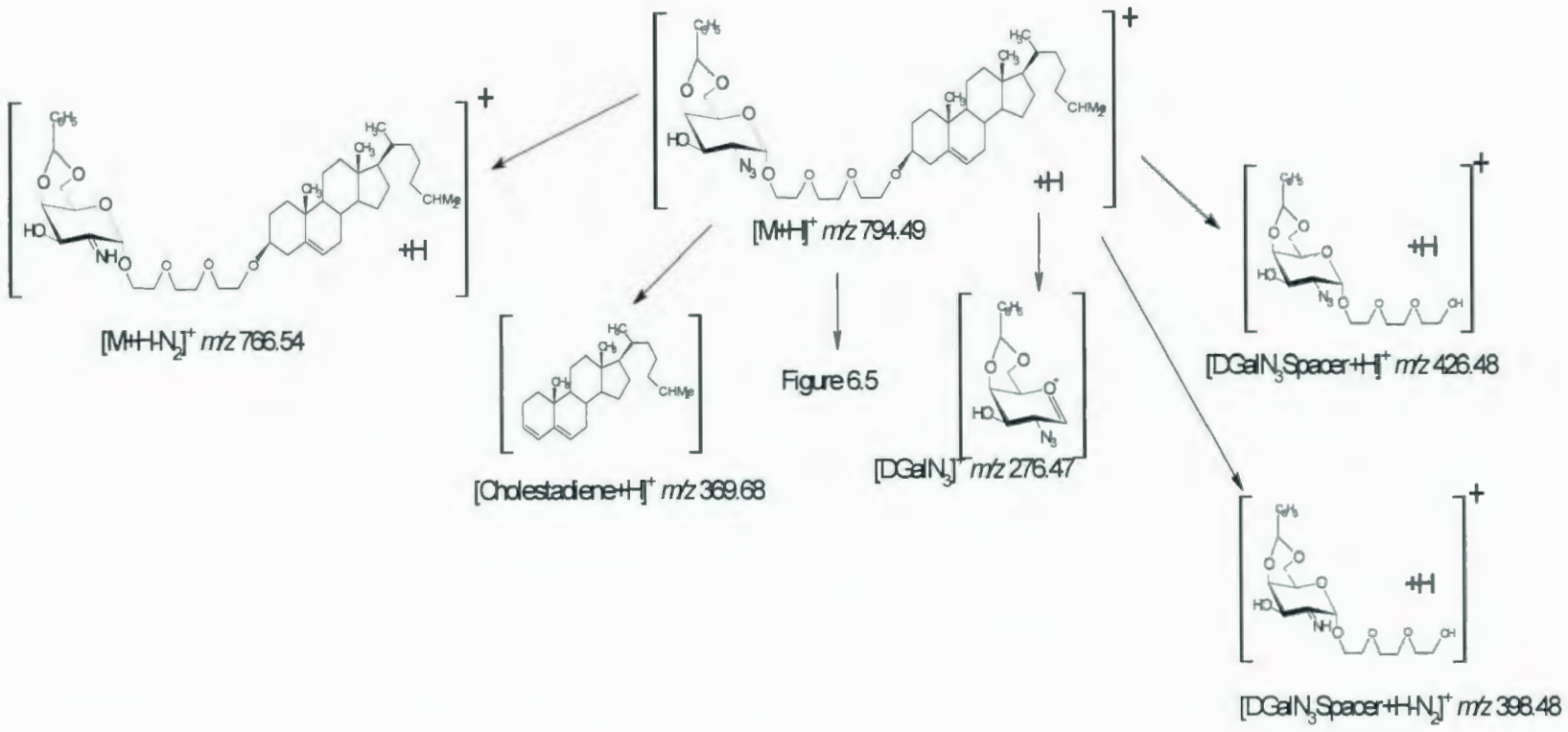

Figure 6.4: Possible fragmentation pathway of the protonated molecule 8-(cholest-5-en-3-β-yloxy)-3,6-dioxaoctyl-2-azido-4,6-*O*-benzylidene-2-deoxy-α-D-galactopyranoside (molecule "11", part 1)

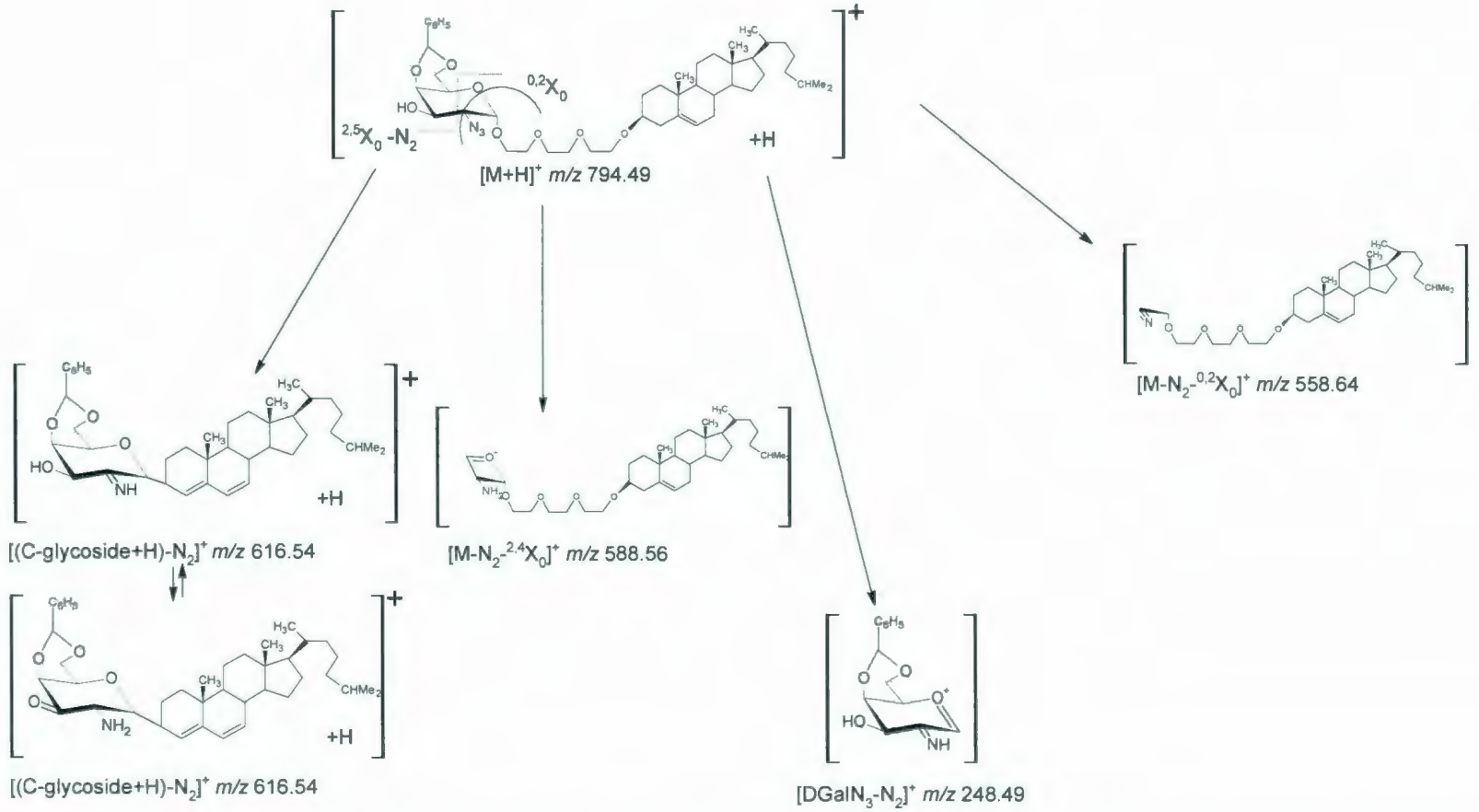

Figure 6.5: Possible fragmentation pathway of the protonated molecule 8-(cholest-5-en-3-β-yloxy)-3,6-dioxaoctyl-2-azido-4,6-*O*-benzylidene-2-deoxy-α-D-galactopyranoside (molecule "11", part 2)

Acquisition of the CID-MS/MS of the protonated molecule $[M+H]^+$ at *m/z* 794.49 was also obtained by increasing the collision energy, to observe whether or not the [C-glycoside+H-N_2]$^+$ ion-species at *m/z* 616.54 disappeared. In addition, the precursor ion scan of [M+H-N_2]$^+$ at *m/z* 766.54 was effected in order to determine if this ion-species arises directly from this ion. Two product ions at *m/z* 408.62 and *m/z* 436.40 were observed when the CE=10 eV. When the CE was increased to 15 eV, only the product ion at *m/z* 408.62 appeared.

The product ion [C-glycoside+H-N_2]$^+$ at *m/z* 616.54 was also selected for a third-generation product ion scan (*quasi*-MS^4). However, even by changing the collision parameters, the ion did not fragment.

6.1.3. 8-(Cholest-5-en-3-β-yloxy)-3,6-dioxaoctyl-2-azido-4,6-*O*-benzylidene-2-deoxy-β-D-galactopyranoside (12)

The CID-MS/MS analyses of the protonated molecule of compounds **11** and **12** were very similar. They both gave the protonated molecule $[M+H]^+$ at *m/z* 794, the [M+H-N_2]$^+$ at *m/z* 766, the cholestadiene at *m/z* 369, the [$DGalN_3$+Spacer]$^+$ at *m/z* 426 andthe [$DGalN_3$]$^+$ at *m/z* 276. Note that the ion corresponding to the formation of the [C-glycoside+H-N_2]$^+$ ion-species at *m/z* 644.55 was identified.

6.1.3.1. CID-MS/MS of the protonated molecule

The CID-MS/MS spectrum of the protonated molecule $[M+H]^+$ at *m/z* 794.50 was acquired (**Figure 6.6**) and yielded the product ion $[M+H-N_2]^+$ at *m/z* 766.51, due to the elimination of the N_2 molecule caused by its instability.[74] The $[SugarSpacer+H]^+$ product ion was formed at *m/z* 426.47 (100%) and the $[Cholestadiene+H]^+$ product ion at *m/z* 369.67. The fragmentation of the $[DGalN_3]^+$ oxonium at *m/z* 276.45 resulting from the cleavage of the disaccharide moiety was noted. The product ions at *m/z* 248.46 and at *m/z* 239.50 were assigned respectively as the product ions $[DGalN_3-N_2]^+$ and $[DGalN_3-N_2-CH_3]^+$, and the $[C\text{-}glycoside+H-N_2]^+$ ion-species was observed at *m/z* 616.57. It is possible that the ion at *m/z* 588.59 is a derivative of the $[C\text{-}glycoside+H-N_2]^+$ ion-species formed by loss of a molecule of methanol assigned as $[C\text{-}glycoside+H-N_2-MeOH]^+$.

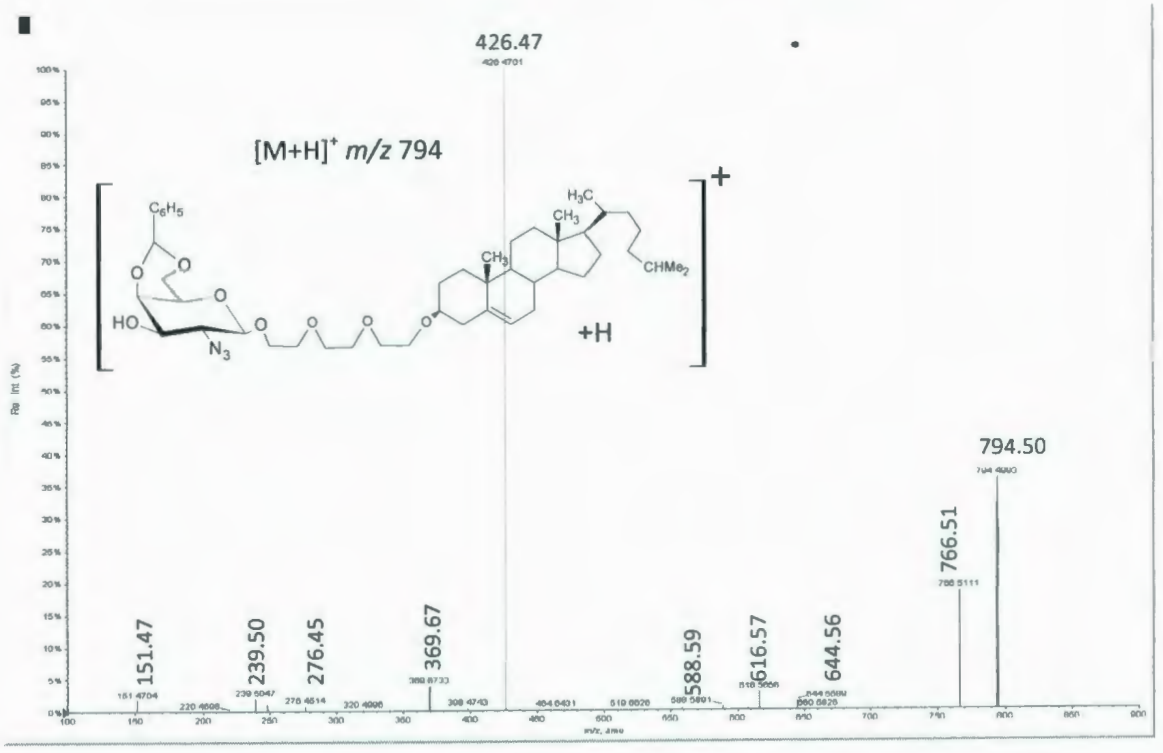

Figure 6.6: Tandem mass spectrum of the protonated molecule $[M+H]^+$ of the 8-(cholest-5-en-3-β-yloxy)-3,6-dioxaoctyl-2-azido-4,6-di-*O*-benzylidene-2-deoxy-β-D-galactopyranoside (molecule "12")

6.1.3.2. CID-MS/MS of the $[M+H-N_2]^+$

To determine if the product ion $[M+H-N_2]^+$ possessing the β-anomeric configuration would fragment, this latter was selected for a *quasi*-MS^3 scan (**Figure 6.7**). The second-generation product ion scan revealed the presence of the [C-glycoside+H-N_2]$^+$ ion-species at *m/z* 616.57, the [M-N_2-$^{0,2}X_0$]$^+$ ion at *m/z* 558.64 and, finally, the [C-glycoside-N_2-C_6H_5CHO-C_2H_5OH-$^{2,4}X_0$]$^+$ at *m/z* 436.45 according to the nomenclature of Domon and Costello[61] (**Figure 6.7** and **Scheme 6.1**).

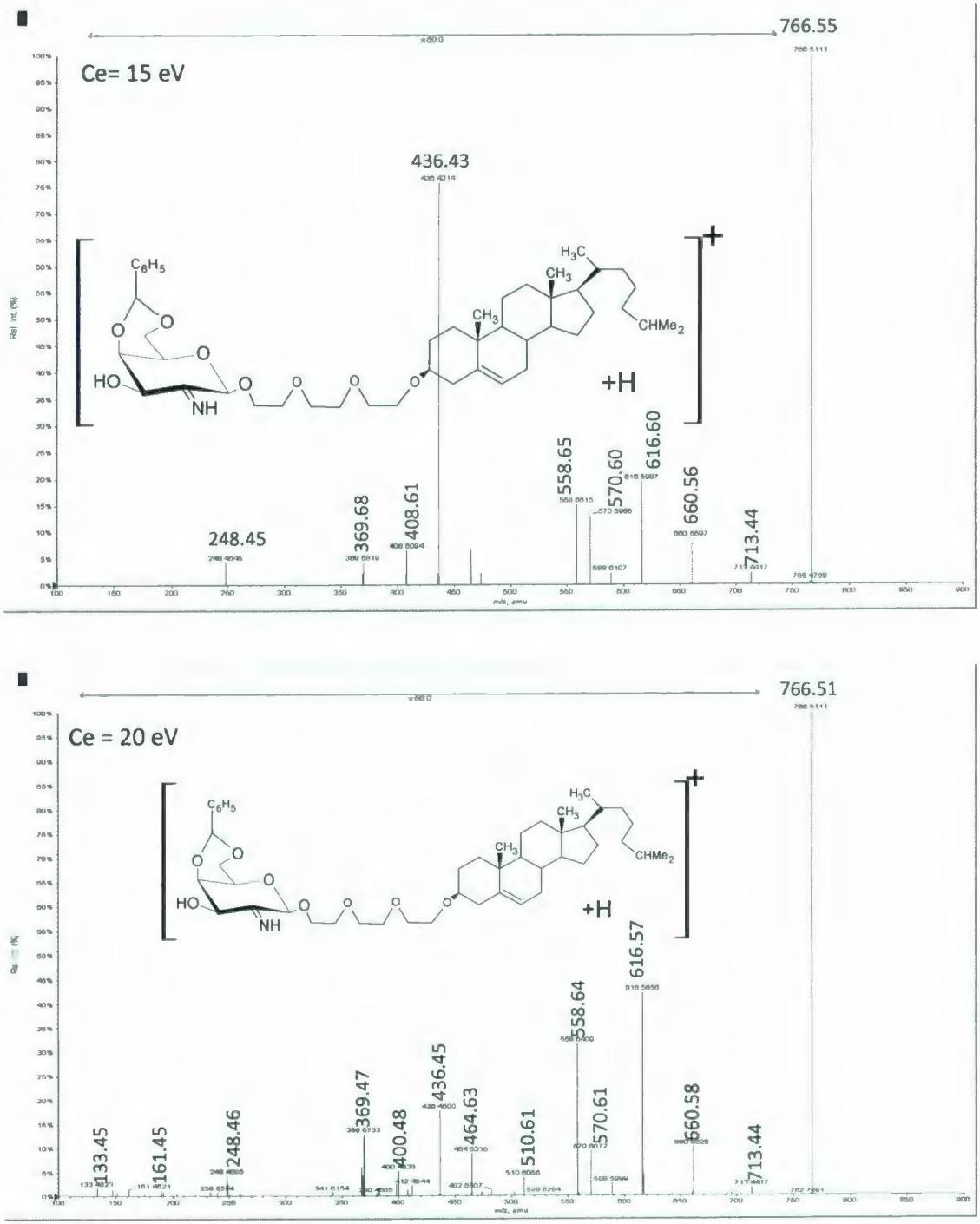

Figure 6.7: CID-MS/MS of the ion $[M+H-N_2]^+$ with different collision energies

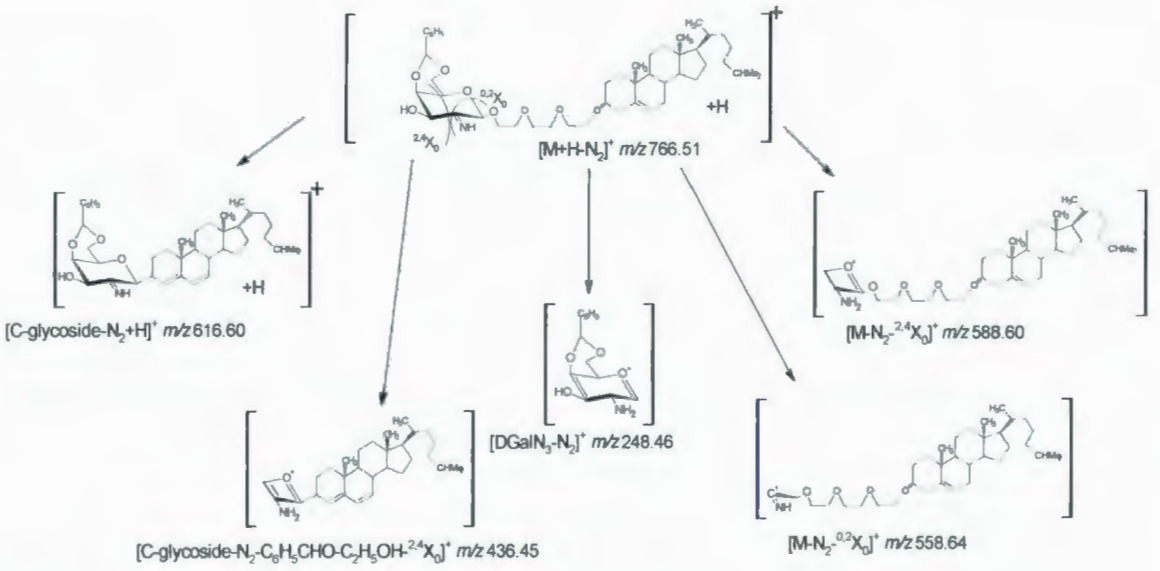

Scheme 6. 1: Presumed product ions formed in the acquisition of *quasi*-MS^3 of the ion $[M+H-N_2]^+$

6.1.3.3. CID-MS/MS of the $[C\text{-glycoside}+H]^+$ ion-species

The formed $[C\text{-glycoside}+H]^+$ product ion-species was observed at *m/z* 644.56 in the CID-MS/MS of the protonated molecule and was also present in the conventional ESI-MS. Usually, it has been observed that the CID-MS/MS of the protonated molecule $[M+H]^+$ affords the expected $[C\text{-glycoside}+H]^+$ product ion and the product ions $[Oxonium]^+$ at *m/z* 248.09 and $[Cholestadiene+H]^+$ at *m/z* 369.31. However, in this case, the product ions obtained were different, due to the presence of the azido group, the 2-deoxy-position of the aminosugar, and the 4,6-di-*O*-benzylidene group attached to the non-reducing sugar moiety of the disaccharide glycosyl portion of the neoglycolipid. Obviously, it is reasonable to expect that the product ion scan of the precursor $[C\text{-glycoside}+H]^+$ ion would form the product ions $[Cholestadiene+H]^+$ at *m/z* 369.68 and

$[DGalN_3\text{-}N_2]^+$ at *m/z* 248.45. The CID-MS/MS of the $[C\text{-glycoside+H}]^+$ ion-species is tentatively depicted in **Scheme 6.2**.

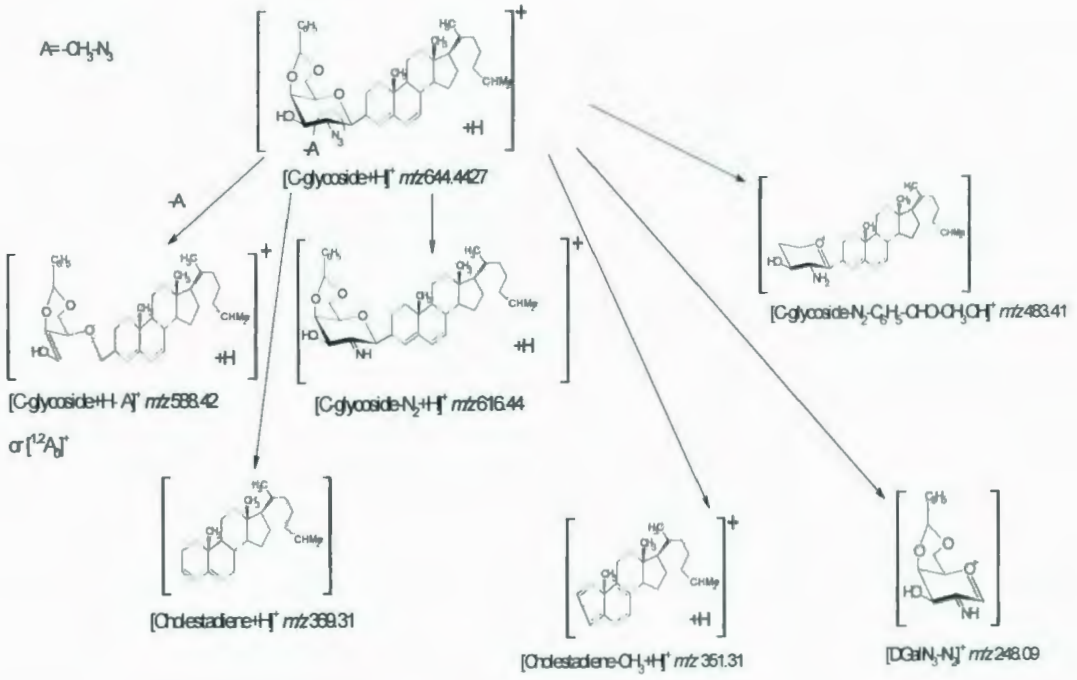

Scheme 6. 2: Possible$[C\text{-glycoside+H}]^+$ fragmentation pathway derived from the second generation tandem mass spectrum

Scheme 6.2 shows that in the second-generation tandem mass spectrum, the $[C\text{-glycoside+H}]^+$ ion-species breaks down spontaneously to the product ion $[C\text{-glycoside+H-N}_2]^+$. In addition, the selected precursor ion creates the diagnostic product ions $[Cholestadiene+H]^+$ and $[DGalN_3\text{-}N_2]^+$.

6.1.3.4. CID-MS/MS of the [C-glycoside+H-N_2]$^+$ ion-species

The third-generation product ion scan (*quasi*-MS^4) of the precursor ion [C-glycoside+H-N_2]$^+$ at *m/z* 616.57 was accomplished more easily than the second-generation CID-MS/MS of the precursor ion [C-glycoside+H]$^+$ at *m/z* 644.57. In fact, only two product ions were observed: the [Oxonium-N_2]$^+$ ion at *m/z* 248.48 and the [Cholestadiene+H]$^+$ ion at *m/z* 369.67 (**Figure 6.8**).

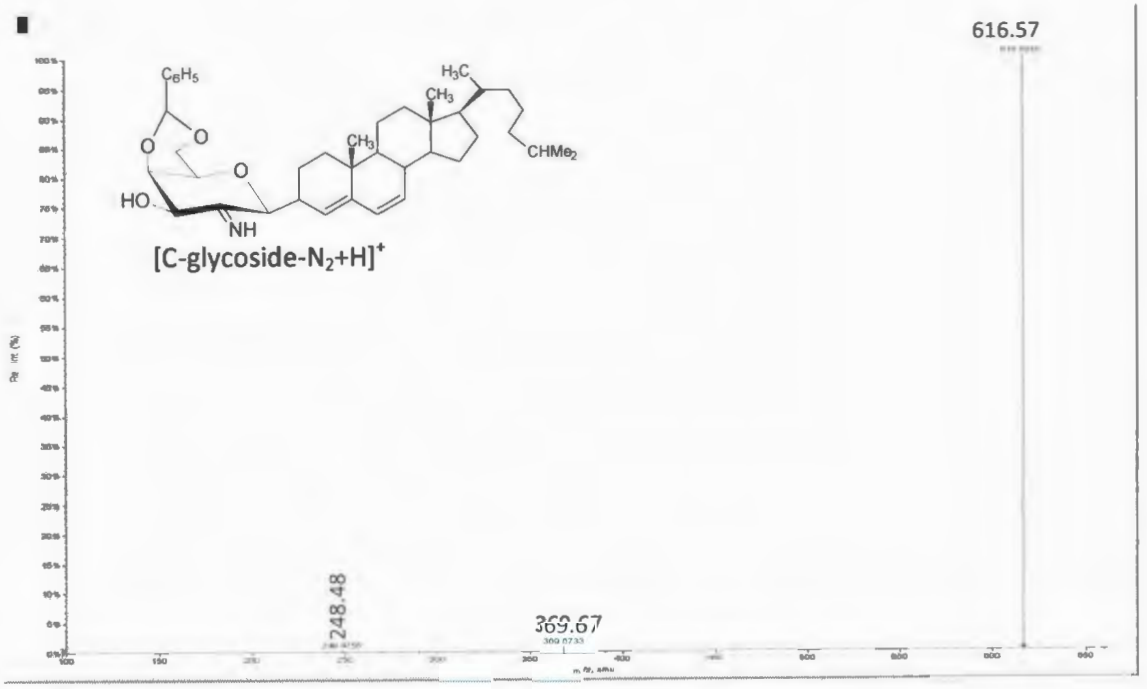

Figure 6.8: Third-generation tandem mass spectrometry of the [C-glycoside+H-N_2]$^+$ product ion at *m/z* 616.57, derived from the 8-(cholest-5-en-3-β-yloxy)-3,6-dioxaoctyl-2-azido-4,6-*O*-benzylidene-2-deoxy-β-D-galactopyranoside (molecule "12")

6.1.4. Discussion

In this study, the product ion scans of the protonated molecule $[M+H]^+$ of compounds **11** and **12** are different and in both scans the $[C\text{-glycoside}+H\text{-}N_2]^+$ ion-species could be observed. However, the molecule **12** also presented the $[C\text{-glycoside}+H]^+$ ion- species. It is proposed that the α-anomeric configuration of compound **11** may be the main reason for the lack of fragmentation of the $[C\text{-glycoside}+H\text{-}N_2]^+$ ion-species.

Table 6.1 shows the differences in abundance of the diagnostic product ions obtained from the two different tandem mass spectra of compounds **11** and **12** (**Figures 6.2** and **6.6**).

Table 6. 1: Comparison of the product ion relative intensities and *m/z* obtained during the acquisition of the CID-MS/MS of both molecules 11 and 12

Ion	11	11 Relative intensity	12	12 Relative intensity
	m/z	(%)	*m/z*	(%)
$[M+H]^+$	794.49	73.64	794.50	35.83
$[M+H-N_2]^+$	766.54	74.55	766.51	18.40
$[C\text{-glycoside}+H]^+$	–	–	644.56	0.07
$[C\text{-glycoside}+H-N_2]^+$	616.54	5.45	616.57	2.79
$[M+H-N_2-{}^{2,4}X_0]^+$	588.56	2.73	588.59	0.58
$[M-N_2-{}^{0,2}X_0]^+$	558.64	0.91	558.62	0.26
$[DGalN_3Spacer]^+$	426.48	100.00	426.47	100.00
$[DGalN_3Spacer+H-N_2]^+$	398.48	2.73	398.47	0.45
$[Cholestadiene+H]^+$	369.68	24.55	369.67	3.82
$[DGalN_3]^+$	276.47	0.91	276.45	0.84
$[DGalN_3-N_2]^+$	248.49	6.36	248.46	1.03
$[DGalN_3-C_6H_5CH-2H_2O]^+$	151.48	4.55	151.47	1.71

The relative abundance of the protonated molecule $[M+H]^+$ was 73.64 % in the CID-MS/MS of the α-anomeric structure, whereas the corresponding relative abundance for the β-anomer was equivalent to 35.83% (**Table 6.1**).

The following graphic (**Figure 6.9**) represents a comparison of the abundances obtained from the fragmentation of the protonated molecules of both molecules **11** and **12**.

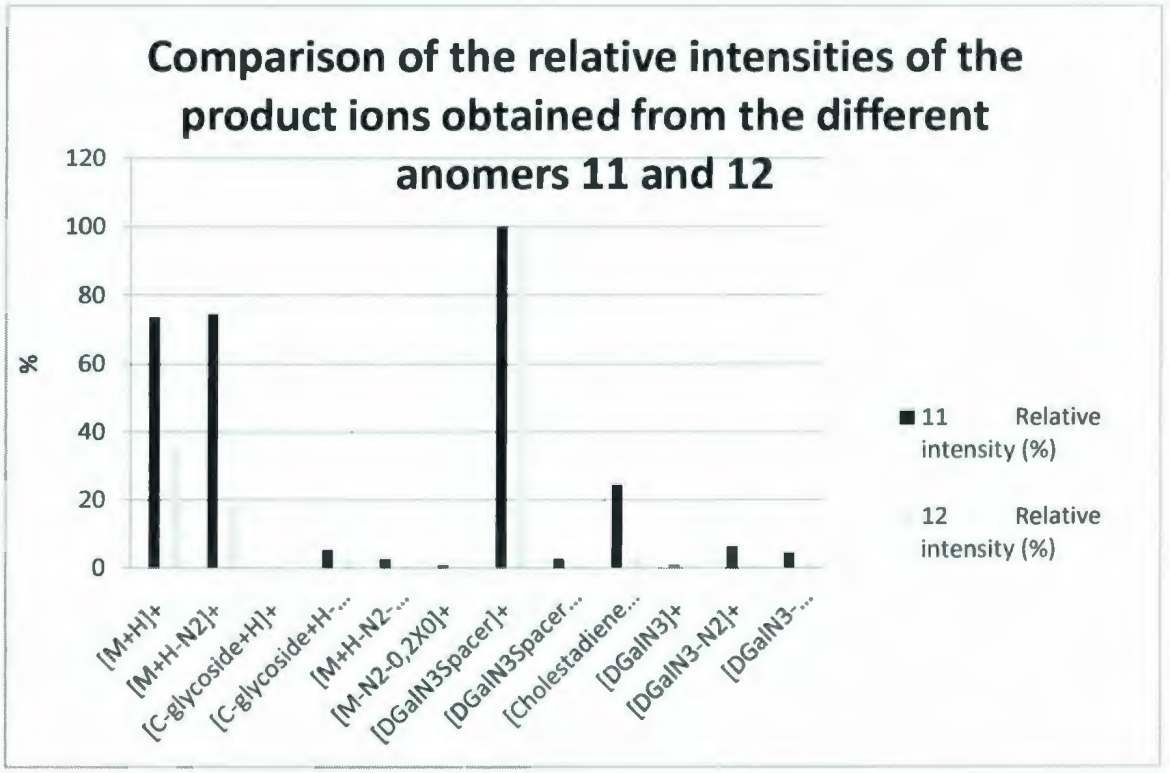

Figure 6.9: Comparison of the relative intensities of the product ions obtained during tandem mass spectrometry of the molecules 8-(cholest-5-en-3-β-yloxy)-3,6-dioxaoctyl-2-azido-4,6-*O*-benzylidene-2-deoxy-α-D-galactopyranoside ("11") and 8-(cholest-5-en-3-β-yloxy)-3,6-dioxaoctyl-2-azido-4,6-*O*-benzylidene-2-deoxy-β-D-galactopyranoside ("12")

It is well known that carbohydrate β-anomers are thermodynamically less stable than the α-anomers.[72] A β-anomer has an eclipsed configuration[72] while the α-anomer has the less energetically favored staggered conformation. For example, the anomerization in solution (mutarotation) of a β-anomer that forms the α–anomeric isomer was observed in the 1920's by Isbell. He also observed that a β-D-glucopyranose reacts faster with bromine than the α-anomer.[72] It has been reported previously that the β-anomeric glycosides fragmented more easily than the α-anomers during electron ionization high energy collision CID-MS/MS analyses.[70,73,74,75,76] It would be reasonable to expect that

this phenomenon would also apply for low energy CID-MS/MS analyses obtained using ESI ionization of the protonated molecule **11** having the α-configuration *vis-a-vis* the protonated molecule **12** having the β-configuration. However, the ESI-QqToF-MS and CID-QqTOF-MS/MS analyses obtained did not support these observed features, as it was shown, that the α-anomer **11** formed more abundant fragment ions.

It is interesting to note that a series of reactions were probably occurring *in situ* the collision cell like for the molecules **7** and **8** studied in **Chapter 5**. These reactions were: i) the excision of the spacer; ii) elimination of the N_2 molecule from the protonated molecule; iii) formation of the $[C\text{-glycoside}+H]^+$ ion-species, as well as the formation of the $[C\text{-glycoside}+H\text{-}N_2]^+$ ion-species. The last ion gave rise to the expected $[Oxonium\text{-}N_2]^+$ ion and the protonated molecule of cholesta-3,5-diene **(Scheme 6.3)**.

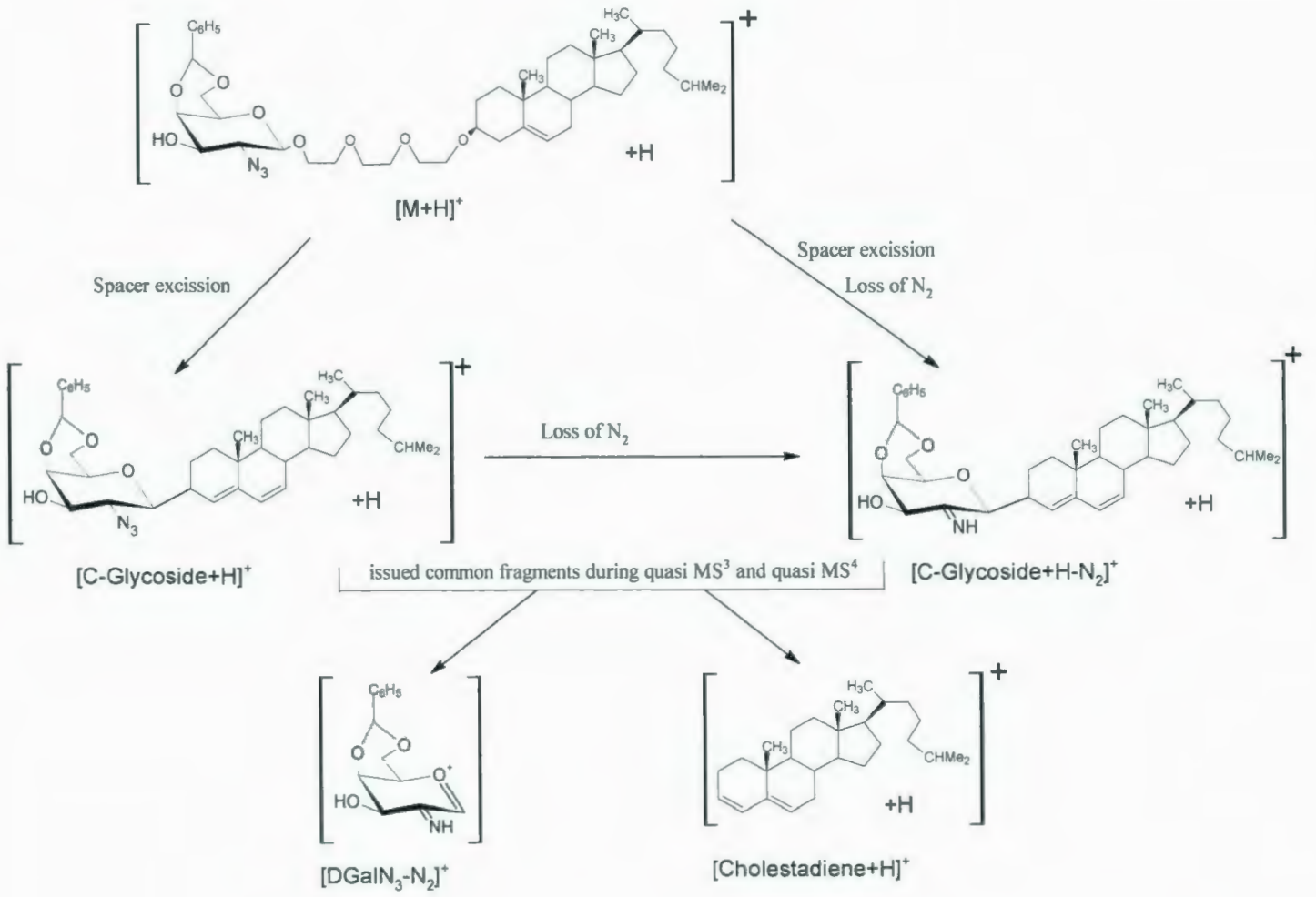

Scheme 6. 3: Possible consecutive reactions occurring *in situ* in the cell collision.

Figure 6.9 represents the relative abundance differences between both anomers. As seen in **Table 6.1**, the α-anomer seems to create product ions having a higher relative abundance than those from the β-anomer. This seems to contradict the findings obtained by electron ionization in conjunction with high-energy collision CID-MS/MS analyses.[70,73,74,75,76] In **Table 6.1**, which summarizes the fragmentation data, it was observed that the β-anomer produced an additional product ion, presumably due to its relative instability compared to the protonated molecule of the α–anomer. Note that it has previously been reported in several articles that β-structures give more fragment ions than the α-anomer.[73,76]

In addition, the $[C\text{-glycoside}+H\text{-}N_2]^+$ ion-species was found in both cases, and could be isolated and fragmented into the $[Oxonium\text{-}N_2]^+$ ion and the protonated molecule of $[Cholestadiene+H]^+$. This could not be accomplished with molecules **7** and **8**, due to the protection afforded by the per-*O*-acetylated groups present on the carbohydrate moiety.

6.1.5. Cholest-5-en-3-β-yl-2-acetamido-2-deoxy-β-L-glucopyranoside (2) vs cholest-5-en-3-β-yl-2-acetamido-2-deoxy-β-D-glucopyranoside (9)

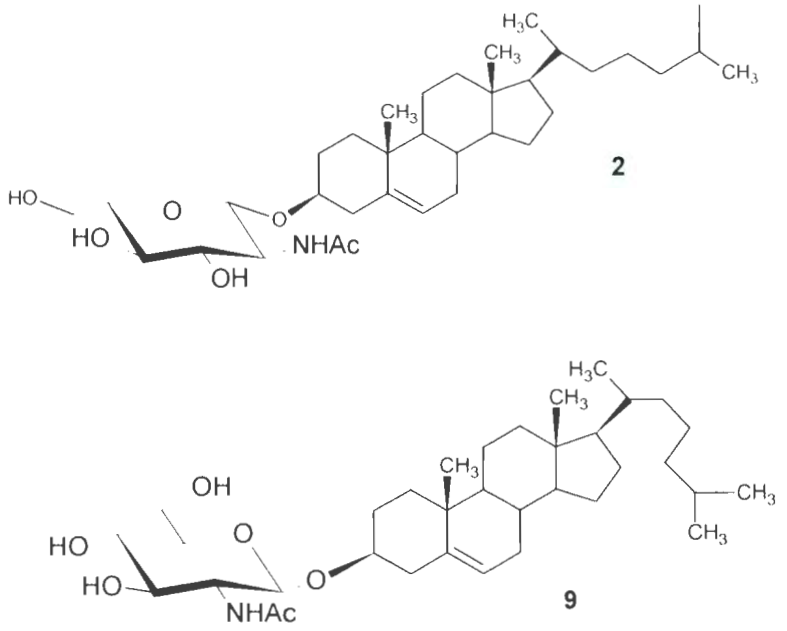

Figure 6.10: Representation of molecules 2 and 9

The ESI-MS of compound **2** gave the expected fragment ions such as the protonated molecule $[M+H]^+$ at *m/z* 590, the [Cholestadiene+H]$^+$ ion at *m/z* 369, the [SugarOH]$^+$ ion at *m/z* 222 and the [Oxonium]$^+$ ion at *m/z* 204, as well as its derivatives (data not shown). The ESI-MS of compound **9** gave the same expected fragment ions as molecule **2** (data not shown). The product ion scans of the protonated molecules **2** and **9** (**Figure 6.10**) are shown in **Figures 6.11** and **6.12**.

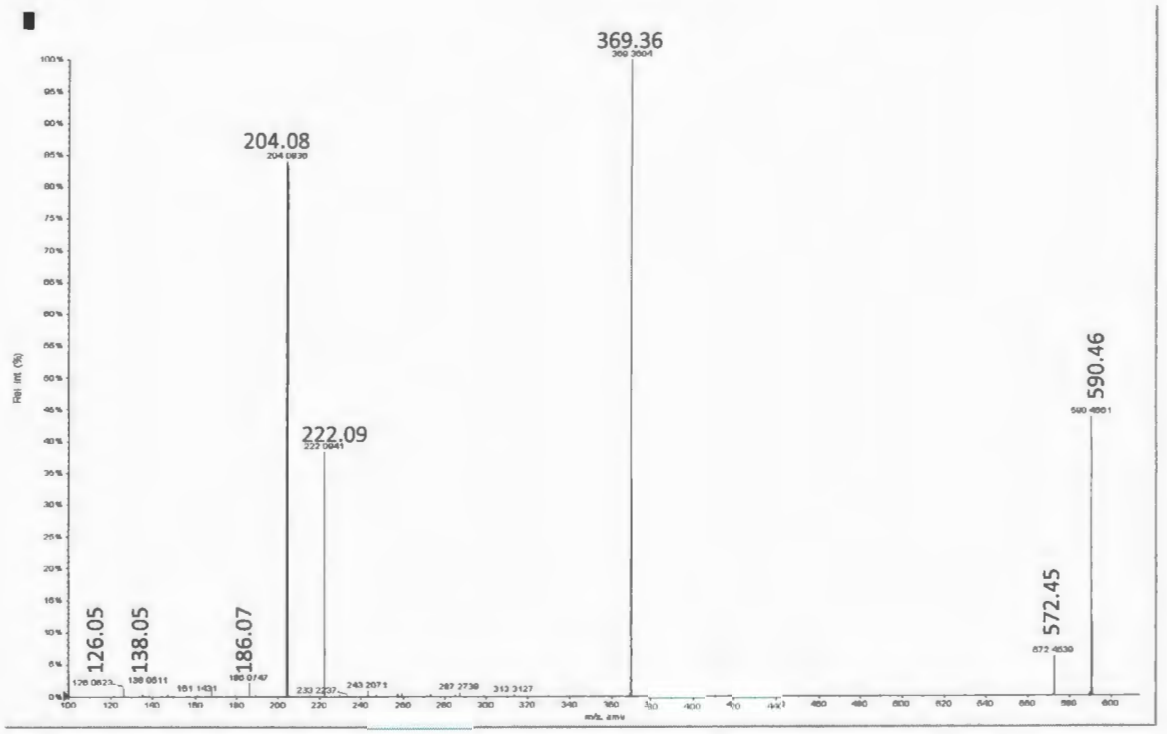

Figure 6.11: Low energy collision tandem mass spectrum of the protonated molecule of cholest-5-en-3-β-yl-2-acetamido-2-deoxy-β-D-glucopyranoside $[M+H]^+$ (molecule "9")

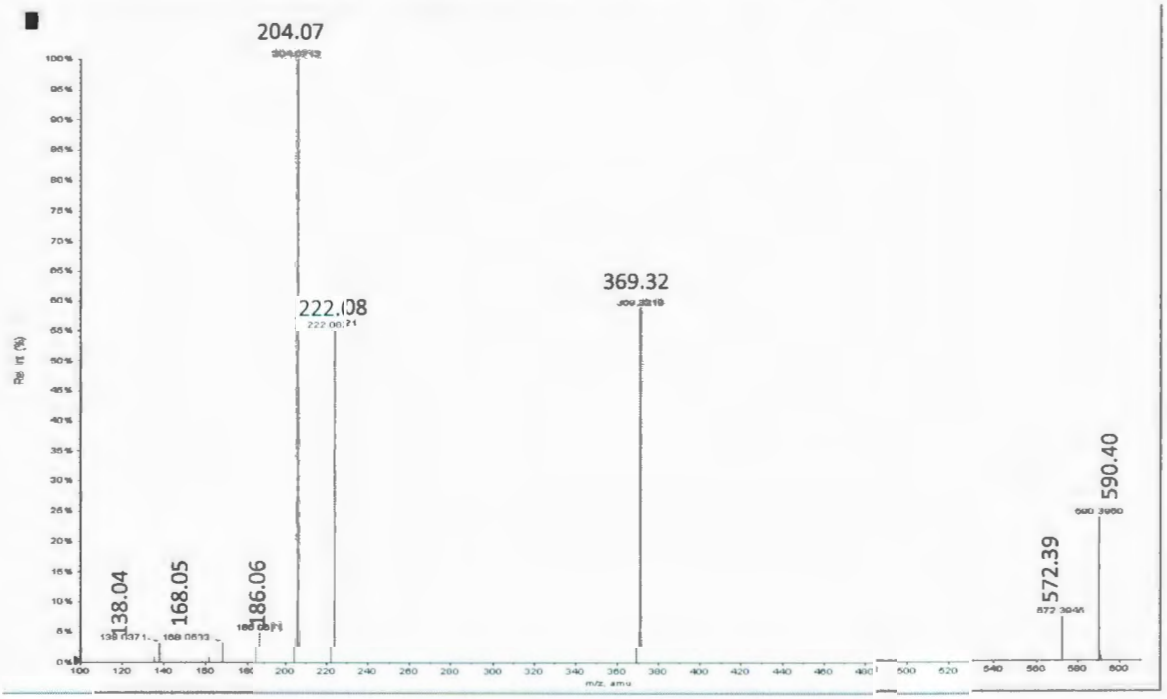

Figure 6.12: Low energy collision tandem mass spectrum of the protonated molecule cholest-5-en-3-β-yl-2-acetamido-2-deoxy-β-L-glucopyranoside $[M+H]^+$ (molecule "2")

The abundances of the product ions obtained in both cases are summarized in **Table 6.2**. It should be noted that, for these two CID-MS/MS analyses, the fragmentation patterns are almost the same, even though the $[Oxonium\text{-}2H_2O\text{-}CH_2CO]^+$ product ion did not appear in the case of **2**. Even though the relative abundance for the protonated molecule and the cholestadiene were higher for **9** than for **2**, it appeared that the precursor ion scan of the β-L-configuration **9** produced a higher relative abundance for all the diagnostic product ions. In fact, the $[GlcNAc]^+$ product ion at *m/z* 204.08 was found to be the base peak for compound **9**, and the different fragments derived from the $[Oxonium]^+$ gave almost twice the relative abundance than the value obtained with the structure D (**9**). Finally, the abundance of the $[C\text{-}glycoside+H]^+$ ion-species is ~ 1.15 % higher in the case of **2** than **9**.

Table 6. 2: Relative intensities and *m/z* obtained for each product ions, when acquiring the tandem mass spectrometry of the protonated molecule $[M+H]^+$ of the molecules 2 and 9

Ion	2 *m/z*	2 Relative intensity (%)	9 *m/z*	9 Relative intensity (%)
$[M+H]^+$	590.40	23.58	590.46	43.74
$[C\text{-}glycoside+H]^+$	572.39	7.32	572.45	6.18
$[Cholestadiene+H]^+$	369.32	58.54	369.36	100.00
$[SugarOH]^+$	222.08	55.28	222.09	38.32
$[Oxonium]^+$	204.07	100.00	204.08	84.05
$[Oxonium\text{-}H_2O]^+$	186.06	4.88	186.07	2.14
$[Oxonium\text{-}2H_2O]^+$	168.05	3.25	168.07	1.60
$[Oxonium\text{-}2H_2O\text{-}CO]^+$	138.04	3.25	138.05	1.76
$[Oxonium\text{-}2H_2O\text{-}CH_2CO]^+$	-	-	126.05	1.37

It should be noted that the *O*-Glycoside **2** has the β-L-configuration and is levorotatory, while the *O*-glycoside **9** has the β-D-configuration and is dextrorotatory. It is interesting, in this case, to observe that the slightly different diastereoisomeric

conformations in space can influence the fragmentation pathways and the relative abundances of the product ions obtained. Therefore, it is postulated that the reason for obtaining different relative abundances may be due to the fact that the β-L- and β-D-anomers are diastereoisomers (not mirror images). While the percentage abundance is double for the protonated molecule $[M+H]^+$ and for the $[Cholestadiene+H]^+$ in the case of the β-D-configuration, the abundance was higher for the other product ions obtained with the β-L-configuration. Those differences are represented in the following chart (**Figure 6.13**).

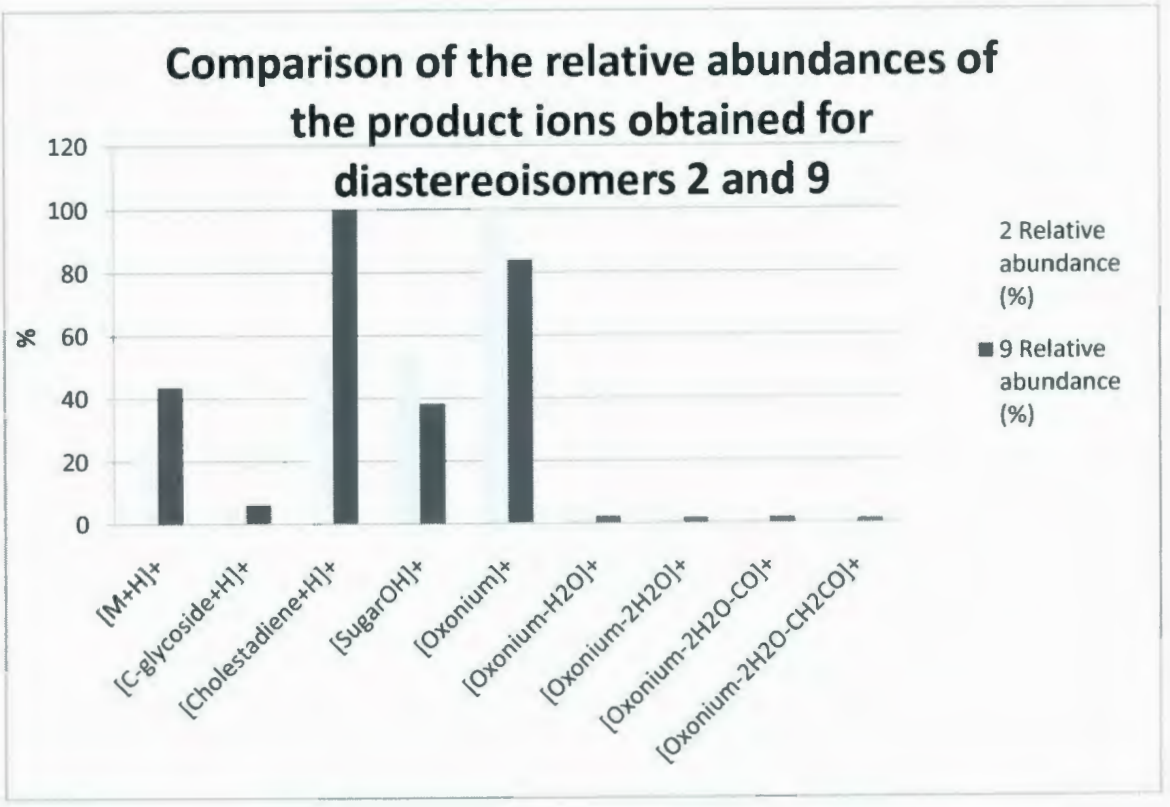

Figure 6.13: Comparison of the relative abundances of the product ions obtained for diastereoisomers 2 and 9

In summary, the formation of the $[C\text{-glycoside}+H]^+$ ion-species was obtained *in situ* in the collision cell for both diastereoisomers **2** and **9** and the relative abundance for this product ion was identical.

6.2. Differentiation of constitutional isomers

6.2.1. 8-(Cholest-5-en-3-β-yloxy)-3,6-dioxaoctyl-2-acetamido-2-deoxy-3-*O*-β-D-galactopyranosyl-α-D-galactopyranoside (3) vs 8-(cholest-5-en-3-β-yloxy)-3,6-dioxaoctyl-2-acetamido-2-deoxy-4-*O*-β-D-galactopyranosyl-β-D-glucopyranoside (10)

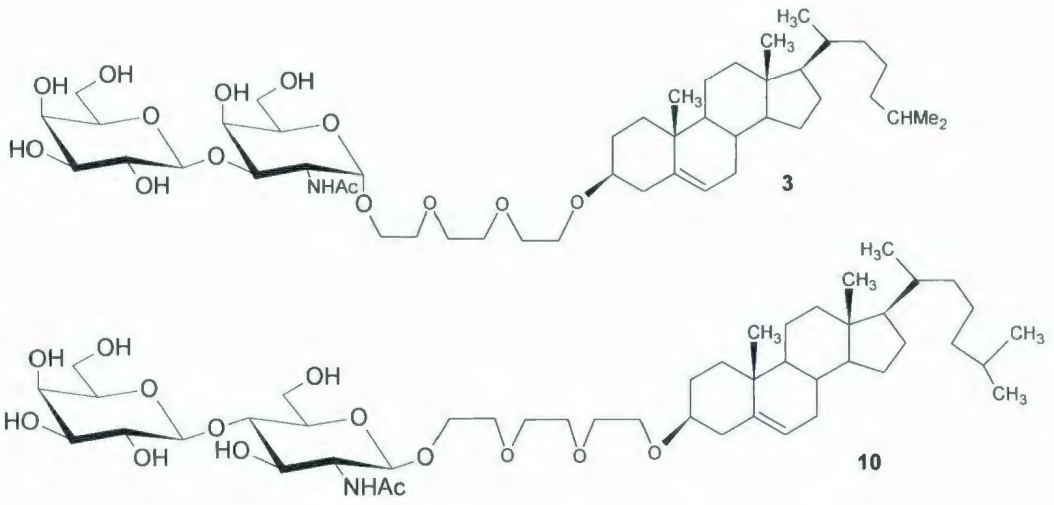

Figure 6.14: Representation of the molecules 3 and 10

The ESI-MS of compound **3** gave the expected fragment ions such as the protonated molecule $[M+H]^+$ at *m/z* 884, the $[M+H\text{-DGal}]^+$ at *m/z* 722, the $[Cholestadiene+H]^+$ at *m/z* 369, the $[Sugar]^+$ at *m/z* 516 and the $[Oxonium]^+$ at *m/z* 204.

The ESI-MS of compound **10** revealed the same expected fragment ions as observed for molecule **3**. In order to compare compound **3** with compound **10** (**Figure 6.15**), it was decided to inject compound **3** once more, this time using the same parameters used in a previously published work.[23] The aim of this comparison was to see if, with those parameters, it was possible to obtain the product ions $[C\text{-glycoside}+H]^+$ and $[C\text{-glycoside-DGal}]^+$, and also to observe any diversity in abundances due to the conventional isomerism of both structures. In fact, the saccharide of molecule **3** is connected by a β-1→3 *O*-glycosidic link, whereas the saccharide of molecule **10** is connected by a β-1→4 *O*-glycosidic link. Moreover, the reducing end group of the disaccharide is a β-D-glucosaminyl unit in **10**, whereas it is an α-D-galactosaminyl residue in **3**. However, the structure of the glucosamine and galactosamine are similar and should not interfere with the fragmentation. The comparison was based on the tandem mass spectrum of the protonated molecule only (**Figures 6.15** and **6.16**).

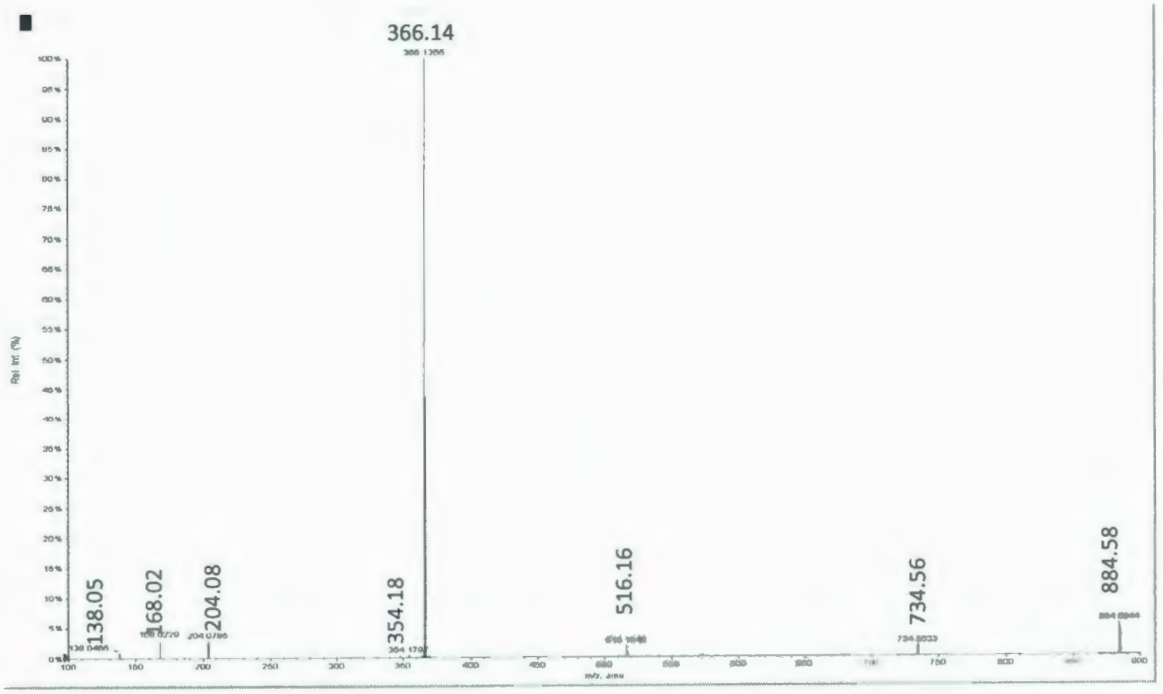

Figure 6.15: CID-MS/MS of the protonated molecule 8-(cholest-5-en-3-β-yloxy)-3,6-dioxaoctyl-2-acetamido-2-deoxy-4-*O*-β-D-galactopyranosyl-β-D-glucopyranoside $[M+H]^+$ (molecule "10")

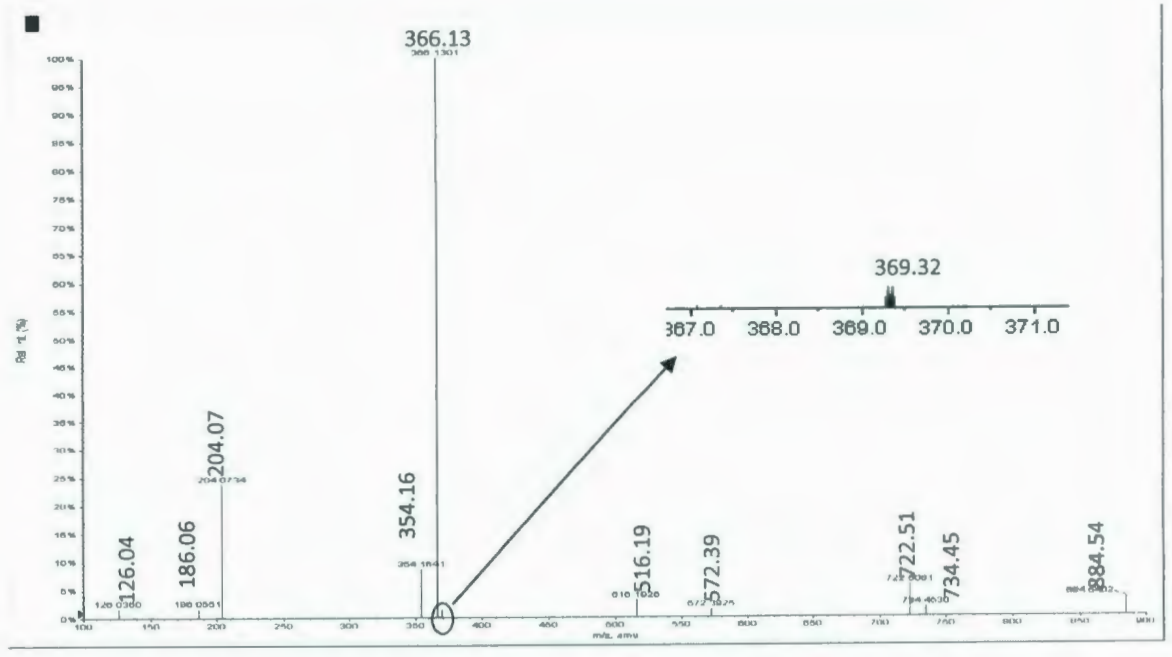

Figure 6.16: CID-MS/MS of the protonated molecule 8-(cholest-5-en-3-β-yloxy)-3,6-dioxaoctyl-2-acetamido-2-deoxy-3-*O*-β-D-galactopyranosyl-α-D-glucopyranoside $[M+H]^+$, molecule 3.

Table 6.3 highlights the results obtained from the low energy collision tandem mass spectrometry analyses of the protonated molecule $[M+H]^+$ for both molecules **3** and **10**. The formation of the $[GlcNAc]^+$ oxonium product ion has been observed for both molecules to have the same relative abundance (100%). The $[SugarSpacer]^+$ product ion appeared also to be identical in both cases and the relative abundances were equal to 3.05 % in **3** and 3.09% in **10**. These were the only similarities seen. Note that the abundance of the protonated molecule **3** was very low (3.29%) when compared to molecule **10**, which was greater by a factor of 8. In addition, it was observed that **3** gave more information regarding the structure and fragmentation of the $[DGal(1\rightarrow3)DGalN_3]^+$ disaccharide. For example, the $[Oxonium\text{-}H_2O]^+$ product ion at *m/z* 186.06 and the $[Oxonium\text{-}H_2O\text{-}^{2,4}X_0]^+$ product ion at *m/z* 126.04 formed by a $^{2,4}X_0$ cleavage were observed.[61] Moreover, the $[Cholestadiene+H]^+$ product ion at *m/z* 369.31 was not detected in the case of **10**. The $[Oxonium\text{-}2H_2O]^+$ product ion at *m/z* 168.05 was only seen in **10**. Finally the [C-glycoside+H]$^+$ ion-species was observed in both cases, with different abundances: the percentage abundance of this complex in **3** was higher, than in **10**. However, **10** did not give the [C-glycoside-DGal]$^+$ ion-species actually derived from either precursor ions $[M+H]^+$ or the $[M+H\text{-}DGal]^+$. Therefore, it is hypothesized that the disaccharide protonated molecule **10** is less prone to fragmentation due to the presence and stability of its β-1→4 linkage, *vis-a-vis* the gas-phase fragmentation than the protonated molecule **3**, which has a β-1→3 linkage. Furthermore, no second C-glycoside ion-species or other product ions seen with **3** were observed with **10**.

Table 6. 3: Product ions *m/z* and relative intensities obtained from the scans of the protonated molecules 3 and 10 by low collision energy tandem mass spectrometric analyses

Ion	CID-MS/MS of 3 m/z	CID-MS/MS of 3 Relative abundance (%)	CID-MS/MS of 10 m/z	CID-MS/MS of 10 Relative abundance (%)
$[M+H]^+$	884.54	3.29	884.58	26.64
$[C\text{-glycoside}+H]^+$	734.45	1.64	734.56	0.77
$[M+H\text{-DGal}]^+$	722.51	5.63	722.53	0.39
$[C\text{-glycoside-DGal}]^+$	572.39	1.41	-	-
$[SugarSpacer]^+$	516.19	3.05	516.16	3.09
$[Cholestadiene+H]^+$	369.32	0.23	-	-
$[Sugar]^+$	366.13	100.00	366.14	100.00
$[OxoniumSpacer]^+$	354.16	8.69	354.18	0.39
$[Oxonium]^+$	204.07	23.71	204.08	1.54
$[Oxonium\text{-}H_2O]^+$	186.06	1.64	-	-
$[Oxonium\text{-}2H_2O]^+$	-	-	168.02	0.77
$[Oxonium\text{-}H_2O\text{-}{}^{2,4}X_0]^+$	126.04	1.64	-	-

To conclude, there are several questions that still need to be answered concerning these CID-MS/MS analyses. Interestingly, second-generation CID-MS/MS or *quasi*-MS^3 product ion scans of the $[C\text{-glycoside}+H]^+$ ion-species or $[C\text{-glycoside-DGal}]^+$ at *m/z* 734.45 and *m/z* 572.39, respectively, did not produce any product ions. As observed in **Chapter 3**, the $[C\text{-glycoside}+H]^+$ and $[C\text{-glycoside-DGal}]^+$ ion-species were able to be gas-phase isolated and fragmented. Hence, it is possible that this was due to the change of the chemical structures of the molecules, or perhaps to the use of ideal gas declustering and focusing voltage parameters, which need to be different for the different neoglycoconjugates. In addition, the fully β-anomer **10** produced less abundant product ions compared to the partially-β-anomer **3** (**Figure 6.17**). This confirms the postulation that before making a theoretical prediction, the analyses of the gas-phase fragmentations have to be done.

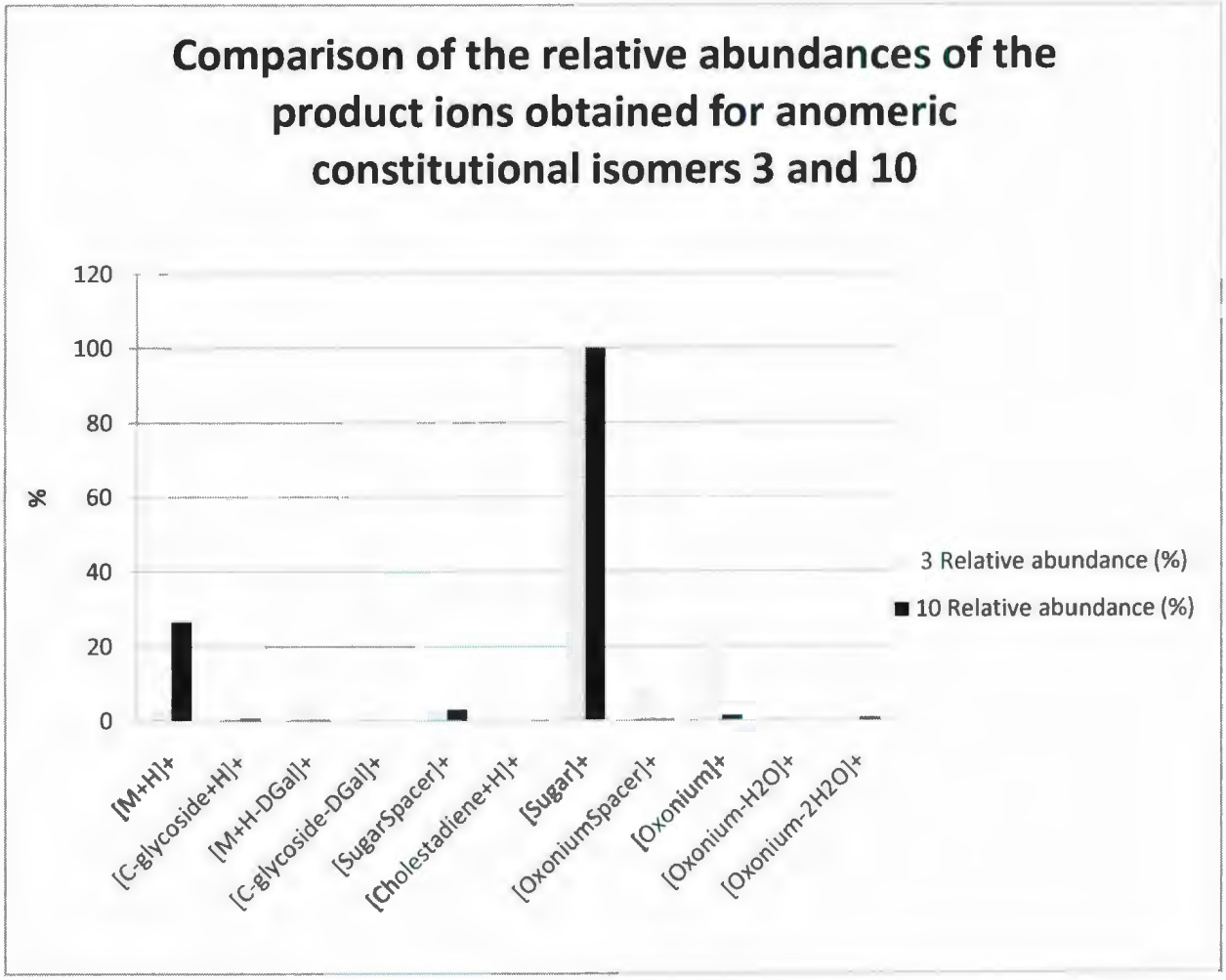

Figure 6.17: Comparison of the relative abundances of the product ions obtained for anomeric constitutional isomers 3 and 10

Chapter 7: Simple neoglycolipid containing the 2-deoxy-2-N-acetyl or 2-deoxy-2-amino-glucosaminyl residues

This section assesses the fragmentation pathway of the simple neoglycolipid during ESI-QqToF-MS analysis. As the samples did not possess any cholesteryl moiety (**Figure 7.1**), no C-glycoside ion-species was anticipated to be formed. In fact, the fragmentation of the neoglycolipids containing the $[GlcNAc]^+$ portion was of more interest, in order to see if the gas-phase fragmentation would be affected by the presence of the 2-deoxy-2-*N*-acetyl group on the amino sugar with respect to a free-2-amino-2-deoxy-glucosaminyl glycolipid.

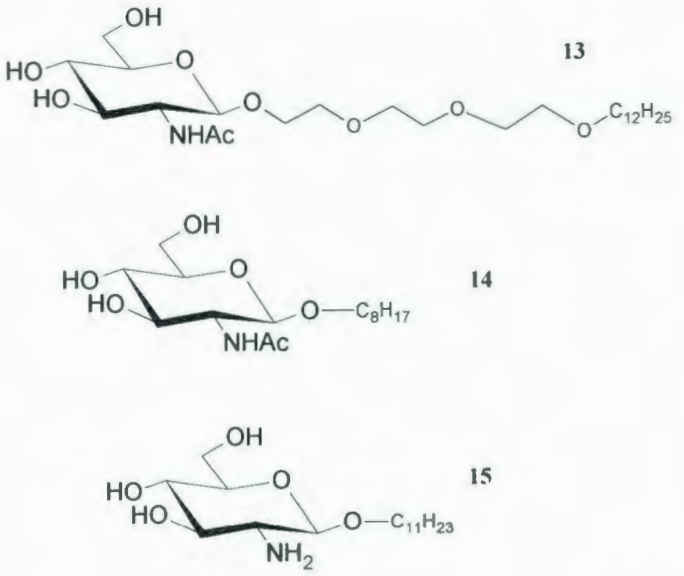

Figure 7.1: Representation of the molecules 13, 14 and 15

7.1. Ethoxy-[2-2-ethoxy]-dodecanoxyl-2-*N*-acetyl-2-deoxy-β-glucopyranoside (13)

A comparison between the ESI-MS conventional full scan and the CID-MS/MS was attempted. It was observed that the conventional ESI-MS of molecule **13** was similar to that of the product ion scan of the protonated molecule $[M+H]^+$ at *m/z* 522.3646 (**Figure 7.2**).

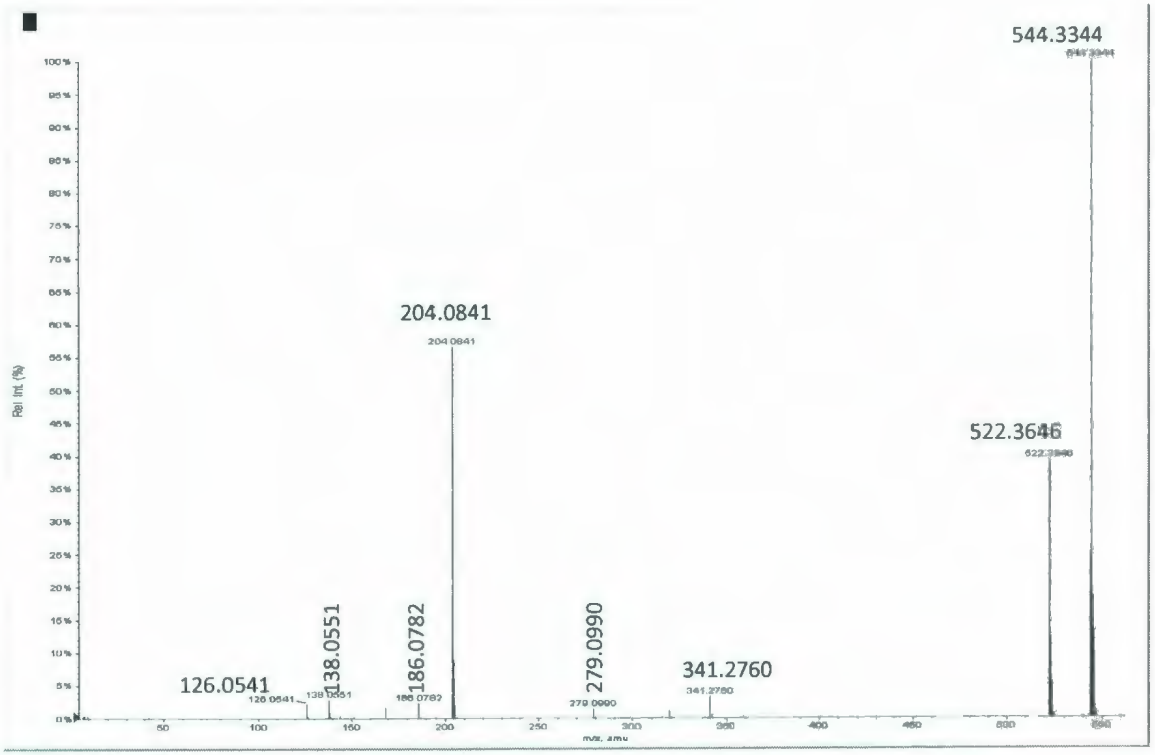

Figure 7.2: Conventional scan of the ethoxy-[2-2-ethoxy]-dodecanoxyl-2-*N*-acetyl-2-deoxy-β-glucopyranoside, molecule "13".

Hence, the CID-tandem mass spectrum of the protonated molecule $[M+H]^+$ was recorded, to determine if the product ions were formed from the $[GlcNAc]^+$ moiety (**Table 7.1, Figure 7.3**).

Table 7. 1: Data obtained from the full conventional scan and the CID-MS/MS-QqToF analyses of the protonated molecule of 1-ethoxy-[2-2-ethoxy]-dodecanoxyl-2-*N*-acetyl-2-deoxy-β- glucopyranoside (13).

Ion	ESI-MS *m/z*	CID-MS/MS 522.36 *m/z*
$[M+Na]^+$	544.3344	-
$[M+H]^+$	522.3646	522.61
[Polyethoxy chain+Allyl Chain +H]$^+$	-	319.65
[Oxonium]$^+$	204.0841	204.48
[Oxonium-H_2O]$^+$	186.0782	186.47
[Oxonium-$2H_2O$]$^+$	-	168.45
[Oxonium-$2CH_3OH$]$^+$	-	144.45
[Oxonium-$2H_2O$-CH_3OH]$^+$	138.0551	138.44
[Oxonium-CH_2CO-$2H_2O$]$^+$	126.0541	126.43

The ESI-MS and CID-MS/MS shared some common fragment ions, however, the CID-MS/MS contained more elimination product ions obtained by losses of molecules of water from the $[GlcNAc]^+$ oxonium. The product ions were $[Oxonium\text{-}2H_2O]^+$ at *m/z* 168.45, $[Oxonium\text{-}2CH_3OH]^+$ at *m/z* 144.45 and [Polyethoxy chain+Allyl Chain+H]$^+$ was observed at *m/z* 319.65.

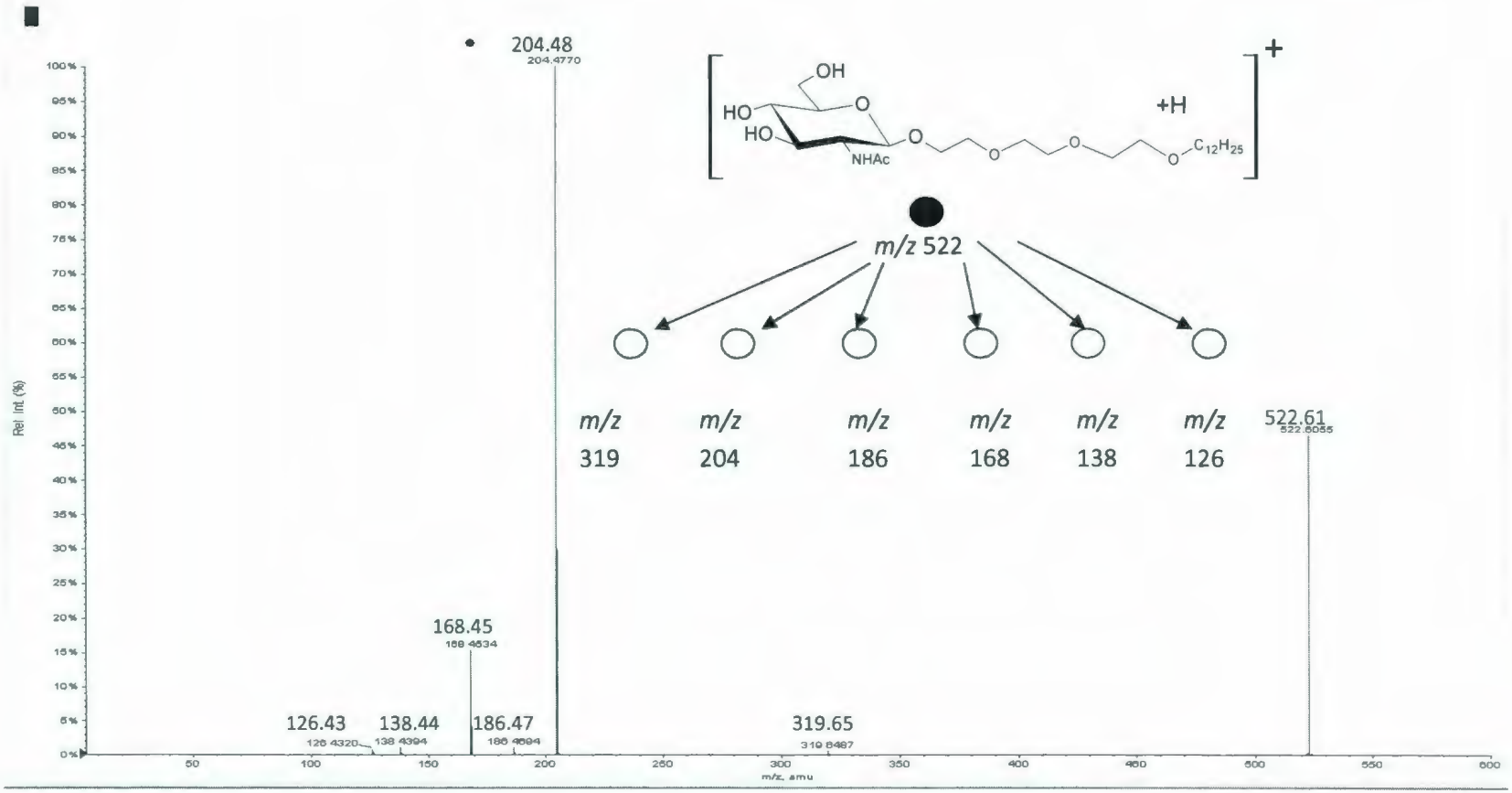

Figure 7.3: Tandem mass spectrometry of the protonated molecule $[M+H]^+$ of ethoxy-[2-2-ethoxy]-dodecanoxyl-2-*N*-acetyl-2-deoxy-β-glucopyranoside at *m/z* 522.61, molecule "13".

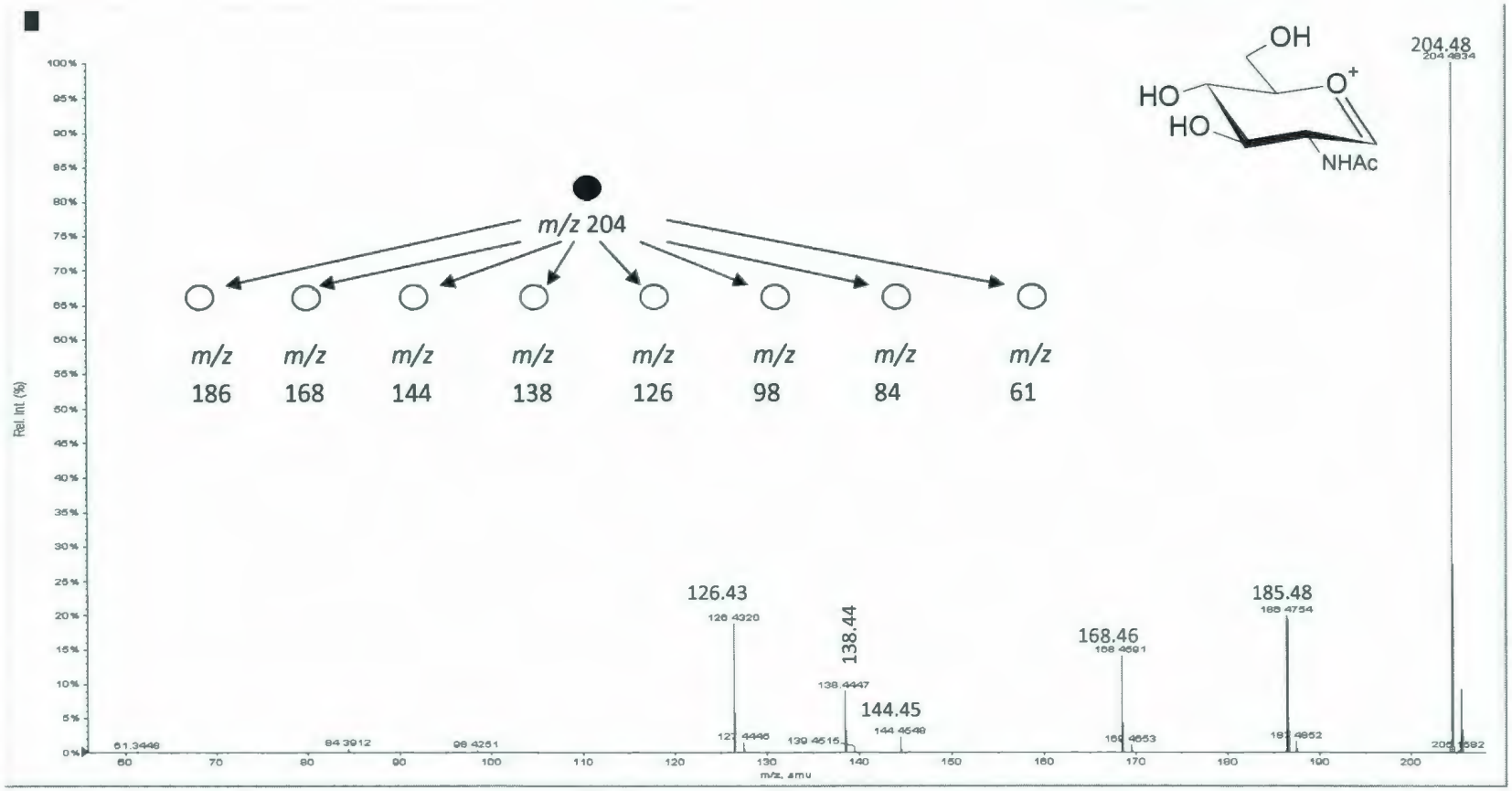

Figure 7.4: *Quasi*-MS^3 of *m/z* 204.48.

Second-generation *quasi*-MS^3 analysis was performed on the $[GlcNAc]^+$ oxonium at *m/z* 204.48. This precursor ion generated the product ions at *m/z* 185.48, 168.46, 138.44 and 126.43, which are assigned in **Table 7.1**. It was observed that the product ion at *m/z* 126.43 was able to eliminate ammonia to produce the ion at *m/z* 84.39 (**Figures 7.4** and **Scheme 7.1**). **Scheme 7.1** represents the proposed fragmentation pathway of the protonated molecule $[\mathbf{13}+H]^+$.

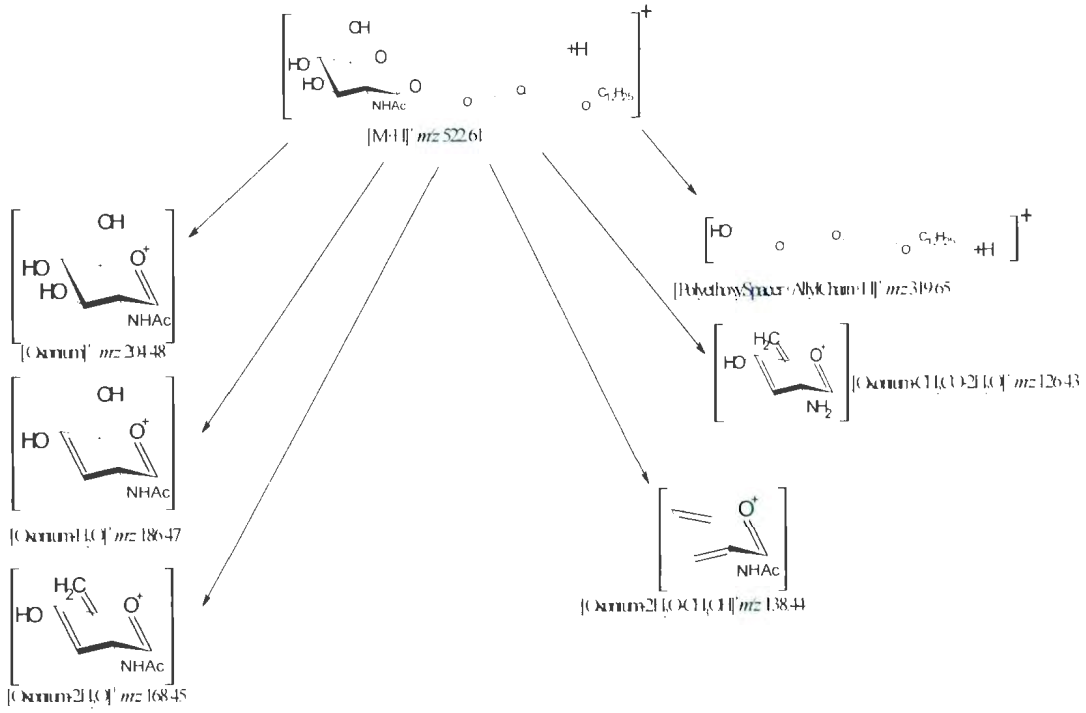

Scheme 7. 1: Proposed fragmentation pathway of the ethoxy-[2-2-ethoxy]-dodecanoxyl-2-*N*-acetyl-2-deoxy-β-glucopyranoside, molecule "13".

7.2. Octanoxyl-2-*N*-acetyl-2-deoxy-β-D-glucopyranoside (14)

The full conventional ESI-MS analysis gave the sodiated molecule $[M+Na]^+$ at *m/z* 356.1258, the protonated molecule $[M+H]^+$ at *m/z* 334.1471, and the $[Oxonium]^+$ ion at *m/z* 204.0866.

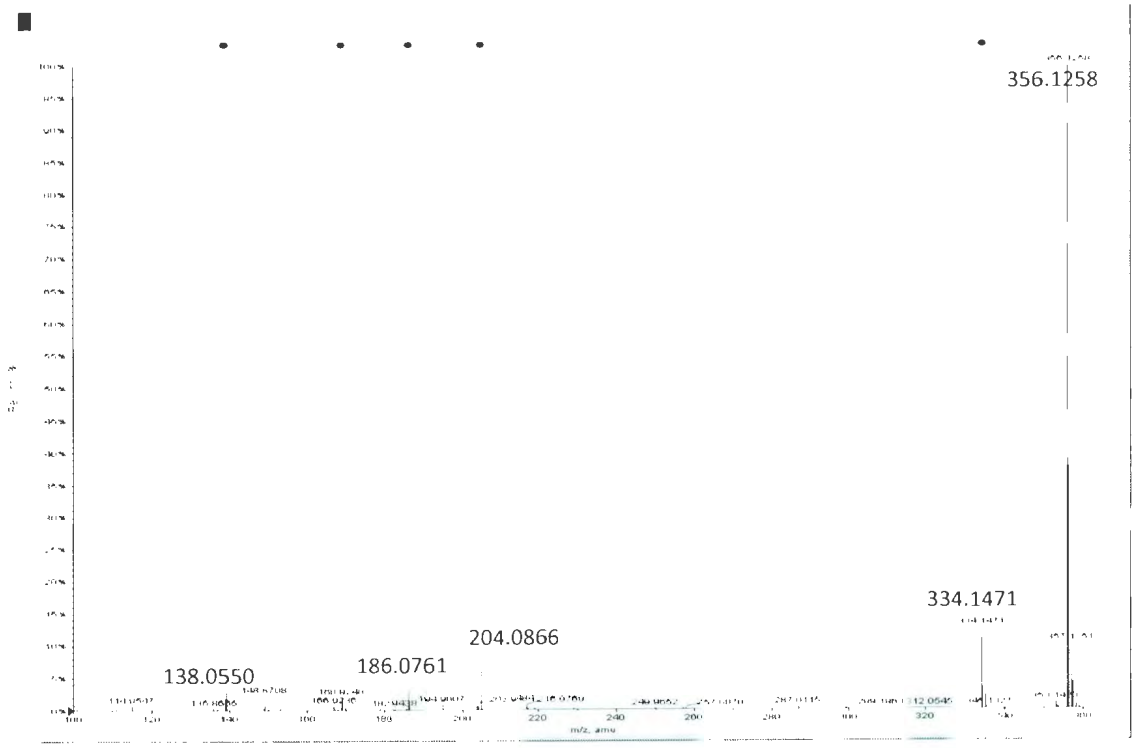

Figure 7.5: ESI-MS of the octanoxyl-2-*N*-acetyl-2-deoxy-β-D-glucopyranoside, molecule "14".

The $[Oxonium]^+$ ion formed a series of secondary fragment ions resulting from the elimination of water molecules (**Figure 7.5**).

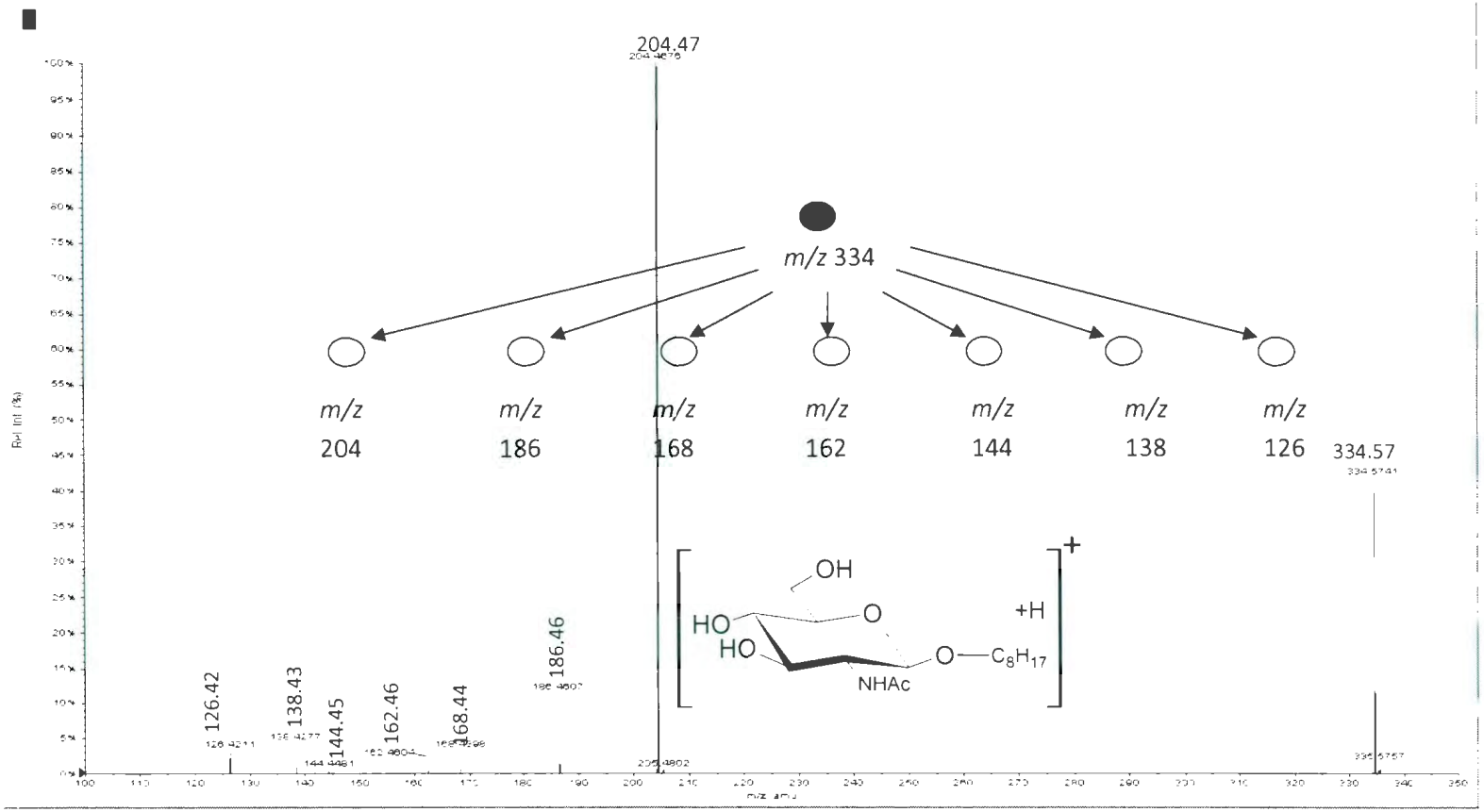

Figure 7.6: Low collision energy tandem mass spectrum of the precursor ion $[M+H]^+$ at *m/z* 334.57, molecule "14".

The CID-MS/MS of the protonated molecule **14** afforded the product $[GlcNAc]^+$ oxonium ion at *m/z* 204, and the series of secondary product ions resulting from elimination of water molecules (**Figure 7.6** and **Scheme 7.2**).

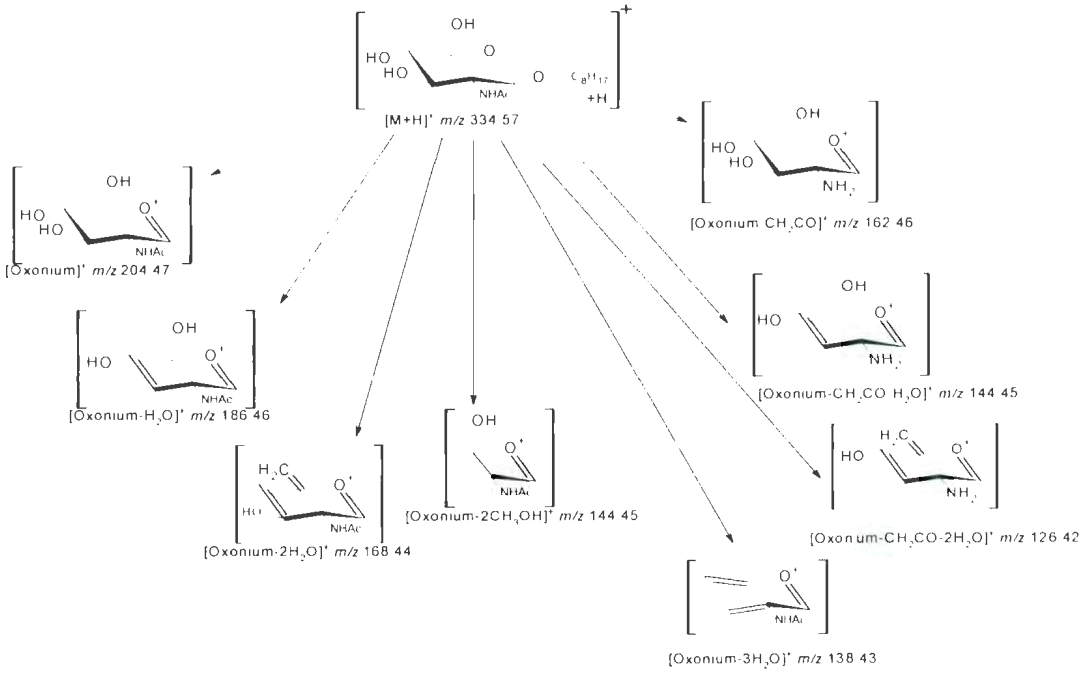

Scheme 7. 2: Proposed fragmentation pathway for the octanoxyl-2-*N*-acetyl-2-deoxy-β-D-glucopyranoside (molecule "14").

In summary, it was observed that the CID-MS/MS fragmentation pathway was governed by the polar carbohydrate moiety (**Table 7.2**).

Table 7. 2: Data obtained from the full conventional scan and the CID-MS/MS-QqToF analyses of the protonated molecule octanoxyl-2-*N*-acetyl-2-deoxy-β-D-glucopyranoside (14).

Ion	ESI-MS *m/z*	CID-MS/MS 334.15 *m/z*
$[M+Na]^+$	356.1258	-
$[M+H]^+$	334.1471	334.58
$[Oxonium]^+$	204.0642	204.47
$[Oxonium-H_2O]^+$	186.0518	186.46
$[Oxonium-2H_2O]^+$	168.0272	168.44
$[Oxonium-2CH_3OH]^+$	-	144.45
$[Oxonium-2H_2O-CH_3OH]^+$	137.9950	138.43
$[Oxonium-CH_2CO-2H_2O]^+$	-	126.42

7.3. Undecyloxyl-2-amino-2-deoxy-β-D-glucopyranoside (15)

The conventional ESI-MS scan of **15**, afforded the major ions $[M+Na]^+$ at *m/z* 356.5771 and $[M+H]^+$ at *m/z* 334.6066. The $[GlcNH_2]^+$ was also observed at *m/z* 162.4661, and its elimination product $[GlcNH_2-H_2O]^+$ formed by loss of water at *m/z* 144.4534 (**Figure 7.7**). The protonated dimer ions $[2M+H]^+$ and $[2M+Na]^+$ at *m/z* 667.5049 and 689.4975, respectively, were also observed.

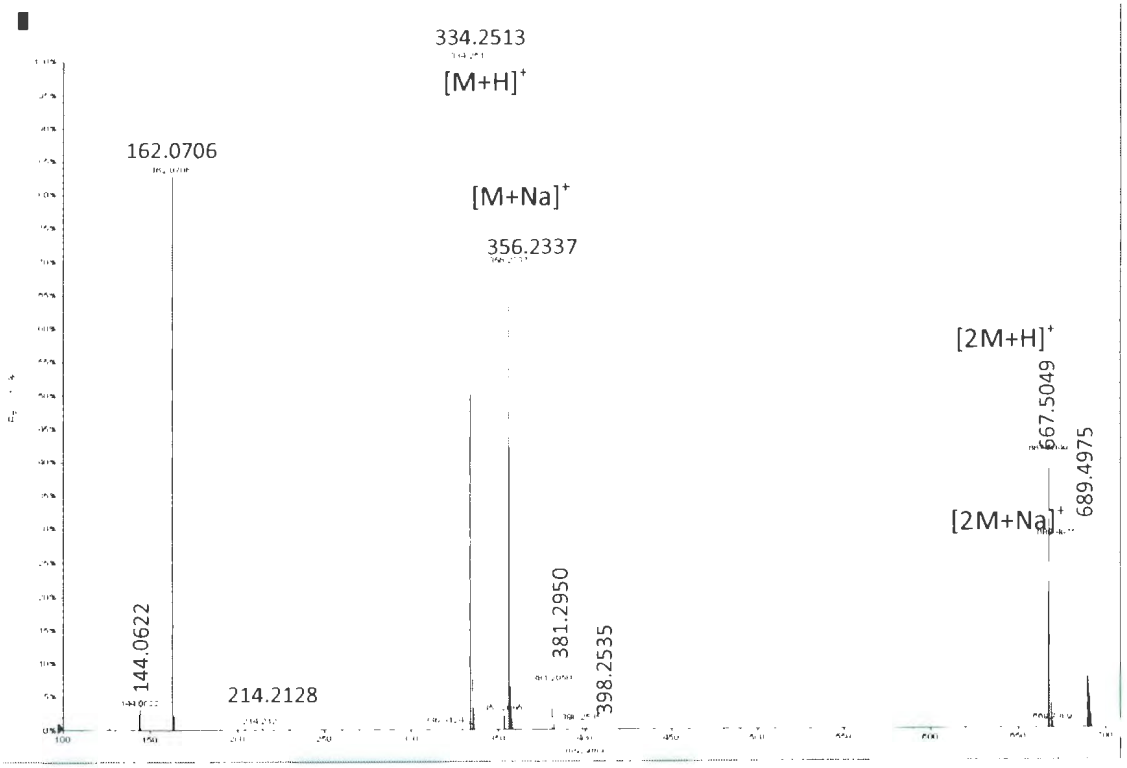

Figure 7.7: Full ESI-MS scan of the undecyloxyl-2-amino-2-deoxy-β-D-glucopyranoside (molecule "15").

Low energy-CID-QqTOF-MS/MS of the protonated dimer $[2M+H]^+$ at *m/z* 667.61 afforded the formation of the protonated molecule $[M+H]^+$ at *m/z* 334.61 and the $[GlcNH_2]^+$ at *m/z* 162.47 (**Figure 7.8**).

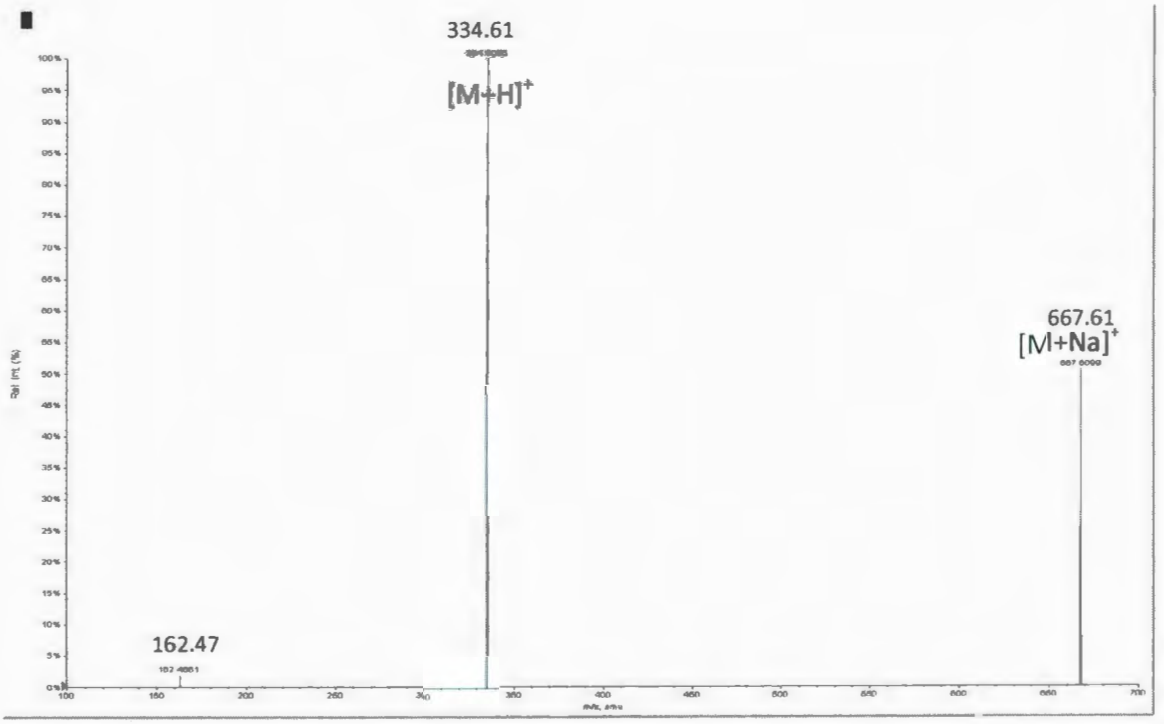

Figure 7.8: Tandem mass spectrum of the dimer protonated molecule $[2M+H]^+$ at *m/z* 667.61

The CID-MS/MS analysis of the protonated molecule $[M+H]^+$ was also performed (**Figure 7.9**), and gave the expected product ions, $[GlcNH_2]^+$ oxonium at *m/z* 162.47, the $[GlcNH_2\text{-}H_2O]^+$ ion at *m/z* 144.45 and the $[GlcNH_2\text{-}2H_2O]^+$ ion at *m/z* 126.44. Finally, the product ion $[M+H\text{-}H_2O]^+$, resulting from loss of water from the precursor $[M+H]^+$ protonated molecule, was observed at *m/z* 317.59. The product ion at *m/z* 299.59 was also formed resulting from the loss of two molecules of water, from the protonated molecule $[M+H\text{-}2H_2O]^+$ ion (**Table 7.3**).

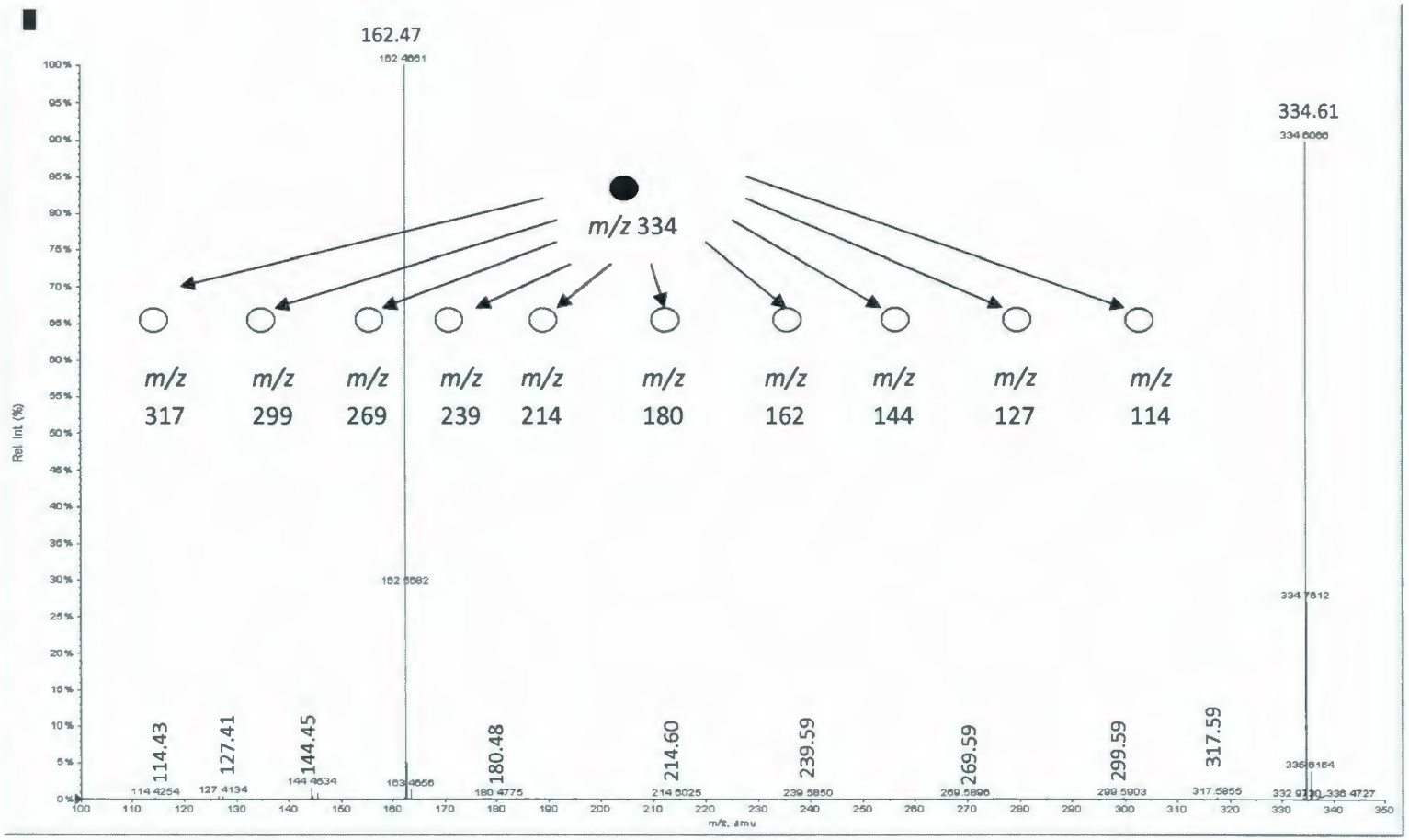

Figure 7.9: CID-MS/MS of the precursor ion $[M+H]^+$ at *m/z* 334.61 of the undecyloxyl-2-amino-2-deoxy-β-D-glucopyranoside (molecule "15").

Table 7. 3: Data from full scan and CID-MS/MS analysis of the undecyloxyl-2-amino-2-deoxy-β-D-glucopyranoside, molecule "15".

Ion	ESI-MS *m/z*	CID-MS/MS 667.61 *m/z*	CID-MS/MS 334.61 *m/z*
$[2M+H]^+$	667.5049	667.61	-
$[M+Na]^+$	356.2337	-	-
$[M+H]^+$	334.2513	334.61	334.61
$[M+H-H_2O]^+$	-	-	317.59
$[Oxonium]^+$	162.0706	162.47	162.47
$[Oxonium-H_2O]^+$	144.0622	-	144.45
$[Oxonium-2H_2O]^+$	-	-	126.44

Scheme 7.3 shows the proposed fragmentation pathway of the protonated molecule **15**.

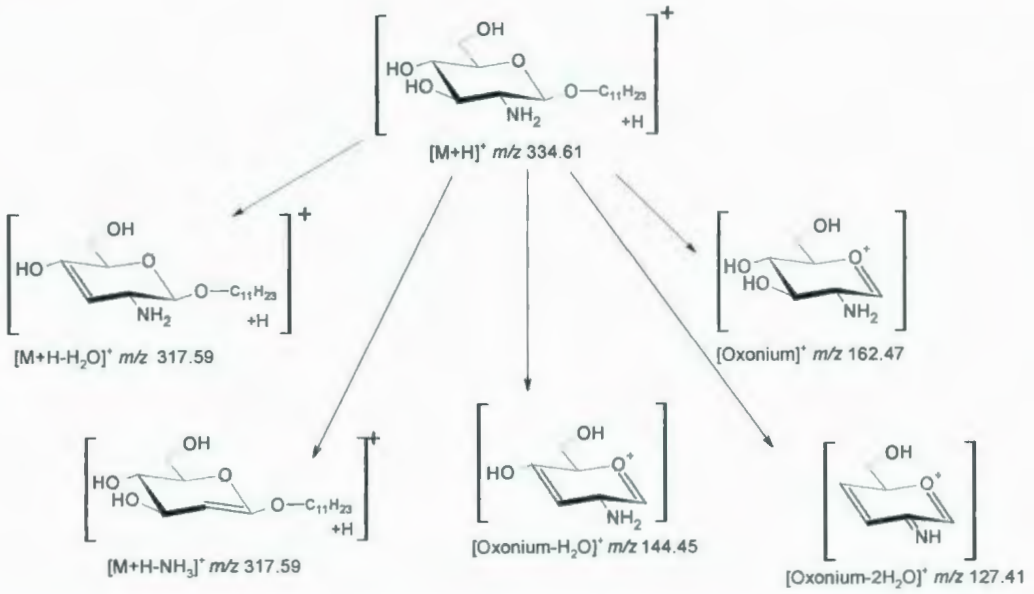

Scheme 7. 3: Proposal fragmentation pathway of the undecyloxyl-2-amino-2-deoxy-β-D-glucopyranoside (molecule "15").

7.4. Discussion

The purpose of this chapter was to detect any difference in the fragmentation of the carbohydrate moiety, compared to the fragmentation of the carbohydrates in the previous neoglycolipids (**1-12**).

The fragmentation pathways of the protonated molecules **13**, **14** and **15** were similar. The difference between these three glycolipids was the presence of an acetyl group linked to the NH-group located on *C*-2 for molecules **13** and **14**. The fragmentation of these molecules provided the expected fragments such as $[GlcNAc\text{-}H_2O]^+$, $[GlcNAc\text{-}2H_2O]^+$, $[GlcNAc\text{-}2H_2O\text{-}CH_3OH]^+$ and $[GlcNAc\text{-}2CH_3OH]^+$. The excision of the polyethoxychain linked to the allylchain was only observed for the molecule **13**, since molecules **14** and **15** did not contain this feature. It is interesting to note the change from an aminoacetyl molecule to an aminomolecule by the presence of the $[GlcNAc\text{-}CH_2CO\text{-}2H_2O]^+$ ion for both molecules. The fact that the acetyl was able to be fragmented from the *N*-acetyl group is new compared to the molecules **1-12**.

The fragmentation of the aminoglucose glycolipid **15** is related to the fragments obtained from molecules **13** and **14**, which lost an acetyl group. The expected fragment ions such as $[GlcNAc\text{-}H_2O]^+$ and $[GlcNAc\text{-}2H_2O]^+$ were observed.

It was of interest to note than no rearrangement occurred between the carbohydrate and the allylchain.

In the MALDI-ToF-MS, these simple neoglycolipid moieties were not observed. This was expected, as the fragment ions of the matrix interfered with detection of the

expected glycosyl ions. The matrices used for the MALDI-ToF technique were CHCA and DHB. Grant and Helleur[77] observed that the addition of a surfactant on the matrix can allow cleaner detection of the analytes. However, this technique is not applicable in every case and is time consuming. ESI-QqTOF-MS and ESI-QqTOF-MS/MS analyses were proven to be efficient for the structural characterization of neoglycolipids **13**, **14** and **15**.

Conclusion

A new series of free-neoglycolipid cholesteryl derivatives was studied in **Chapter 3**. The results obtained confirmed the fragmentation pathway of each neoglycolipid, which is necessary for future therapeutic treatment of HIV or cancer. It also confirmed the formation the formation of a C-glycoside ion-species by an intramolecular mechanism occurring in the activated ion-molecule complex, in both conventional and CID-MS/MS analyses, as indicated in previous research.[5,23] New information was noticed regarding the fragmentation of the C-glycoside ion-species. In fact, its fragmentation can be complex, depending on the parameters used. It was also noticed for the first time that a neoglycolipid containing a disaccharide could produce two different C-glycoside ion species. The first C-glycoside ion-species was not proven to be a parent of the [C-glycoside-DGal]$^+$ using of ESI-QqToF-MS/MS.

Chapter 4 confirmed the previous research[5] on per-*O*-acetylated neoglycolipids and the fragmentation pathway was relatively simple to determine. Elimination of acetic acid and ketene molecules were observed, resulting from the *O*-acetylated group present on the neoglycolipid carbohydrate. No C-glycoside ion-species was observed, due to the protection of the neoglycolipid belonging to the *O*-acetylated groups.

Comparison of the data from **Chapters 3** and **4**, regarding whether the per-*O*-acetylated or free-neoglycolipids give rise to the [C-glycoside+H]$^+$ ion-species within the ESI-QIT mass spectrometer and the FT-ICR mass spectrometer, has been conducted by collaborators Gianluca Giorgi and Jon Amster.[78] The results obtained with the ESI-QIT,

FT-ICR-MS^n were identical to the results acquired using the QqToF-MS/MS. The major point of comparison of the techniques was to observe the formation *in situ* of the C-glycoside ion-species with other cell collisions. The C-glycoside ion-species was noted by both Gianluca Giorgi and Jon Amster. Compared to the ESI-QqToF technique, the ion trap and Fourier-transform mass spectrometers are able to trap any ion before its fragmentation. The quality of the data[79] with those techniques was definitely better than that obtained using the ESI-QqToF mass spectrometer.

Interference of the 2-azido group, the partial *O*-acetylation of the non-reducing end and the presence of the 4,6-*O*-benzylidene group on the azido-D-galactosamine were observed in **Chapter 5**. The formation of a new ion-species was noticed under the $[C\text{-glycoside}+H\text{-}N_2]^+$ even though the neoglycolipid was partially acetylated. The reason that this ion-species was present could be due to the fact that the free acetylated carbohydrate was linked directly to the linker attached to the cholesteryl group. However, it was not possible to fragment this ion-species during *quasi*-MS^3 acquisition.

Chapter 6 focused on the difference in the fragmentation observed with isomeric or anomeric neoglycolipid. It was noticed that an α-anomer would produce ions with a higher intensity than a β-anomer. Occurrence of the $[C\text{-glycoside}+H\text{-}N_2]^+$ ion-species was observed for the family of 2-azido-neoglycolipids. It was possible to isolate this ion to determine its fragmentation pathway, contrary to the partially *O*-acetylated 2-azido-neoglycolipids in **Chapter 5**. Differences in the intensity of the product ions were also observed with β-L and β-D anomers. Finally, the constitutional isomers produced

different results. Some product ions would be seen, favored by the linkage between the carbohydrates.

Simple fragmentation of glycolipids was observed in **Chapter 7**. This allowed confirmation of the fragmentation of the carbohydrate moiety, and related it to the previous chapters. It was shown that no main difference existed in the fingerprint of the sugar moiety compared to the previous fingerprint of the carbohydrate moiety in the neoglycolipids.

Future work

Future experiments should be conducted to confirm in each case if the cholesterol-glycoside ion is either a weak ion or an ion-molecule complex.

The analyses of the simple glycolipids **13-15** could be attempted by using Grant's method[77] with a MALDI-ToF. It would be interesting to see if his method can be applied to the series of glycolipids.

An additional novel series of glycoconjugates, containing the cholesteryl could also be assessed by MALDI-ToF-MS, to be compared to the other techniques used (ESI-QqToF, ESI-QIT, FT-ICR) which revealed the presence of the cholesteryl-glycoside ion.

Finally, it was recently observed that the study of the neoglycoconjugates by high-resolution could affect the relative abundances of the product ions. Studying the CID-MS/MS of the protonated molecules and the C-glycoside ion-molecule formation in the collision cell for the 2-deoxy-2-azido-neoglycolipids with high-resolution FT-ICR-MS^n instrument is a must and would be of primordial interest.

It could be of interest to synthesize a novel series of C-glycosides containing both the cholesteryl aglycon and 2-deoxy-2-acetamido- and 2-deoxy-2-azido-glucosamine to be studied using ESI-QqToF mass spectrometry in low and high-resolution, and compare it to the tandem mass spectrum data of the neoglycolipids, which gave a cholesteryl-glycoside ion or ion-molecule complex structure similar to that of the C-glycoside.

This will be a formidable task to achieve as to our knowledge there are no synthetic method existing that would allow such a synthesis.

Articles based on the work described in this thesis regarding the azido neoglycolipids, the anomeric and isomeric effect, and comparison with the QIT-MS^n and FT-ICR-MS^n will be subject of future publications.

References

[1] Gregoriadis, G. *Liposome Technology*, *3*; Informa Healthcare, USA, 1984.

[2] Banoub, J.; Boullanger, P.; Lafont, D. Synthesis of oligosaccharides of 2-amino-2-deoxy sugars. *Chem. Rev.* **1992**, *92*(6), 1167-1195.

[3] Kiessling, L. L.; Pohl, N L. Strength in numbers: non-natural polyvalent carbohydrate derivatives. *Chem. Biol.* **1996**, *3*(2), 71-77.

[4] Taylor, M E.; Drickamer, K. *Introduction to Glycobiology*, 2nd Ed, Oxford University Press, 2006.

[5] Banoub, J.; Boullanger, P.; Lafont, D.; Cohen, A.; El Aneed, A.; Rowlands, E. In situ formation of C-glycosides during electrospray ionization tandem mass spectrometry of a series of synthetic amphiphilics cholesteryl polyethoxy neogylcolipids contaning *N*-Acetyl-D-Glucosamine. *J. Am. Soc. Mass. Spectrom.*, **2005**, *16*(4), 565-570.

[6] Kuberan, B.; Sikkander, S. A.; Tomiyama, H.; Lindhardt, R. J. Synthesis of a C-glycoside analogue of sTn: an HIV- and tumor-associated antigen. *Angew. Chem. Int. Ed.*, **2003**, *42*(18), 2073-2075.

[7] Dhaneshwar, S. S.; Kandpal, M.; Gairola, N.; Kadam, S. S. Dextran : A promising macromolecular drug carrier. *Indian. J. Pharm. Sci.* **2006**, *68*(6), 705-714.

[8] Wallner, F, *Glycoconjugates. Solid-phase synthesis and biological applications,* Dissertation, Umeå University, Sweden, **2005**.

[9] Minden, H.M., *Synthesis and mesomorphic properties of glycolipids and neoglycolipids,* Dissertation, University of Hamburg, **2000**.

[10] Bardonnet, P-L.; Faivre, V.; Pirot, F.; Boullanger, P.; Falson, F. Cholesteryl oligoethyleneglycol glycosides: Fluidizing effect of their embedment into phospholipid bilayers. *Biochem. Biophys. Res. Commun.* **2005**, *329*(4), 1186-1192.

[11] Duffels, A.; Green, L. G.; Ley, S.V.; Miller, A. D. Cationic lipids for gene therapy, part III. Synthesis of high-mannose type neoglycolipids: Active targeting of liposomes to macrophages in gene therapy. *Chem. Eur. J.* **2000**, *6*(8), 1416-1430.

[12] Lemieux, R U.; Takeda, T.; Chung, B.Y. Synthesis of 2-amino-2-deoxy-β-D-glucopyranosides. Properties and use of 2-deoxy-2-phtalimidoglycosyl halides. *Synthetic methods for carbohydrates. ACS (Am Chem Soc) Symp.*ser. 39, **1976**, 90-115.

[13] Boullanger, P.; Sancho-Camborieux, M-R.; Bouchu, M-N.; Marron-Brignone, L.; Morelis, R.M; Coulet, P R. Synthesis and interfacial behaviour of three homologous glycerol neoglycolipids with various chain lengths. *Chem. Phys. Lipids*, **1997**, *90*(1), 63-74.

[14] Laurent, N.; Lafont, D.; Boullanger, P. Syntheses of α-D-galactosamine neoglycolipids. *Carbohydr. Res.* **2006**, *341*(7), 823-835.

[15] Wang, X.; Gross, P. H. C-Glycoside syntheses.3. Diastereodiversified C-glycosides from D-glucose. *J. Org. Chem.* **1995**, 60, 1201-1206.

[16] Peri, F.; Cipolla, L.; Rescigno, M.; La Ferla, B.; Nicotra, F. Synthesis and biological evaluation of an anticancer vaccine containing the C-glycoside analogue of the T_n epitope. *Bioconjugate. Chem.*, **2001**, *12*(3), 325-328.

[17] Routier, F H.; Nikolaev, A. V.; Ferguson, M. A. J. The preparation of neoglycoconjugates containing phosphodiester linkages as potential anti-Leishmania vaccines. *Glycoconj. J.* **1999**, *16*(12), 773-780.

[18] Guo, C-T.; Sun, X-L.; Kanie, O.; Shortridge, K. F.; Suzuki, T.; Miyamoto, D.; Hidari, K. I-P. J.; Wong, C-H.; Suzuki, Y. An *O*-glycoside of sialic acid derivative that inhibits both hemagglutinin and sialidase activities of influenza viruses. *Glycobiology* **2002**, *12*(3), 183-190.

[19] Boullanger, P.; Chevalier, Y.; Croizier, M-C.; Lafont, D.; Sancho, M-R. Synthesis and surface-active properties of some alkyl 2-amino-2-deoxy-β-D-glucopyranosides. *Carbohydr. Res.* **1995**, *278*, 91-101.

[20] Schmieg, J.; Yang, G.; Franck, R. W.; Tsuji. M. Superior protection against malaria and malanoma metastases by a C-glycoside analogue of the natural killer T cell ligand α-galactosylceramide. *J. Exp. Med.* **2003**, *198*(11), 1631-1641.

[21] Gelhausen, M.; Besson, F., Bonnin, S.; Lafont, D.; Roux, B. Interaction of neoglycolipids with artificial membranes and erythrocytes. Influence of the length of the neoglycolipid ethoxy moiety. *Biotechnol. Lett.* **1998**, *20*(8), 713-716.

[22] Denton, R. W.; Tony, K.A.; Hérnandez-Gay, J. J.; Cañada, F.J.; Jiménez-Barbero, J.; Mootoo, D. R. Synthesis and conformation behaviour of the difluoromethylene linked C-glycoside analog of β-galactopyranosyl-(1↔1)-α-mannopyranoside. *Carbohydr. Res.* **2007**, *342*(12-13), 1624-1635.

[23] El Aneed, A.; Banoub, J.; Koen-Alonso, M.; Boullanger, P.; Lafont, D. Establishment of mass spectrometric fingerprints of novel synthetic cholesteryl neoglycolipids: the presence of a unique C-glycoside species during electrospray ionization and during collision induced dissociation tandem mass spectrometry. *J. Am. Soc. Mass. Spectrom.* **2007**, *18* (2), 294-310.

[24] Campbell, K. M.; Watkins, M. A.; Li, S.; Fiddler, M. N.; Winger, B.; Kenttämaa, H. I. Functional group selective ion/molecule reactions: mass spectrometric identification of the amido functionality in protonated monofunctional compounds. *J. Org. Chem.* **2007**, *72*, 3159-3165.

[25] Liu, J.; Anderson, S. L. Dynamical control of 'statistical' ion-molecule reactions. *Int. J. Mass Spectr.* **2005**, *241*(2-3), 173-184.

[26] Baer, T.; Hase,W. L. *Unimolecular Reaction Dynamics: Theory and Experiments*, Oxford University Press, New York, 1996.

[27] Hase, W. L. Some recent advances and remaining questions regarding unimolecular rate theory. *Acc. Chem. Res.* **1998**, *31*, 659-665.

[28] Steinfeld, J. I; Francisco, J. S.; Hase, W.L. *Chemical Kinetics and Dynamics*, Prentice-Hall International Inc., NJ, 2nd edition, 1989.

[29] Fukui, K. A formulation of the reaction coordinate. *J. Phys. Chem.* **1970**, *74*, 4161-4163.

[30] Marcus, R. A. Unimolecular dissociations and free radical recombination reactions. *J. Chem. Phys.* **1952**, *20*, 359-364.

[31] Marcus, R. A.; Rice, O. K. The kinetics of the recombination of methyl radicals and iodine atoms. *J. Phys. Colloid Chem.* **1951**, *55*, 894-908.

[32] Schranz, H. W.; Sewell, T. D. Statistical and dynamical behaviour in the unimolecular reaction dynamics of polyatomic molecules. *J. Mol. Str. (Theochem)* **1996**, *368*, 125-131.

[33] Sun, L.; Song, K.; Hase, W. L. A SN_2 reaction that avoids its deep potential energy minimum. *Science* **2002**, *296*, 875-878.

[34] Ammal, S. C.; Yamataka, H.; Aida, M.; Dupuis, M. Dynamic-driven reaction pathways in an intramolecular rearrangement. *Science* **2003**, *299*, 1555-1557.

[35] Meagher, J. F.; Chao, K. J.; Barker, J. R.; Rabinovitch, B. S. Intramolecular vibrational energy relaxation. Decomposition of a series of chemically activated fluoroalkyl cyclopropanes. *J. Phys.Chem.* **1974** , *78*, 2535-2543.

[36] Baer, T.; Potts, A. R. Non-statistical chemical reaction: the isomerisation over low barriers in methyl and ethyl cyclohexanones. *J. Phys. Chem. A* **2000**, *104*, 9397-9402.

[37] Chowdhury, P.K. Impulsive IR-multiphoton dissociation of acrolein: observation of non-statistical product vibrational excitation in CO(v=1-12) by time resolved IR fluorescence spectroscopy. *Chem. Phys.* **2000**, *260* (1-2), 151-158.

[38] Oudejans, L.; Miller, R. E. Photofragment translational spectroscopy of weakly bound complexes: probing the interfragment correlated final state distribution. *Ann. Rev. Phys. Chem.* **2001**, *52*, 607-637.

[39] Tonner, D. S.; McMahon, T. B. Non-statistical effects in the gas-phase SN_2 reaction. *J. Am. Chem. Soc.* **2000**, *122* (36), 8783-8784.

[40] Liu, J.; Chen, W.; Hochlaf, M.; Qian, X.; Chang, C.; Ng, C. Y. Unimolecular decay pathways of state-selected CO_2^+ in the internal energy range of 5.2-6.2 eV: an experimental and theoretical study. *J. Chem.Phys.* **2003**, *118*, 149-163.

[41] Smith, R. R.; Killelea, D. R. ; DelSesto, D.F.; Utz, A. L. Preference for vibrational over translational energy in a gas-surface reaction. *Science* **2004**, *304*, 992-995.

[42] Perouzel, E.; Jorgensen, M. R.; Keller, M.; Miller, A. D. Synthesis and formulation of neoglycolipids for the functionalization of liposomes and lipoplexes. *Bioconjug. Chem.* **2003**, *14*(5), 884-898.

[43] Xu, Z.; Jayaseharan, J.; Marchant, R. E. Synthesis and characterization of oligomaltose-grafted lipids with application to liposomes. *J.Colloid Interface Sci.* **2002**, *252*, 57-65.

[44] Gelhausen, M.; Besson, F.; Chierici, S.; Lafont, D.; Boullanger, P.; Roux, B. Lectin recognition of liposomes containing neoglycolipids. Influence of their lipidic anchor and spacer length. Coll. Surf. B. **1998**, *10*, 395-404.

[45] Lafont, D.; Boullanger, P.; Carvahlo, F.; Voltero, P. A convenient access to β-glycosides of N-acetyllactosamine. *Carbohydr. Res.* **1997**, *297*, 117-126.

[46] Lafont, D.; Boullanger, P.; Chierci, S.; Gelhausen, M.; Roux, B. Cholesteryl oligoethyleneglycols as D-glycosamine anchors into phospholipid bilayers. *New. J. Chem.* **1996**, *20*, 1093-1101.

[47] Lafont, D.; Boullanger, P. Syntheses of L-glucosamine donors for 1,2-trans-glycosylation reactions. *Tetrahedron Assymetry* **2006**, *17*, 3368-3379.

[48] Joly, N.; Vaillant, C.; Cohen, A. M.; Martin, P.; El Essassi, M.; Massoui, M.; Banoub, J. Structural determination of the novel fragmentation routes of zwitteronic morphine opiate antagonists naloxonazine and naloxone hydrochlorides using electrospray ionization tandem mass spectrometry. *Rapid Commun. Mass Spectrom.* **2007**, *21*, 1062-1074.

[49] Rida, M.; El Meslouhi, H.; Es-Safi, N-E.; Essassi el, M.; Banoub, J. Gas-phase fragmentation study of novel synthetic 1,5-benzodiazepine derivatives using electrospray ionization tandem mass spectroscopy. *Rapid Commun. Mass Spectrom.* **2008**, *22* (14), 2253-2268.

[50] www.munichbiotech.com

[51] Esposito, C.; Masotti, A.; Del Grosso, N.; Malizia, D.; Bianco, A.; Bonadies, F.; Napolitano, R.; Ortaggi, G.; Mossa, G. Function/structure correlation in novel pH-dependent cationic liposomes for glioma cells transfection in vitro. *C. R. Chimie* **2003**, *6*(5-6), 617-622.

[52] Chaudhuri, A. Cationic liposomes-promising gene carriers in non-viral gene therapy, *Business briefing: Pharmatech* **2002**, 1-4.

[53] Zou, Y.; Zong, G.; Ling, Y-H.; Perez-Soler, R. Development of cationic liposome formulations for intratracheal gene therapy of early lung cancer. *Cancer. Gene. Ther.* **2000**, *7*(5), 683-696.

[54] Yerushalmi, N.; Brinkmann, U.; Brinkmann, E.; Paia, L.; Pastan, I. Attenuating the growth of tumors by intratumoral administration of DNA encoding pseudomonas exotoxin via cationic liposomes. *Cancer. Gene. Ther.* **2000**, *7*(1), 91-96.

[55] Miyata, T.; Yamamoto, S.; Sakamoto, K.; Morishita, R.; Kaneda, Y. Novel immunotherapy for peritoneal dissemination of murine colon cancer with macrophage inflammatory protein-1 beta mediated by a tumor-specific vector, HVJ cationic liposomes. *Cancer.Gene.Ther.* **2001**, *8*(11), 852-860.

[56] The Use of Zeta Potential and PCS Measurements in Gene Therapy Research. Application Note by Malvern Instrument.
Website:www.azonaco.com/details.asp?ArticleID=1233

[57] Dass, C. R. Formation and quality control of cationic liposomes. *S. Pac. J. Nat. Sci.* **2001**, *19*, 18-23.

[58] Stopeck, A. T.; Hersh, E. M.; Akporiaye, E. T.; Harris, D. T.; Grogan, T.; Unger, E.; Warneke, J.; Schluter, S. F.; Stahl, S. Phase I study of direct gene transfer of an allogeneic histocompatibility antigen, HLA-B7, in patients with metastatic melanoma. *J. Clin. Oncol.* **1997**, *15*, 341-349.

[59] Xing, X.; Zhang, S.; Chang, J. Y.; Tucker, S. D.; Chen, H.; Huang, L.; Hung, M. C. Safety study and characterization of E1A- liposome complex gene delivery protocol in an ovarian cancer model. *Gene. Ther.* **1998**, *5*(11), 1538-1544.

[60] El Aneed, A.; Banoub, J. Elucidation of the molecular structure of lipid A isolated from both a rough mutant and a wild strain of Aeromonas salmonicida lipopolysaccharides using electrospray ionization quadrupole time-of-flight tandem mass spectrometry. *Rapid Commun. Mass Spectrom.* **2005**, *19*, 1-13.

[61] Domon, B.; Costello C. E. A systematic nomenclature for carbohydrate fragmentations in FAB-MS/MS spectra of glycoconjugates. *Glycoconj. J.* **1988**, *5*(4), 397-409.

[62] Irigoras, A.; Ugalde, J. M.; Lopez, X.; Sarasola, C. On the dissociation energy of $Ti(OH_2)^+$. An MCSCF, CCSD(T), and DFT study. *Can. J. Chem.* **1996**, *74*, 1824-1829.

[63] Harrison, A. G. Site of gas-phase ethyl ion attachment. *Can. J. Chem.* **1986**, *64*(6), 1051-1053.

[64] Lau, Y. K.; Kebarle, P. Substituent effects on the intrinsic basicity of benzene: proton affinities of substituted benzenes, *J. Am. Chem. Soc.* **1976**, *98*(23), 7452-7453.

[65] Li, X.; Hoffmann, E. Ion chemistry of deprotonated phenylthiocarbamyl-phenylalanine, *J. Am. Soc. Mass. Spectrom.* **1997**, *8*(10), 1078-1084.

[66] Veenstra, T. D.; Tomlison, A. J.; Benson. L.; Kumar, R.; Naylor, S. Low temperature aqueous electrospray ionization mass spectrometry of noncovalent complexes. *J. Am. Soc. Mass. Spectrom.* **1998**, *9*(6), 580-584.

[67] Reid, G. E.; O'Hair, R. A. J.; Styles, M. L.; McFayden, W. D.; Simpson, R. J. Gas phase ion-molecule reactions in a modified ion-trap: H/D exchange of non-covalent complexes and coordinatively unsaturated platinum complexes. *Rapid. Comm. Mass. Spectrom.* **1998**, *12*(22), 1701-1708.

[68] Low, W.; Kang, J.; DiGruccio, M.; Kirby, D.; Perrin, M.; Fischer, W. F. MALDI-MS analysis of peptides modified with photolabile arylazido groups. *J. Am. Soc. Mass. Spectrom.* **2004**, *15*, 1156-1160.

[69] Oliveira, A. M.; Barros, M. T.; Martins, A. M.; Cabral, M. A. R.; Dias, A. A.; Costa, M. L.; Cabral, M. H.; Moutinho, A. M. C.; and Jennings, K. R. Mass spectrometry of aliphatic azides. *Rapid. Comm. Mass. Spectrom.* **1999**.*13*(7), 559-561.

[70] Dinya, Z.; Benke, P.; Gyorgydeak, Z.; Somsak, L.; Jeko, J.; Pinter, I.; Kuszman, J.; Praly, J-P. Mass spectrometric studies of anomeric glycopyranosyl azides. *J. Mass. Spectrom.* **2001**, *36*(2), 211-219.

[71] Clayden, J.; Greeves, N.; Warren, S.; Wothers, P. *Organic Chemistry*, Oxford, 2001.

[72] El Khadem, H. S. *Carbohydrate Chemistry. Monosaccharide and their Oligomers*, Academic Press: New York, **1988**.

[73] Brakta, M.; Lhoste, P.; Sinou, D.; Becchi, M.; Fraisse, D.; Banoub, J. Differentiation of anomeric unsaturated C-glycosides by fast-bombardment ionization-collision activated dissociation/mass-analyzed ion kinetic energy analysis. *Organic. Mass. Spectrom.* **1990**, *25*, 249-252.

[74] Brakta, M.; Sinou D.; Becchi, M.; Banoub, J. Negative ion mass spectra of some unsaturated C-glycosides following keV ion bombardment. *Organic. Mass. Spectrom.* **1992**, *27*, 621-624.

[75] Brakta, M.; Lhoste, P.; Sinou, D.; Banoub, J. Electron impact mass spectra of phenyl 2,3 unsaturated O-Glycosides. *Organic. Mass. Spectrom.* **1990**, *25*, 243-244.

[76] Brakta, M.; Chaguir, B.; Sinou, D.; Banoub, J; Becchi, M. Differentiation of anomeric C-glycosides by mass spectrometry using fast atom bombardment, mass-analyzed ion kinetic energy and collision-activated dissociation. *Organic. Mass. Spectrom.* **1992**, *27*, 331-339.

[77] Grant, D. C.; Helleur, R. Rapid screening of anthocyanins in berry samples by surfactant-mediated matrix-assisted laser desorption/ionization time-of-flight mass spectrometry, *Rapid. Comm. Mass. Spectrom.* **2007**, *22*(2), 156-164.

[78] Hoffman, L. L.; Thomsberry, L.; Robbins, R., Amster, I. J.; Vaillant, C.; Banoub, J. MS^3 confirms the composition of in situ generated "internal elimination" product ions that arise from synthetic neoglycolipid derivatives. *J. Am. Soc. Mass. Spectrom.* 2007-3438. (manuscript submitted in July 2007)

[79] Siuzdak, G. *The expanding role of mass spectrometry in biotechnology*, Second Ed, 2006.

TurbolonSpray

Gas 1 of QSTAR XL connected to Neb gas
Gas 2 of QSTAR XL connected to Turbo gas

QSTAR XL TurbolonSpray			
NEB GAS		TURBO GAS	
Gas 1		Gas 2	
Setting	**Value (L/ min)**	**Setting**	**Value (L/min)**
0	0.00	0	0.0
10	0.62	10	1.5
20	1.16	20	2.5
30	1.56	30	3.0
40	1.95	40	4.0
50	2.85	50	4.8
55	**3.03**	60	5.5
60	3.33	70	6.0
70	3.77	80	6.5
80	4.10	**90**	**7.5**
90	4.35		

Appendix 1: Flow conversion table for QSTAR XL (QSTAR XL System, Hardware Guide, Applied Biosystems, July 2002)